

ATR

AUSTRALIAN TELECOMMUNICATION RESEARCH



- Editor-in-Chief* G. F. JENKINSON, B.Sc.
- Executive Editor* H. V. RODD, B.A., Dip.Lib.
- Deputy Executive Editor* M. A. HUNTER, B.E.
- Secretary* H. V. RODD, B.A., Dip.Lib.
- Editors* D. W. CLARK, B.E.E., M.Sc.
G. FLATAU, F.R.M.I.T. (Phys.)
A. J. GIBBS, B.E., M.E., Ph.D.
R. J. HARRIS, B.Sc.(Hons.), Ph.D.
D. KUHN, B.E.(Elec.), M.Eng.Sc.
I. P. MACFARLANE, B.E.
C. W. PRATT, Ph.D.
G. K. REEVES, B.Sc.(Hons.), Ph.D.
- Corresponding Editors* R. E. BOGNER, M.E., Ph.D., D.I.C., *University of Adelaide*
J. L. HULLETT, B.E., Ph.D., *University of Western Australia*

ATR is published twice a year (in May and November) by the Telecommunication Society of Australia. In addition special issues may be published.

ATR publishes papers relating to research into telecommunications in Australia.

CONTRIBUTIONS: The editors will be pleased to consider papers for publication. Contributions should be addressed to the Secretary, ATR, c/- Telecom Australia Research Laboratories, 770 Blackburn Rd., Clayton, Vic., 3168.

RESPONSIBILITY: The Society and the Board of Editors are not responsible for statements made or opinions expressed by authors of articles in this journal.

REPRINTING: Editors of other publications are welcome to use not more than one third of any article, provided that credit is given at the beginning or end as: ATR, the volume number, issue and date. Permission to reprint larger extracts or complete articles will normally be granted on application to the General Secretary of the Telecommunication Society of Australia.

SUBSCRIPTIONS: Subscriptions for ATR may be placed with the General Secretary, Telecommunication Society of Australia, Box 4050, G.P.O., Melbourne, Victoria, Australia, 3001. The subscription rates are detailed below. All rates are post free. Remittances should be made payable to the Telecommunication Society of Australia, in Australian currency and should yield the full amount free of any bank charges.

The Telecommunication Society of Australia publishes the following journals:

- 1. The Telecommunication Journal of Australia** (3 issues per year)
Subscription — Free to members of the Society* resident in Australia
Non-members in Australia \$15.00
Non-members or Members Overseas \$22.00
 - 2. ATR** (2 issues per year).
Subscription — To members of the Society* resident in Australia \$11.00
Telecom Payroll Deduction 43c/pay
Non-members in Australia \$22.00
Non-members or Members Overseas \$26.50
Single Copies — To Members of the Society resident in Australia \$8.50
Non-members within Australia \$14.00
Non-members or Members Overseas \$16.50
- *Membership of the Society \$9.00

All overseas copies are sent post-free by surface mail.
Prices are for 1985. Please note the revised rates.

Enquires and Subscriptions for all publications may be addressed to:
The General Secretary, Telecommunications Society of Australia,
Box 4050, G.P.O.
Melbourne, Victoria, Australia, 3001

Contents

- 2 Challenge**
- 3 Satellite Propagation in the South Pacific Region**
E. BACHMANN
- 13 Optimum Pulse Shapes for Local Digital Transmission Systems with Impulsive Noise**
P.G. POTTER
- 23 Echo Canceller Structures for Digital Loop Access Systems**
F.G. BULLOCK
- 43 Protocols for Message Handling**
R. EXNER
- 53 A Model for Carrier Recovery, Timing Recovery and Adaptive Equalisation in High-Capacity Digital Radio Systems**
P.V. KABAILA, J.L. ADAMS

Challenge . . .

1985 will see the launch of the first of the AUSSAT satellites. With this launch, Australia will join the small but increasing number of countries operating their own domestic communication satellite systems.

It will not be the first time, however, that Australia has used satellites for domestic communications. In 1969, an international INTELSAT satellite provided trunk telephone service relief between Sydney and Perth, and more recently Intelsat has been providing the ABC with TV relay facilities to remote transmitters.

Aussat Pty. Ltd., a wholly government-owned company, will operate Australia's national satellite system. Two satellites are to be launched this year, using the US Space Shuttle. A third will be launched later by the European Ariane rocket. The Aussat system will provide a wide range of communication services to the whole of the country. It will provide direct TV broadcasting to remote homesteads, TV program relays, telephone services to isolated settlements, various types of data transmission for businesses, and communication links for aircraft operations, to name just some applications.

The Aussat spacecraft manufacture and launches are, of necessity, and with minor exceptions, being done overseas. However, offset clauses in their contracts have resulted in other, complementary, work being brought into Australia.

There are considerable opportunities in the production and marketing of earth stations and associated components and systems. Those currently being purchased are very largely from overseas. Whilst large earth stations may never be needed in sufficient quantities to justify Australian production, some satellite applications will require large quantities of small earth terminals. The challenge for Australian industry is to develop its skills in space-related technology, with a view to the design and manufacture of such terminals for the domestic, and export, markets.

A further challenge for Australia lies in the development of new applications for satellite-related technology to meet the country's unique communication needs. This will require an innovative approach and a degree of risk to identify potential new developments and pursue appropriate ones to generate new markets.

By such means, Australia could, and should, progress towards a viable space-communication related industry, and maximize the returns from the nation's investment in space.

1985 is also a very important year for all nations who will, in the future, use communication satellites. In August, a World Administrative Radio Conference on the Geostationary Satellite Orbit (WARC ORB (1)) will be convened in Geneva. The challenge for Australia, and for all other nations attending, is to find a mutually acceptable basis for an agreement which will ensure that the geostationary satellite orbit, a unique, limited natural resource, can be shared on an equitable basis by all nations which need to use it.

G.F. JENKINSON

Satellite Propagation in the South Pacific Region

E. BACHMANN

Overseas Telecommunications Commission (Australia)

This paper examines the propagation impairments associated with the various frequency bands that could be used for a South Pacific satellite system. In particular, the effects of rain attenuating a satellite signal are investigated. Available climatological information tends to indicate that eastern tropical Australia, Papua New Guinea and the South Pacific countries belong to the same climatological region. On this basis, reliable long term rain intensity measurements for eastern tropical Australia and Papua New Guinea have been used for extrapolation to South Pacific countries. Rain intensity values for these countries are then converted to rain attenuation using an empirical formula.

System margins are proposed for trunk and concentrated subscriber telephone circuits, and transmission margins at 14 and 11 GHz are calculated for 25 representative potential earth station locations in the South Pacific region. Two other prediction methods are used for checking the results, and satisfactory agreement with the latest ITU method has been obtained.

KEYWORDS: Propagation, Satellite systems, Rain attenuation, Ku-Band, South Pacific

1. INTRODUCTION

The information presented in this paper was prepared in the course of a feasibility study of the implementation of a satellite communication system for the South Pacific region (Rural Telecommunications Study of the South Pacific Countries). The study was funded by the Governments of Australia and New Zealand and was carried out in 1981/82 under the convenorship of the South Pacific Bureau for Economic Cooperation (SPEC).

The paper considers propagation aspects for the selection of a frequency band which would be suitable for a South Pacific satellite system. The possible bands are 6/4 GHz and 14/11 GHz (uplink/downlink frequencies). Consideration has been given to ionospheric scintillation, depolarisation and rain attenuation, the latter being the most serious propagation impairment, especially above 10 GHz.

Satellite path rain attenuation studies have been carried out for a number of years in telecommunications laboratories overseas and in Australia (Telecom Australia). Several empirical models are now available for predicting rain attenuation statistics for a given location on the basis of available rain intensity (or rain rate, mm/hr) statistics for that location (several models are listed in Ref.1). However, rain intensity data is not available for the South Pacific region, and therefore these models have not been used for predicting rain attenuation statistics at the potential earth station sites.

Other models derive rain intensity data from local long-term data, such as annual rainfall as in Ref.2. However, little experience is available using such models for maritime tropical climates, such as the South Pacific region, especially above 10 GHz. In summary, an urgent need is seen for a new reliable empirical method for predicting rain attenuation in a maritime tropical climate.

2. PROPAGATION AVAILABILITY OBJECTIVES

The adoption of availability objectives will have a significant economic impact on a satellite system operating above 10 GHz. Availability to the user is a function of equipment and propagation availabilities. The use of a propagation availability in the lower part of the range being considered (99.9% to 99.0%) would lead directly to improvements in satellite capacity and to economies in earth station hardware and site engineering.

CCIR Recommendation No. 579 states that the mean annual equipment availability of a hypothetical reference satellite circuit for telephony should not be less than 99.8%; it also suggests that the required propagation availability should be the subject of a separate Recommendation, following further study.

In the absence of firm guidelines from the ITU, an independent set of propagation objectives are proposed for planning purposes. It is suggested that the mean annual propagation availability objective for South Pacific telephony trunk circuits should be the same as that which is recommended

Paper received 12 December 1983.
Final revision 14 January 1985.

for the equipment, namely 99.8%. Depending on the severity of the rainy season at a particular location, the worst month naturally would be subject to more interruptions than the annual monthly average. The proposed objectives are summarised in Table 1.

TABLE 1 - Proposed Availability Objectives

	TRUNK CIRCUITS	
	AVAILABILITY OBJECTIVE	UNAVAILABILITY PER WEEK
EQUIPMENT, MEAN ANNUAL	99.8%	
PROPAGATION, MEAN ANNUAL	99.8%	
TOTAL MEAN ANNUAL	99.6%	40 Min.

3. TRANSMISSION IMPAIRMENTS

3.1 Ionospheric Scintillation

Ionospheric scintillations are variations in amplitude, phase, polarisation and angle-of-arrival, produced when radio waves pass through electron density irregularities in the ionosphere. They were first noticed during the late 1960's (Refs. 3,4,5) and have been confirmed by INTELSAT measurements at 1.4, 4 and 6 GHz (impairments do not appear to be significant above 10 GHz). Analysis of the measurements indicates scintillation fading rates of between 2 and 6 fades per minute. The geographical area of significant scintillations is located in a band of 30° latitude above and below the geomagnetic equator. Maximum activity generally occurs about one hour after local ionospheric sunset, and around the two annual equinox periods.

Scintillation activities are highly Sunspot dependent (Ref.5). Ref.5 summarizes INTELSAT measurements carried out in Hong Kong over a 10 year period, incorporating almost the whole 11 year solar cycle including the high peak in 1979-80. These measurements showed that during a medium sized sunspot number (in the range of 45-110), scintillation fades (i.e. negative signal excursions) would be less than about 2 dB for 99.8% of the average year. As mentioned above, this phenomenon has a strong diurnal dependence and since the daytime occurrence and depth of fading is minimal, the effect on traffic will be much less than indicated by the Hong Kong statistics. Hence it is proposed not to incorporate special transmission margins for a South Pacific 6/4 GHz satellite system as far as ionospheric scintillations are concerned.

At the elevation angles being considered for the system (more than 40°), tropospheric scintillations are also not expected to be a problem.

3.2 Depolarisation

The electromagnetic waves in a satellite communications link can be depolarised by propagation anomalies such as heavy rain, ionospheric irregularities and tropospheric turbulences. Two nominally isolated channels using the same frequency, but orthogonally polarised signals, can interfere with each other when depolarisation occurs. At frequencies in the GHz-range, rain is the most significant cause of depolarisation. Ref.6 provides a theoretical and practical investigation of rain depolarisation, including the calculation of 4,6 and 11 GHz depolarisation for various rain rates, based on the differential attenuation and differential phase shift due to oblate raindrops. Reasonable agreement was observed between the theory and experimental results. On the basis of the calculated values in Ref.6 and using a typical tropical rain height of 3 km, it is noted that during heavy rain conditions (say 65mm/hour which is a typical 99.8% of year South Pacific worst case value) circular polarisation isolation may decrease to some 19 dB at 4 GHz, 15dB at 6 GHz, and 10 dB at 11 GHz.

It is not proposed to use dual polarisation transmission above 10 GHz for the South Pacific area. Dependent on detailed analysis, in a dual polarised 6/4 GHz system it may be necessary to stagger the voice channels on the two orthogonal beams; this may cause a minor reduction of the calculated single-channel-per-carrier (SCPC) transponder capacity values.

3.3 Rain Attenuation

By far the most serious propagation impairment to be considered is that of signal attenuation due to rain. While this is not a serious problem at lower frequencies, above 10 GHz it becomes a major cause of transmission loss. Proper design of a satellite system operating above 10 GHz therefore requires prediction of the rain attenuation statistics associated with the particular up and down paths.

Attenuation is generally described by a cumulative distribution curve which shows the percentage of time when attenuation is larger than a certain value. As the equiprobable attenuation along the slant path is related to the equiprobable rain intensity measured at a point, the relevant rain statistics is the rain rate (mm/hr) and not the other more available data such as rain accumulation.

The most reliable prediction of attenuation statistics on earth/space paths involves the long-term monitoring of a satellite beacon signal. In the absence of a suitable satellite beacon transmission the generally accepted approach has been to monitor sky noise temperature with a ground based radiometer and to convert the measured results to equivalent attenuation figures for the particular slant path being monitored.

4. CLIMATOLOGY OF SOUTH PACIFIC REGION*

The South Pacific region can be characterised as wet and tropical and much of the region satisfies the ITU classification P which represents the wettest climate in the world.

4.1 Summer

During southern hemisphere summer months, an area of low pressure extends from Indonesia in an easterly direction to at least 180° longitude, incorporating tropical Australia, Papua New Guinea and most of the South Pacific. Both incidence and intensity of rainfall are determined largely by the instability and amount of moisture available in the lower layer of the atmosphere, which in turn depend on the temperature of the upper few metres of the sea. Sea surface temperatures are very high in the Timor, Arafura and Coral Seas but decrease gradually eastwards to relatively low values off the South American Coast.

Most of the high intensity rainfall in tropical Australia, Papua New Guinea and the South Pacific occurs during the summer months.

During this period the area under discussion incorporates several major breeding grounds for tropical cyclones; there are also occasional semi-organised systems called cloud clusters containing numerous cumulonimbus cells.

4.2 Winter

The southeast trade winds dominate the South Pacific area during southern hemisphere winter months. Cumulus clouds are common but their height is limited by the trade wind inversion, particularly in the eastern part of the South Pacific. Showers are frequent on those parts of an island exposed to the southeasterlies and can be heavy at times, especially on the sides of hills or mountains. Records from New Caledonia and the Solomon Islands show some high intensity falls during this season.

4.3 Tropical Cyclones

By definition, a tropical cyclone must have associated wind speeds of at least 63 km/hour (i.e. gale force wind or above). According to Australian meteorological records (Ref.7), about one quarter of tropical cyclones produce "flood-type" rain; some very spectacular rainfall events associated with tropical cyclones and hurricanes are documented in the literature (Refs.8 to 14).

At any one place the incidence of exposure varies from more than five times per decade in the Loyalty Islands (170°E) to once or twice per decade for Vanuatu, Samoa, Tonga and Southern Cook Islands. The incidence decreases in the easterly direction, as the seawater temperature drops towards South America.

* This chapter is based on information provided by the Australian Bureau of Meteorology

4.4 Rainfall

An area of high rainfall extends from northern Australia/Papua New Guinea to 180° longitude along a latitude band approximately 5°S to 20°S. Between 160°E and 170°E mean annual rain accumulation totals are about 5000mm. In the Solomon Islands (around 160°E) almost all the rainfall recording stations are situated in coastal areas but much higher rainfall accumulation values have been noted in inland exposed mountainous regions. In such locations annual accumulation totals of at least 9000mm are indicated. The isohyets show decreasing annual rainfall totals to the east of the Solomon Islands, to 3000mm at 180°, falling to 1500mm at 30°S, 150°W.

The ITU has classified the world's geographical rainfall intensity distribution into 14 different rain climatic zones designated from A to P in order of increasing rain intensity (see Ref.15). As shown in Table 2, the South Pacific countries belong to three different rain climatic zones, namely D, N and P. (For more detailed information on the climatology of the South Pacific region, see Refs.16 to 20 which were referenced by the Australian Bureau of Meteorology.)

TABLE 2 - ITU Rain Climatic Zones In South Pacific

ITU RAIN CLIMATIC ZONE	0.2% OF YEAR RAIN INTENSITY IN ZONE	SOUTH PACIFIC COUNTRY
P	45 mm/hr	AMERICAN SAMOA, FSM (KOSRAE, PONAPE, TRUK, YAP), NORTHERN VANUATU, SOLOMON ISLANDS
N	20 mm/hr	FIJI, NIUE, NORTHERN COOK, SOUTHERN VANUATU, TONGA, TUVALU, WESTERN KIRIBATI, WESTERN SAMOA
D	6.5 mm/hr	EASTERN KIRIBATI, SOUTHERN COOK

5. METHODOLOGY FOR PREDICTING RAIN ATTENUATION

A simple method of calculating rain attenuation is available from CCIR (Ref.21) using empirical formulae to calculate path length and rain height when the rain rate for a given location is known. In the case of the South Pacific, the only source for rain intensity figures was CCIR Report 563-2 (Ref.15) which quoted for a given probability a fixed rain rate value for each rain climatic zone (i.e. with no

variation between locations in the same zone). While it is believed that this broad brush approach is too simplistic for predicting attenuation at the various potential earth station sites in the South Pacific area, the approach can serve as a check on calculated rain margins employing local rain accumulation data.

A computer program based on the Rice-Holmberg rain rate model was generously made available by AUSSAT Pty. Ltd. (Ref.2); it relates rain intensity to annual rainfall, taking account of local thunderstorm rain activity. The calculation of effective path length is based on experience from temperate climates, and the experience with the use of this program for maritime tropical climates is very limited. Recently it has been recognised (see Ref.1 and 21) that the top of the rain in tropical areas is often well below the freezing level and that a rain height correction factor should be applied in the rain path length calculation (Ref.21 applies a correction factor of 0.6). Therefore one would expect that this computer program, which bases the path length calculation on experience from temperate climates, would tend to over-estimate the path length and thus the rain attenuation, when it is applied to a tropical climate. Nevertheless, this program may be useful as another independent check on otherwise predicted rain attenuation at potential earth station sites.

5.2 Availability of Basic Data

Early in this study, approaches were made to INTELSAT, COMSAT, Papua New Guinea P and T Department and Telecom Australia, concerning attenuation statistics for the South Pacific region. As a result, useful radiometer measurement results were received from Telecom Australia for Darwin (Northern Territory) and Innisfail (North Queensland). However, no information was available for the countries covered by this study.

In order to ensure that no available rainfall data for the region was overlooked, the author visited the local meteorology department in each of the South Pacific countries concerned. Requests for data were also sent to the meteorology departments in New Zealand, Australia, Hawaii, Papua New Guinea, Hong Kong and the Philippines. As a result, Telecom Australia made available cumulative rain intensity distribution graphs for 19 locations in eastern tropical Australia and Papua New Guinea. These graphs were based on pluviograph charts (average site measurement period of about 15 years), which had been analysed following digitisation by the Australian Bureau of Meteorology. Apart from a single graph for Laucala Bay in Fiji, however, no rain intensity information was available from the countries covered by the study.

5.3 Proposed Methodology

Examination of the climatology information provided by the Australian Bureau of Meteorology indicated that the South Pacific, Papua New Guinea and the eastern part of

tropical Australia are subjected to the same external influences in regard to rainfall, although the impact of these varies within the area. The Bureau advised that this area forms a single climatological region. Since the relationship between rain intensity and mean annual rain accumulation could be established for part of this region, it would be reasonable to investigate the feasibility of estimating the required rain intensity values for the South Pacific countries on the basis of the mean annual rain accumulation which is available for each potential South Pacific site. This approach would be somewhat akin to the Rice-Holmberg method, but with the notable difference that prediction is carried out only within the same climatological region.

Mean annual rain accumulation, as well as measured rain intensities (6-minute integration) were available from Telecom Australia for 19 locations in eastern tropical Australia and Papua New Guinea. The rain intensity values were converted to equivalent 1-minute integration values (see Table 3) using the following empirical formula advised by Telecom Australia (Ref.1) to be valid for tropical climates:

TABLE 3 - Total Annual Rainfall and Rain Intensity for Australia and PNG

LOCATION	1 MIN RAIN INTENSITY EXCEEDED FOR 0.2% OF YEAR (mm/hr)	TOTAL ANNUAL RAINFALL (mm)
THURSDAY ISLAND	28.2	1729
PORT MORESBY	16.6	1201
WILLIS ISLAND	14.8	1320
RABAU	26.3	2012
COOKTOWN	27.0	1784
MADANG	51.5	3552
LAE	45.2	4610
LAUCALA BAY	39.0	3160
KUM RIVER	22.1	2642
UPPER STRICKLAND	15.4	3036
KAINANTU	18.4	2037
NAMBARE	35.7	2235
INNISFAIL	42.9	3192.5
NORFOLK ISLAND	15.4	1381
MACKAY	14.0	1640
ROCKHAMPTON	10.0	834
CAIRNS	23.3	2150
WEIPA	30.0	1961
GOVE	22.0	1401

$$R_1 = 0.990 R_6^{1.054} \text{ mm/hr} \quad (1)$$

where:

R_1 is the 1-minute integration rain intensity, and

R_6 is the 6-minute integration rain intensity.

A rain intensity (1-minute) versus annual rainfall regression plot for these 19 locations (Fig.1) indicated that one location should be classified as an extreme outlier (Upper Strickland in Papua New Guinea). Map examination revealed that this station is located on the southerly side of the Central Range and therefore would appear to be sheltered from the summer weather systems which incorporate the highest rain intensities. This station had a much lower intensity than the value indicated by its annual rainfall. Accordingly, this location was removed from the plot. Linear regression analysis resulted in a correlation coefficient of 0.87 when it was excluded. While a correlation coefficient of 0.87 is only moderately encouraging, it must be emphasised that no reliable method for predicting tropical rain attenuation was known to exist. Therefore it was decided to proceed with this regression method.

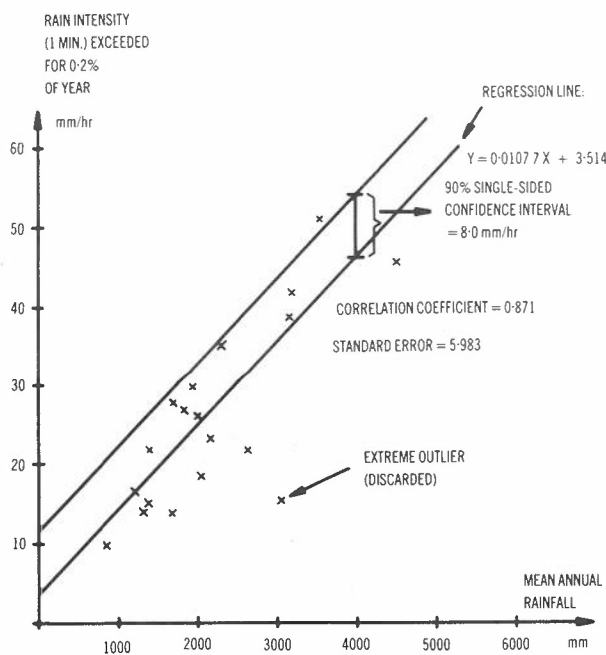


Fig. 1 - Regression analysis. 1 minute rain intensity exceeded for 0.2% of year versus mean annual rainfall. Locations in PNG and east tropical Australia.

The basis for the derivation of rain attenuation would be measured rain intensity and 11 GHz attenuation (downlink frequency) data over a three year period at Innisfail on the North Queensland coast in Australia (as graphed

in Ref.22). As discussed in Ref.1, based on the measured rain intensity/attenuation relationship for Innisfail, the following relation may be used for tropical areas such as the South Pacific region:

$$A_T = 0.020 R^{1.383} \text{ (dB)} \quad (2)$$

where:

A_T is the tropical rain attenuation at 11 GHz in dB, and R is the rain intensity in mm/hr

A possible objection to this simplistic method may be that it fails to recognise any elevation angle dependence. However, there are strong reasons to believe that in tropical areas for elevation angles above 30°, the elevation angle dependence is minimal, as demonstrated in Ref.1.

6. DERIVATION OF RESULTS

6.1 Rain Attenuation for 25 South Pacific Locations

Statistical analysis on the regression line in Fig.1 indicated a standard error of 6.0 mm/hr for rain intensity. The derivation of the confidence interval depends on the distribution function of the plotted values. Statistical tables show that, with a Gaussian distribution, there would be 90% confidence that the 11 GHz rain intensity value, R, would be less than $A+SE$ (1.28) mm/hr where:

A is the regression line value, and SE is standard error of estimate.

Therefore, for a standard error of 5.98 mm/hr,

$$R = A + 7.7 \text{ mm/hr} \quad (3)$$

Similarly, t-distribution tables (16 degrees of freedom) indicate that there would be 90% confidence that the rain intensity value would be less than $A + SE(1.337)$ mm/hr, or

$$R = A + 8.0 \text{ mm/hr} \quad (4)$$

The difference between the two results is insignificant, and it was decided to apply the larger value, i.e., $A + 8.0$ mm/hr.

Long term mean annual rainfall values for 25 representative South Pacific locations (Table 4) were converted to rain intensity values (1-minute integration, 99.8% annual availability), simply by applying the formula of the regression line in Fig.1, and the results are shown in the left hand column of Table 5.

From these rain intensity values 11 GHz rain attenuation values were predicted in accordance with relation (2) (see Table 5 middle column). The right hand column of Table 5 shows the 14 GHz attenuation figures which were calculated from the 11 GHz values using the following formula (Ref.1):

TABLE 4 - Mean Annual Rainfall for 25 South Pacific Locations

	MEAN ANNUAL RAINFALL (mm)
PAGO PAGO, AMERICAN SAMOA	4915
AFIAMALU, WESTERN SAMOA	5080
APIA, WESTERN SAMOA	2938
SANTO, VANUATU	3095
VILA, VANUATU	2365
TANNA, VANUATU	1589
FUNAFUTI, TUVALU	4003
VAVAU'U, TONGA	2289
NUKUALOFA, TONGA	1878
HA'APAI, TONGA	1801
ATAFU, TOKELAU	2683
RENDOVA, SOLOMON ISLANDS	4616
AUKI, SOLOMON ISLANDS	3321
HONIARA, SOLOMON ISLANDS	2177
NIUE	2079
NORTHERN GILBERTS, KIRIBATI	3000
FANNING, KIRIBATI	2515
TARAWA, KIRIBATI	1996
LAUCALA BAY, FIJI	3059
NADI, FIJI	1892
PONAPE, FSM	4875
TRUK, FSM	3493
YAP, FSM	3086
MANIHIKI, COOK ISLANDS	2482
RARATONGA, COOK ISLANDS	2012

$$F(f) = 1 + B(f-11), \quad (5)$$

where:

F(f) is the dB ratio of rain attenuation at the frequency f (GHz) to the rain attenuation at 11 GHz, and

B is 0.20 for tropical climates.

Table 6 indicates the equivalent 90% confidence rain attenuation values for 11 and 14 GHz, applying the additional 8.0 mm/hr rain intensity in accordance with the 90% single sided confidence interval (see equation (4) above).

As a check, the AUSSAT computer program mentioned in Section 5.1 above was used for predicting 11 GHz attenuations at 7 different locations, see Table 7. As anticipated in section 5.1 above, the computer calculation results gave higher values than those based on the regression line method.

TABLE 5 - 11 And 14 GHz Rain Attenuation for 25 South Pacific Locations

	RAIN INTENSITY EXCEEDED 0.2% OF YEAR (mm/hr)	11 GHz ATTENUATION EXCEEDED 0.2% OF YEAR (dB)	14 GHz ATTENUATION EXCEEDED 0.2% OF YEAR (dB)
PAGO PAGO, AMERICAN SAMOA	56.5	5.3	8.5
AFIAMALU, WESTERN SAMOA	58.2	5.5	8.8
APIA, WESTERN SAMOA	35.2	2.8	4.5
SANTO, VANUATU	36.9	2.9	4.6
VILA, VANUATU	29.0	2.1	3.4
TANNA, VANUATU	17.1	1.3	2.1
FUNAFUTI, TUVALU	46.6	4.1	6.6
VAVAU'U, TONGA	28.2	2.0	3.2
NUKUALOFA, TONGA	23.7	1.6	2.6
HA'APAI, TONGA	22.9	1.5	2.4
ATAFU, TOKELAU	32.4	2.5	4.0
RENDOVA, SOLOMON ISLANDS	53.2	4.9	7.8
AUKI, SOLOMON ISLANDS	39.3	3.2	5.1
HONIARA, SOLOMON ISLANDS	27.0	1.9	3.0
NIUE	25.9	1.8	2.9
NORTHERN GILBERTS, KIRIBATI	35.8	2.8	4.5
FANNING, KIRIBATI	30.6	2.3	3.7
TARAWA, KIRIBATI	25.0	1.7	2.7
LAUCALA BAY, FIJI	36.5	2.9	4.6
NADI, FIJI	23.9	1.5	2.4
PONAPE, FSM	56.0	5.2	8.3
TRUK, FSM	41.1	3.4	5.4
YAP, FSM	36.8	2.9	4.6
MANIHIKI, COOK ISLANDS	30.3	2.2	3.5
RARATONGA, COOK ISLANDS	25.2	1.7	2.7

TABLE 6 - 11 And 14 GHz Rain Attenuation (90% Confidence) for 25 South Pacific Locations

	90% CONFIDENCE RAIN INTENSITY EXCEEDED 0.2% OF YEAR (mm/hr)	90% CONFIDENCE 11GHz ATTENUATION EXCEEDED 0.2% OF YEAR (dB)	90% CONFIDENCE 14GHz ATTENUATION EXCEEDED 0.2% OF YEAR (dB)
PAGO PAGO, AMERICAN SAMOA	64.5	6.4	10.2
AFIAMALU, WESTERN SAMOA	66.2	6.6	10.6
APIA, WESTERN SAMOA	43.2	3.7	5.9
SANTO, VANUATU	44.9	3.9	6.2
VILA, VANUATU	37.0	3.0	4.8
TANNA, VANUATU	25.1	1.7	2.7
FUNAFUTI, TUVALU	54.6	5.1	8.2
VAVAU'U, TONGA	36.2	2.9	4.6
NUKUALOFA, TONGA	31.7	2.4	3.8
HA'APAI, TONGA	30.9	2.3	3.7
ATAFU, TOKELAU	40.4	3.3	5.3
RENDOVA, SOLOMON ISLANDS	61.2	5.9	9.4
AUKI, SOLOMON ISLANDS	47.3	4.1	6.6
HONIARA, SOLOMON ISLANDS	35.0	2.7	4.3
NIUE	33.9	2.6	4.2
NORTHERN GILBERTS, KIRIBATI	43.8	3.7	5.9
FANNING, KIRIBATI	38.6	3.1	5.0
TARAWA, KIRIBATI	33.0	2.5	4.0
LAUCALA BAY, FIJI	44.5	3.8	6.1
NADI, FIJI	31.9	2.4	3.8
PONAPE, FSM	64.0	6.3	10.1
TRUK, FSM	49.1	4.4	7.0
YAP, FSM	44.8	3.8	6.1
MANIHIKI, COOK ISLANDS	38.3	3.1	5.0
RARATONGA, COOK ISLANDS	33.2	2.5	4.0

TABLE 7 - Comparison of 11 GHz Rain Attenuation Calculated By Regression Line Versus Aussat Computer Program

	11 GHz RAIN ATTENUATION EXCEEDED 0.2% OF YEAR (dB)	
	REGRESSION LINE (90% CONFIDENCE)	AUSSAT COMPUTER PROGRAM
RAROTONGA, COOK ISLANDS	2.5	4.2
TANNA, VANUATU	1.7	2.3
LAUCALA BAY, FIJI	3.8	5.0
FUNAFUTI, TUVALU	5.1	6.5
RENDOVA, SOLOMON ISLAND	5.9	7.1
AFIAMALU, WESTERN SAMOA	6.6	8.4
PONAPE, FEDERATED STATES OF MICRONESIA	6.3	7.5

6.2 System Margins

Further analysis is required, in order to derive appropriate system design margins to cover rainfall attenuation. It is proposed that the validity of such margins should be based on 90% probability; in other words, the margins should take account of the uncertainty involved in the regression line method by using the single sided confidence interval.

In a practical South Pacific satellite system, it would be necessary to compute the rain attenuation for each site. While the system should be designed generally to provide sufficient power margins above clear-sky transmission for the various stations, it would not be economical to set that margin for the worst cases, (i.e. for the most rainy locations), as this would place too great a burden on the space segment in terms of loss of channel capacity. Therefore the worst case sites may need to use slightly larger antennas or receivers with lower noise figures than the other stations in the system (antenna diversity is not expected to be an option for the South Pacific, in view of the real estate and cost requirements).

It is proposed that the system design margins should be suitable for 90% of the sites. The 99.8% attenuation values for the sites in Table 4 were plotted in a cumulative distribution graph (Fig.2), indicating that 90% of the sites should have down-link attenuations of no more than approximately 5 dB, the equivalent 99.8% rain intensity value being 54.2 mm/hr. As

mentioned above, the system design values should take account of the 90% confidence interval for the regression line. The aggregate 99.8% rain intensity value therefore would be:

$$54.2 + 8.0 = 62.2 \text{ mm/hr,}$$

resulting in a system design margin for 11 GHz of:

$$0.02 \times 62.2^{1.383} = 6.05 \text{ dB, say } \underline{6.1 \text{ dB.}}$$

The equivalent up-link attenuation (14 GHz) is derived by using formula (5) above. The resulting uplink attenuation is 9.76 dB, say 9.8 dB.

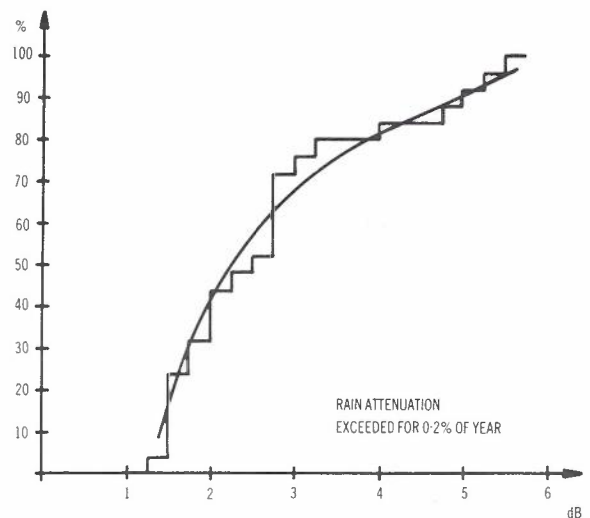


Fig. 2 - Rain attenuation exceeded for 0.2% of year. Cumulative distribution for South Pacific Sites.

In order to maintain power at the satellite during rain, it is customary to provide automatic up-link power control, on the basis of continuous monitoring of a satellite beacon at each earth station. In practice, the susceptibility of the transponder to damage in the case of malfunction of the automatic power control system would place a limit on the range of power control that could be applied.* In this regard, a maximum range of 0-6 is believed to be safe. The adoption of this range would lead to a system margin requirement of about 4 dB, in addition to the 0-6 dB transmit power control range.

As a check, system margins were calculated using the ITU method shown in Ref.21. In view of the significant number of climate P countries in the region (see Table 2), it is proposed that the system margins be based on climate P. Using typical South Pacific climate P parameters of 45°

* In the case of multiple carrier operation for telephony, the result of malfunction may be interference to other carriers, but in the case of a full transponder TV carrier, excessive power levels may result in damage to a travelling wave tube amplifier in the satellite.

elevation angle to the satellite and 10° latitude, the 0.2% of year rain attenuation at 11 GHz was calculated to be 6.5 dB. Conversion to 14 GHz, using formula (6), resulted in an attenuation of 10.4 dB. Table 8 shows 0.2% of year rain attenuation for 14/11 and 6/4 GHz, calculated for climates P, N and D as found in the South Pacific.

TABLE 8 - Rain Attenuation Calculated for ITU Climates D, N and P Using ITU Method (Ref.21)

	RAIN ATTENUATION, EXCEEDED 0.2% OF YEAR (dB)			
	4 GHz	6 GHz	11 GHz	14 GHz
CLIMATE D	0.02 dB	0.1 dB	0.6 dB	1.0 dB
CLIMATE N	0.1 dB	0.6 dB	3.8 dB	6.1 dB
CLIMATE P	0.2 dB	1.0 dB	6.5 dB	10.4 dB

7. APPLICATION OF RESULTS

The agreement between the results of the regression line prediction method and the climate P results of the ITU prediction method at 11 and 14 GHz is considered to be satisfactory, see Table 9. Because of this agreement, the 4 and 6 GHz attenuations for climate P, calculated by the ITU method, are believed to give a good indication of the required system margins at these frequencies.

TABLE 9 - Comparison of 11 and 14 GHz Rain Attenuation Calculated By Regression Line Versus ITU Method

	RAIN ATTENUATION, EXCEEDED 0.2% OF YEAR (dB)	
	REGRESSION LINE, 90% CONFIDENCE	ITU CALCULATION CLIMATE P
11 GHz	6.1 dB	6.5 dB
14 GHz	9.8 dB	10.4 dB

In applying the results of this study, one must recognise the vagaries and uncertainties involved in meteorological phenomena. Plus and minus 50% variation around the annual and worst month rain accumulation are not unusual in the South Pacific countries. Thus, even if accurate long term rain intensity distributions could be predicted, large year to year variations of the attenuation exceeded for a fixed percentage of time must still be anticipated.

It is also necessary to recognise the seasonal variation of propagation performance. Based on inspection of calculated attenuation statistics for eastern tropical Australia and

Papua New Guinea, one could expect the mean worst month unavailability to be of the order of twice the mean annual unavailability.

Finally, it is evident that the long term incidence of tropical cyclones in the South Pacific area is high and that such cyclones may be accompanied by prolonged rainfall that would prevent the operation of a satellite system working above 10 GHz, at affected earth stations. Statistically, the associated unavailability is already allowed for but it does not seem desirable to have a major communications system which is known to be unreliable during heavy rain.

8. CONCLUSIONS

It is concluded that the mean annual propagation availability objective for trunk and concentrated subscriber circuits for a possible South Pacific satellite system should be 99.8%.

The following system margins are indicated for such circuits for the propagation availability objectives:

6/4 GHz:

Up-link 1.0 dB
Down-link 0.2 dB

14/11 GHz:

Up-link 3.8 dB plus a dynamic power control range of 0-6 dB
Down-link 6.1 dB

9. ACKNOWLEDGEMENTS

The assistance of Mr. M.R. Kennedy of the Australian Bureau of Meteorology and Mr. R.K. Flavin of Telecom Australia Research Laboratories is gratefully acknowledged. The author also wishes to thank the Overseas Telecommunications Commission (Australia), the Department of Communications and the South Pacific Bureau for Economic Cooperation (SPEC) for their permission to publish the paper.

10. REFERENCES

1. Flavin, R.K., "Rain Attenuation Considerations for Satellite Paths in Australia", Australian Telecommunications Research Journal, Vol. 16, No. 2, 1982.
2. Rice, P.L. and Holmberg, N.R., "Cumulative Time Statistics of Surface-Point Rainfall Rates", IEEE Trans Comm., Vol. COM-21, No. 10, pp 1131-1136; 1973.
3. Taur, R.R., "Ionospheric Scintillations of 4 and 6 GHz", COMSAT Technical Review, Vol. 3, 1973, pp 145.
4. Taur, R.R., "Ionospheric Propagation - Scintillation at

- Frequencies above 1 GHz", COMSAT Technical Review, Vol. 4, 1974, pp 462.
5. Fang, D.J. and Pontes, M.S., "4/6 GHz Ionospheric Scintillation Measurements during the Peak of Sunspot Cycle 21", COMSAT Technical Review, Vol. 11, No. 2, 1981, pp 294.
 6. Taur, R.R., "Rain Depolarisation Measurements on a Satellite-Earth Propagation Path at 4 GHz", COMSAT Laboratories.
 7. Kennedy, M.R., Climatologist, Australian Bureau of Meteorology, Conversations with author.
 8. Revell, C.G., "Tropical Cyclones in the Southwest Pacific", New Zealand Meteorological Service Miscellaneous Publication 170, Wellington, 1981, pp 3.
 9. Gabites, J.F., "The Threat of Tropical Cyclones in the Southwest Pacific", Technical Note, Fiji Meteorological Service, 1976, pp 5.
 10. Lourensz, R.S., "Tropical Cyclones in the Australian Region", July 1909 to June 1975, Australian Bureau of Meteorology, January 1977.
 11. Letter from the Meteorological Service in Reunion to Australian Bureau of Meteorology, September, 1969, attached copy of pluviograph chart.
 12. Henry, W.K., "An Excessive Rainfall in Panama, 1954", Water Resources Research, Vol. 2., No. 4, 1966, pp 894.
 13. Appadu, S.N., "Rainfall in Mauritius", World Meteorological Organisation Bulletin, October, 1980, pp 255.
 14. Davis, E.R. and Bridges, W.C., "Weather Note", Monthly Weather Review, April 1972, pp 294.
 15. CCIR Report 563-2, Green Book 1982, Volume V, XVTH Plenary Assembly, Geneva, 1982.
 16. Brookfield, H.C. and Hart, D., "Rainfall in the Tropical Southwest Pacific", National University Dept., Geographical Publication G.3.
 17. Girard, J. and Rignot, D., "Climatologie de la Nouvelle-Caledonie", Monographie No. 82 de la Meteorologie Nationale, Ministry of Transport, Paris, France.
 18. Hansell, R.F. and Wall, J.R.D., "Land Resources of the Solomon Islands, Vol. 1", Introduction and Recommendations, Land Resource Study 18, Ministry of Overseas Development, United Kingdom, pp 36.
 19. Thomsen, H., "Climates of the Oceans," World Survey of Climatology, Vol. 15, Elsevier Publishing Company.
 20. Ocean Atlas for Pacific Ocean, USSR Ministry of Defence, Moscow.
 21. Report of CCIR Conference Preparatory Meeting (CPM), Geneva, June/July 1984, Part II, pp 7-17.
 22. Flavin, R.K., "Earth-Space Rain Attenuation for 11 and 14 GHz - Darwin, Australia", Australian Telecommunications Research Journal, Vol. 12, No. 2, 1978, pp 15.

BIOGRAPHY



ERIK BACHMANN graduated with an M.E. in 1955 from the Technical University of Copenhagen, Denmark. He spent a few years with the Royal Danish Navy, L.M. Ericsson (Stockholm), Broadcasting Control Board (Melbourne), ICI Australia (Sydney). Since joining the Overseas Telecommunications Commission (Australia) in 1963, he has worked on the planning and construction of a variety of projects in the fields of international switching and transmission. Between 1971 and 1977, he was the regular Australian delegate to the INTELSAT Board of Governors Advisory Committee on Technical Matters. He was the expert responsible for satellite matters on the Rural Telecommunications Study of the South Pacific Countries, which was carried out under the convenorship of the South Pacific Bureau for Economic Cooperation from late 1981 to late 1982. Mr. Bachmann's current responsibility at OTC(A) is the planning of Australian international satellite earth stations.

Optimum Pulse Shapes for Local Digital Transmission Systems with Impulsive Noise

P.G. POTTER

Telecom Australia Research Laboratories

Impulsive noise due to signalling transitions on nearby pairs in the cable limits the performance of local digital reticulation systems. It is shown that impulsive noise limits interact with compatibility constraints. The transmit level of the digital system is constrained by crosstalk interference into other types of system in the same cable and also by limitations on power feeding to remote transmitters. This paper proposes an approximate near-end crosstalk (NEXT) impulsive noise model based on the total energy in the impulsive noise response at the decision point. The model adequately predicts the relative performance of systems with several different transmit and receive pulse shapes for 2- and 3-level codes. This total energy model is optimized over both transmit and receive pulse shapes. For cases where the total transmit power is constrained, a sensible choice of practical pulse shapes can give near optimal impulsive noise performance.

KEYWORDS: Impulsive Noise, Local Digital Transmission, Crosstalk in Multipair Cable

1. INTRODUCTION

In this paper an approximate model for impulsive noise interference into digital transmission systems is proposed. The new performance measure described herein is based on the ratio of the total energy in the impulsive noise response at the decision point to the square of the eye opening. Since increase in the signal level at the decision point improves the impulsive noise performance, the formulation of constraints on this signal level must be recognised as a necessary part of the process of determining line loss limits due to impulsive noise (Ref.1). These constraints may be due to power feed limitations for remote transmitters, or due to crosstalk from the digital system into other types of system within the same cable (Refs.2,3).

Given a particular constraint, the relative impulsive noise performance of systems with different practical transmit and receive pulse shapes is assessed. The optimum performance is also derived and compared with the practical cases. The proposed measure is shown to be in good agreement with the NEXT impulsive noise figure (Ref.1) which is considered to be the most appropriate measure of impulsive noise susceptibility.

2. TRANSMISSION MODELS

Consider one direction of a digital transmission system on pair cable (Fig.1) consisting of a transmitted code with average spectrum $W(f)$, transmit pulse shaping $S(f)$,

a line transfer function $G(f)$ and an equalizer $E(f)$. The pulse shape at the receiver's decision point is $d(t)$ with Fourier transform given by $D(f)$,

$$D(f) = S(f)G(f)E(f) \quad (1)$$

and the transmit average power spectral density $P(f)$ is

$$P(f) = W(f)|S(f)|^2 \quad (2)$$

For step disturbances on the near-end of nearby pairs the average over the ensemble of realizations of the p^{th} pair combination of the NEXT impulsive noise energy spectrum due to a step disturbance event is given by (Ref.1):

$$I(f) = I_p \frac{\alpha(f_0)}{\alpha(f)} \quad (3)$$

where α is the cable attenuation per unit length and I_p is independent of frequency.

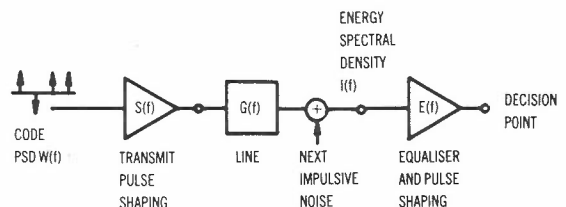


Fig. 1 - Transmission Model for NEXT Impulsive Noise Energy Spectrum

Paper received 19 December 1984.
Final revision 1 February 1985.

The frequency dependence of $l(f)$ differs from the frequency dependence on mean NEXT attenuation (Ref.5) by the factor f^{-2} due to the step disturbance.

The impulsive noise energy spectrum at the decision point is given by $N(f)$,

$$N(f) = \left| \frac{D(f)}{S(f)G(f)} \right|^2 I_p \frac{\alpha(f_0)}{\alpha(f)} \quad (4)$$

and the total impulsive noise energy per event at the decision point is \bar{N} .

$$\bar{N} = 2I_p \int_0^\infty \left| \frac{D(f)}{S(f)G(f)} \right|^2 \frac{\alpha(f_0)}{\alpha(f)} df \quad (5)$$

The code description and the receive pulse shape $d(t)$ will now be used to obtain the minimum eye opening. The basic code element is described by the impulse train representation (compare with equation (2) of Ref.4).

$$\sum_{i=-\infty}^{\infty} w_i \delta(t-iT)$$

$$\Rightarrow W(f) = \frac{1}{T} \left| \sum_{i=-\infty}^{\infty} w_i e^{-ji2\pi fT} \right|^2 \quad (6)$$

The basic code elements for binary, duobinary and alternate mark inversion (AMI) codes illustrated in Fig.2 are based on the partial response scheme in which a precoder precedes the basic code element and pulse shaping (Ref.4).

The response at the decision point to this basic code element is $p(t)$.

$$p(t) = \sum_{i=-\infty}^{\infty} w_i d(t-iT) \quad (7)$$

The basic responses are multiplied by the (pre-coded) data $b_j \in \{-1,+1\}$ at time instant j and summed to obtain the overall signal at the decision point (as in Fig.3).

$$v(t) = \sum_{j=-\infty}^{\infty} b_{-j} \sum_{i=-\infty}^{\infty} w_i d(t+(j-i)T) \quad (8)$$

The nominal signal levels at the sampling instant t_0 are determined by the possible sets of b_{-j} for j such that $w_j \neq 0$. All other terms are intersymbol interference (ISI) and the extreme voltages for a given nominal signal level occur when the remainder of the b_{-j} are chosen so that all ISI terms have the same sign.

$$\text{Nominal signal level} = \sum_{j, w_j \neq 0} b_{-j} p(t_0+jT)$$

for each set of b_{-j}

(9)

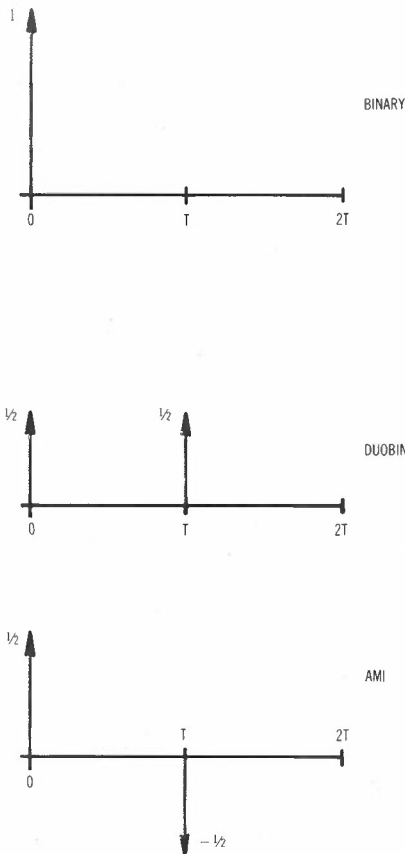


Fig. 2 - Basic Code Elements for Binary, Duobinary and AMI Codes

$$\text{Extreme signal levels} = \sum_{j, w_j \neq 0} b_{-j} p(t_0+jT) \pm \sum_{j, w_j = 0} |p(t_0+jT)| \quad (10)$$

For example, for AMI $w_0 = 1/2$, $w_1 = -1/2$, otherwise $w_i = 0$.

$$\text{Hence } \{b_{-j}\} \equiv \{(b_{-1}, b_0) = (1, 1), (-1, 1), (-1, -1) \text{ or } (1, -1)\}$$

The corresponding nominal signal levels are $\{0, d(t_0), 0, -d(t_0)\}$ for sampling at t_0 in $(-T/2, T/2)$. The difference between each extreme signal level from (10) and the relevant decision threshold in the receiver (assumed to exactly bisect the minimum eye opening) gives the noise voltage V_T which causes an error.

A summary of the definitions of 2- and 3-level linear codes with basic codes covering 1 or 2 symbol periods is presented in Table 1. The basic code element is normalized so that:

$$\sum_{i=-\infty}^{\infty} |w_i| = 1 \quad (11)$$

Most 2-level linear codes (e.g. WAL1,

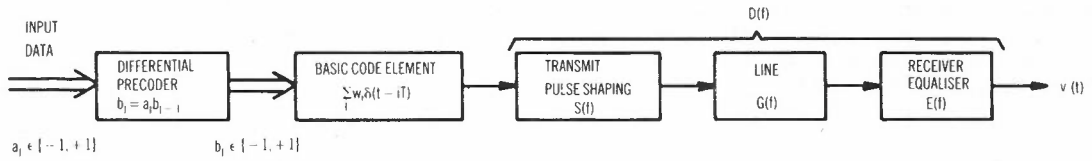


Fig. 3 - Block Diagram for Determination of the Signal $V(t)$ at the Decision Point

WAL2, MWAL2) may be considered as pre-distortions of binary coding, having multimodal $d(t)$ functions.

The value of the noise threshold V_T obtained from the analysis of intersymbol interference may be used to produce an expression for the total impulsive noise energy which is independent of the receiver gain.

$$\bar{N}_O = \frac{\bar{N}}{V_T^2} = \frac{2I_p}{V_T^2} \int_0^\infty \left| \frac{D(f)}{S(f)G(f)} \right|^2 \frac{\alpha(f_0)}{\alpha(f)} df \quad (12)$$

This expression is independent of the scale of the receive pulse shape $d(t)$.

TABLE 1 - Linear Codes with 2 or 3 Levels

Code	w_0	w_1	$W(f)$
BINARY	1	0	$\frac{1}{T}$
AMI	1/2	-1/2	$\frac{1}{T} \sin^2 \pi f T$
DUOBINARY	1/2	1/2	$\frac{1}{T} \cos^2 \pi f T$

3. CONSTRAINTS ON THE TRANSMITTED POWER SPECTRUM

The transmitted average power spectrum may be constrained for two reasons. Firstly crosstalk into other types of system in the same cable may degrade the performance of those systems unless the transmit level in the digital system is limited to some maximum value. Secondly, the power feeding requirements may also limit the total power which can be transmitted from the remote part of the system (e.g. the subscribers' terminal in local digital reticulation systems). In most cases these constraints may be expressed in terms of the frequency weighted total power which is transmitted. If we define a weight function $H(f)$, then the weighted total power is constrained to be less than P_0 .

$$P_0 \geq 2 \int_0^\infty H(f)W(f)|S(f)|^2 df \quad (13)$$

For the case of power feed limitations, $H(f)=1$. For crosstalk interference into another system with equalizer $E_1(f)$, $H(f)$ is given by:

$$H(f) = A_0 \frac{f^2}{\alpha(f)} |E_1(f)|^2 \quad (14)$$

where A_0 is a constant depending on mean NEXT attenuation (Ref.5).

In either case, the constraint may be met by scaling $S(f)$ (i.e., by adjusting the transmit signal level):

$$S(f) = a S_1(f) \Rightarrow a^2 = \frac{P_0}{2 \int_0^\infty H(f)W(f)|S_1(f)|^2 df} \quad (15)$$

This constrain leads to an expression for \bar{N}_O .

$$\bar{N}_O = \frac{4I_p}{P_0 V_T^2} \int_0^\infty \left| \frac{D(f)}{S_1(f)G(f)} \right|^2 \frac{\alpha(f_0)}{\alpha(f)} df \cdot \int_0^\infty H(f)W(f)|S_1(f)|^2 df \quad (16)$$

This expression has the constraint incorporated, and is independent of the scale of the transmit pulse shaping $S_1(f)$.

4. COMPARISON OF PERFORMANCE MEASURES FOR A RANGE OF TRANSMIT PULSE WIDTHS

It is proposed that \bar{N}_O , when expressed in dB, should give a relative measure which is comparable to the NEXT Impulsive Noise Figure (Ref.1) for the same length of cable. The NEXT Impulsive Noise Figure $R_{IN}(f_0)$, referred to $f_0 = 1/2T$ say, is a measure of the susceptibility of a digital receiver to impulsive noise and is equal to the difference between the mean NEXT attenuation and the mean margin in dB (both over the ensemble of pair combinations) against a prescribed number of errors per event ϵ_{max} . It may be obtained from the properties of the disturbing event, the transmission path and the receiver properties as follows:

$$R_{IN}(f_0) = -20 \log_{10} \phi - 10 \log_{10} \left(\frac{\pi^2 f_0^2}{\alpha(f_0)} \right) + 2.5 \quad (17)$$

where ϕ is obtained from the expression for the required number of errors per event ϵ_{max} :

$$\epsilon_{max} = \frac{2V}{T} \int_0^\infty Q \left(\frac{V_T}{\phi r(t)} \right) dt \quad (18)$$

where the coding factor ν is the ratio of the number of errors to the times that the absolute value of the noise voltage exceeds V_T (equal to 3/4 for AMI), Q is the area in the upper tail of the standard normal probability density, and $r(t)$ is the normalized r.m.s. impulsive noise voltage.

$$r^2(t) = \int_0^{\infty} z^2(x,t) dx \quad (19)$$

where the Fourier transform of $z(x,t)$ is $Z(x,f)$.

$$Z(x,f) = j2\pi fV(f) E(f) e^{-2\gamma(f)x} \quad (20)$$

where $\gamma(f)$ is the cable propagation constant and $V(f)$ is the Fourier transform of the disturbing event ($j2\pi fV(f) = V_0$, the height of the step voltage disturbance, for the example considered).

That \bar{N}_0 provides a measure of relative impulsive noise performance for different transmit pulse shapes is demonstrated by comparison with the NEXT Impulsive Noise Figure in the following example. Consider a pulse shape $d(t)$ at the receiver decision point corresponding to a 100% raised cosine function in the frequency domain, with AMI detection.

$$D(f) = \frac{T}{2} \{1 + \cos(\pi fT)\} \quad (21)$$

$$W(f) = \frac{\sin^2(\pi fT)}{T} \quad (22)$$

$$V_T = 1/2 \quad (23)$$

The transmit pulse shape is rectangular and of width η symbol.

$$S_1(f) = \frac{\sin(\eta\pi fT)}{\pi f} \quad (24)$$

The total transmitted power is constrained to be less than P_0 ; hence $H(f) = 1$ in the constraint.

Since $|G(f)| = e^{-\alpha(f)\ell}$ for a length ℓ , the expression for \bar{N}_0 is:

$$\bar{N}_0 = \frac{I_p \eta}{P_0} \int_0^{1/T} \left[\frac{\{1 + \cos(\pi fT)\} (\pi fT)}{\sin(\eta\pi fT)} \right]^2 \frac{\alpha(f_0)}{\alpha(f)} e^{2\alpha(f)\ell} df \quad (25)$$

In order to obtain a valid comparison for the case of a constraint on the total transmitted power, the quantity

$$10 \log_{10} \left(\frac{\bar{N}_0 P_0 T}{I_p} \right)$$

is compared in Fig.4 with the NEXT Impulsive Noise Figure R_{IN} (1/2T) referred to one half of the line rate (for AMI code). R_{IN} (1/2T) is computed for two values of the expected number of errors per event ϵ_{max} which correspond to the typical range of this parameter in a system designed for a bit error ratio of the order of 10^{-7} . The comparison in Fig.4 is for 144 kbit/s transmission over 4 km of 0.4 mm polyethylene insulated copper pair cable. Because \bar{N}_0 provides only a relative measure of performance for the various pulse widths, both quantities in Fig.4 have been referred to the value at $\eta=1$. The variation with the pulse width η in the proposed model is in good agreement with the more exact R_{IN} . Both have optima at about $\eta = 0.75$, while remaining within 1 dB of the optimum for pulse widths between 0.5 and 1.0 symbol.

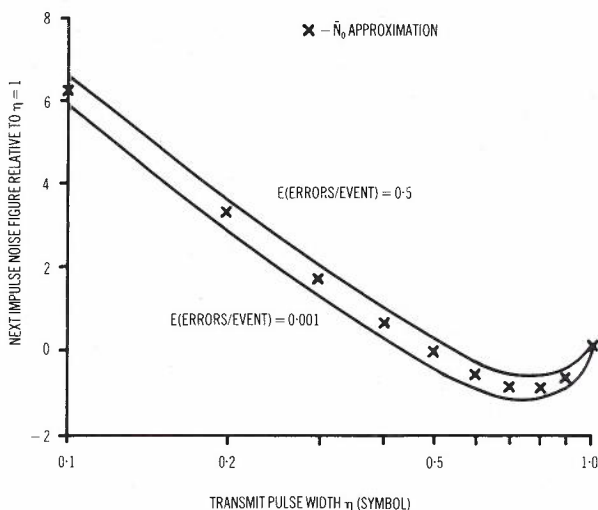


Fig. 4 - Variation of Impulsive Noise Performance with Transmit Pulse Width for AMI Code (Comparison of Total Energy Model, Normalized to the value at $\eta=1$, with NEXT Impulsive Noise Figure, R_{IN})

5. OPTIMIZATION OF TRANSMIT PULSE SHAPE FOR GIVEN RECEIVE PULSE SHAPE

For a given receive pulse shape $d(t)$, weighting function $H(f)$ and code w_i , the dependence of \bar{N}_0 on the transmit pulse shape is described by:

$$\bar{N}_0 \propto \int \frac{A(f)}{|S_1(f)|^2} df \int B(f) |S_1(f)|^2 df \quad (26)$$

For the case of 100% raised cosine received pulse shaping and a constraint on total transmitted power, $A(f)$ and $B(f)$ are as follows:

$$A(f) = \{1 + \cos(\pi fT)\}^2 \frac{\alpha(f_o)}{\alpha(f)} e^{2\alpha(f)l} \quad (27)$$

$$B(f) = W(f)T = \begin{cases} 1 & \text{for binary} \\ \sin^2 \pi fT & \text{for AMI} \\ \cos^2 \pi fT & \text{for duobinary} \end{cases} \quad (28)$$

In Fig.5 these are plotted over $(0, 2/T)$ for a 144 kbit/s system on 4 km of 0.4 mm polyethylene insulated copper pair cable. Inspections of these curves indicates the conditions under which \bar{N}_o is minimized. Any spectral components of $S_1(f)$ outside $(0, 1/T)$ are wasted in the sense that they contribute to the second integral and yet don't reduce the value of the first integral. Within $(0, 1/T)$ the optimum $S_1(f)$ should be large where $A(f)$ is large and small where $B(f)$ is large. A solution for the optimum is possible by applying the Rayleigh-Ritz method directly to (26). However a more elegant solution using Lagrange multipliers is preferred. This is based on the original expression (12) and the constraint equation (13). The resulting Euler-Lagrange equation, using $y = |S_1(f)|^2$, is:

$$\frac{\partial}{\partial y} \left(\frac{A(f)}{y} - \lambda B(f)y \right) = 0 \quad (29)$$

$$\Rightarrow y^2 = \frac{A(f)}{\lambda B(f)} \quad (30)$$

Since $S_1(f)$ is scale independent, the optimum transmit pulse shaping is given by:

$$|S_1(f)|^2_{opt} = \sqrt{\frac{A(f)}{B(f)}} = \left| \frac{D(f)}{G(f)} \right| \sqrt{\frac{\alpha(f_o)}{\alpha(f)W(f)H(f)}} \quad (31)$$

and the value of \bar{N}_o at the optimum is equal to:

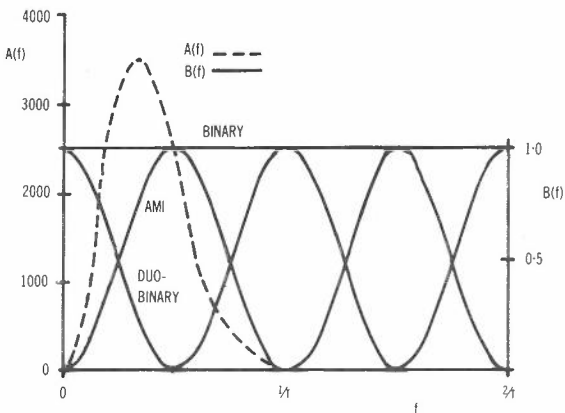


Fig. 5 - Factors in Integrals which affect Optimization of Transmit Pulse Shape (for 100% Raised Cosine Received Pulse Shape)

$$\bar{N}_{opt} = \frac{4l}{P_o T V_T^2} \left[T \int_0^{\infty} \left| \frac{D(f)}{G(f)} \right| \sqrt{\frac{\alpha(f_o)}{\alpha(f)}} W(f)H(f) df \right]^2 \quad (32)$$

For the case plotted in Fig.5, with binary code the optimum $S_1(f)$ is given by:

$$|S_1(f)|^2_{opt} = \{1 + \cos(\pi fT)\} \sqrt{\frac{\alpha(f_o)}{\alpha(f)}} \cdot e^{\alpha(f)l}, \quad 0 < f < \frac{1}{T} \quad (33)$$

For AMI code, the optimum is:

$$|S_1(f)|^2_{opt} = \frac{1 + \cos(\pi fT)}{\sin(\pi fT)} \sqrt{\frac{\alpha(f_o)}{\alpha(f)}} e^{\alpha(f)l}, \quad 0 < f < \frac{1}{T} \quad (34)$$

This contains an integrable singularity at $f=0$ and then approximates to linear roll-off from $0.1/T$ to $1/T$. The value of $10 \log_{10} (\bar{N}_{opt} P_o T / l_p)$ is 31.9 dB, which is only 0.5 dB smaller than for 0.75 width rectangular AMI code. Hence the optimum is fairly broad and the impulsive noise performance is not very sensitive to the shape of the transmit pulse.

For duobinary code, the optimum is:

$$|S_1(f)|^2_{opt} = \frac{1 + \cos(\pi fT)}{|\cos(\pi fT)|} \sqrt{\frac{\alpha(f_o)}{\alpha(f)}} e^{\alpha(f)l}, \quad 0 < f < \frac{1}{T} \quad (35)$$

This contains a singularity at $0.5/T$, and hence is difficult to realize.

For non-unity weighting functions $H(f)$ the optimization produces some interesting practical results. Consider the interference from the digital system into a subscriber carrier system with frequency bands at 36 to 44 kHz and 60 to 68 kHz.

$$H(f) = \begin{cases} a, & 36 \text{ kHz} < f < 44 \text{ kHz} \\ b, & 60 \text{ kHz} < f < 68 \text{ kHz} \\ 0, & \text{otherwise} \end{cases} \quad (36)$$

In this case there will be one constraint for each frequency band.

$$P_a \geq 2a \int_{36}^{44} W(f) |S(f)|^2 df$$

$$P_b \geq 2b \int_{60}^{68} W(f) |S(f)|^2 df \quad (37)$$

From (31), the optimum $|S_1(f)|^2$ is zero inside these bands and non zero (but arbitrary) outside these bands. This corresponds to removal of all frequency components within these bands from the transmitted signal of the digital system. Adequate performance in this situation might also be achieved by the choice of a transmit pulse shape which has very little energy in these bands (i.e., a near optimal solution).

6. OPTIMIZATION OF THE RECEIVE PULSE SHAPE

Because of the nonlinear operation required for the determination of eye opening in (16), the following analysis is restricted to those pulse shapes $d(f)$ without intersymbol interference. For these cases $D(f)$ satisfies the Nyquist criterion:

$$\sum_{n=-\infty}^{\infty} D(f - \frac{n}{T}) = T \tag{38}$$

This provides a constraint for the optimization of the expression for \bar{N}_{opt} in (32) with respect to the receive pulse shaping $D(f)$. This may be abbreviated to read:

$$\bar{N}_{opt}^{1/2} = \int_0^{\infty} |D(f)| C(f) df \tag{39}$$

where

$$C(f) = \frac{2}{V_T} \cdot \frac{1}{\sqrt{\frac{I_p}{P_o T}}} \cdot \frac{1}{|G(f)|} \cdot \sqrt{\frac{\alpha(f_o)}{\alpha(f)} W(f)H(f)} \tag{40}$$

Equation (38) ensures that $V_T = d(0) = 1$ for binary code and $V_T = \frac{d(0)}{2} = 1/2$ for AMI and duobinary codes.

If the constraint is expressed in integral form as:

$$\int_{-\infty}^{\infty} D(f) \sum_{n=-\infty}^{\infty} \delta(f - \frac{n}{T}) df = T \tag{41}$$

then the Euler-Lagrange equation from (39) and (41), assuming $y=D(f) \geq 0$ for all f , has no solution because

$$\frac{\partial}{\partial y} \{C(f)y - \lambda y \sum_{n=-\infty}^{\infty} \delta(f - \frac{n}{T})\} \neq 0 \tag{42}$$

It follows that the optimum for $D(f) \geq 0$ is not differentiable. It is possible that the optimum $D(f)$ is not positive for all f .

It is possible to obtain an optimum over the restricted class of $D(f)$ which have 100% raised cosine shaping ($0 < v < 1$).

$$D(f) = \begin{cases} T & , f < \frac{(1-v)}{2T} \\ \frac{T}{2} \{1 - \sin((\pi f T - \pi/2)/v)\} & , \frac{1-v}{2T} < f < \frac{1+v}{2T} \end{cases} \tag{43}$$

$$\frac{\partial D(f)}{\partial v} = \frac{T\pi}{2v^2} (fT - \frac{1}{2}) \cos \{(\pi f T - \pi/2)/v\} , \frac{1-v}{2T} < f < \frac{1+v}{2T} \tag{44}$$

$$\Rightarrow \frac{\partial \bar{N}_{opt}^{1/2}}{\partial v} = \frac{\pi T}{v^2 V_T} \sqrt{\frac{I_p}{P_o T}} \int_{\frac{1-v}{2T}}^{\frac{1+v}{2T}} (fT - 1/2) \cos((fT - \frac{1}{2})\pi/v) \cdot e^{\alpha(f)\ell} \sqrt{\frac{\alpha(f_o)W(f)H(f)}{\alpha(f)}} df \tag{45}$$

$$= \frac{\pi}{v^2 V_T} \sqrt{\frac{I_p}{P_o T}} \cdot \int_{-\frac{v}{2}}^{\frac{v}{2}} f' \cos(\frac{\pi f'}{v}) \cdot e^{\alpha(\frac{f'+1/2}{T})\ell}$$

$$\cdot \sqrt{\frac{\alpha(f_o)W(\frac{f'+1/2}{T})H(\frac{f'+1/2}{T})}{\alpha(\frac{f'+1/2}{T})}} df' \tag{46}$$

The location of the optimum depends on the form of the weight function $H(f)$. For $H(f)=1$ over the frequency range of the integral it is possible to show that the RHS of (46) is always positive. This occurs because the W, H and cosine terms are even functions of f' , while the f' term is an odd function; the remaining terms containing $\alpha(f)$ are larger at $f' > 0$ than at $-f'$, hence making the overall expression

positive. Since $\frac{\partial \bar{N}_{opt}^{1/2}}{\partial v}$ is always positive the optimum for $H(f)=1$ occurs at $v=0$.

$$D_{opt} = \begin{cases} T & , \quad f < 1/2T \\ 0 & , \quad f > 1/2T \end{cases} \quad (47)$$

This is also the optimum for many other $H(f)$

for which $\frac{\alpha(f_o)H(f)}{\alpha(f)} \cdot e^{\alpha(f)\ell}$

increases with increasing frequency over $(0, 1/2T)$.

Next it is shown that $D_{opt}(f)$ is also a local optimum in function space for $H(f)=1$.

Consider a function $D(f)$ defined on $(\frac{2m-1}{2T}, \frac{2m+1}{2T})$,

$$D(f) = D_m(f - \frac{m}{T}) \quad , \quad -\frac{1}{2T} < f - \frac{m}{T} < \frac{1}{2T} \quad (48)$$

and let D_m be a perturbation to the basic function $D_{opt}(f)$, so that in order to satisfy the constraint (38) we have:

$$D(f) = T - D_m(f) \quad , \quad -1/2T < f < 1/2T \quad (49)$$

Substitution in (39) yields,

$$\begin{aligned} \bar{N}_{opt}^{1/2} &= T \int_{-1/2T}^{1/2T} C(f)df - \int_{-1/2T}^{1/2T} D_m(f)C(f)df \\ &+ \int_{\frac{m}{T} - \frac{1}{2T}}^{\frac{m}{T} + \frac{1}{2T}} |D_m(f - \frac{m}{T})| C(f)df \end{aligned} \quad (50)$$

where the modulus sign is missing from $D_m(f)$ because it is a small perturbation of the positive $D_{opt}(f)$, ($D_m(f) < T$). Hence the change from the D_{opt} case is:

$$\Delta \bar{N}_{opt}^{1/2} = \int_{-1/2T}^{1/2T} \{ |D_m(f)| C(f + \frac{m}{T}) - D_m(f) C(f) \} df \quad (51)$$

Since $C(f)$ is always positive, any negative part of $D_m(f)$ results in a positive contribution to the integral. For positive parts of $D(f)$, it is only necessary to show that $C(f)$ increases with increasing frequency to show that their contribution to the integral is also positive. This is indeed true for $H(f)=1$, because of the rapid increase of $|G(f)|^{-1}$ with frequency. Since it is possible to make any function $D(f)$ by superposition of perturbations $D_m(f)$,

$m=\pm 1, \pm 2, \pm 3, \dots$, and each perturbation produces an increase in the impulsive noise energy at the decision point, we have shown that $D_{opt}(f)$ is a local optimum. It is also most likely to be the global optimum, for $H(f)=1$, over all pulse shapes $D(f)$ which satisfy the Nyquist criterion. Although the pulse shape $d_{opt}(t)$ would result in extreme sensitivity to the sampling times, it does provide a theoretical limit to the performance which could be achieved by systems with no ISI. It is unlikely that the introduction of intersymbol interference in $d(t)$ would result in better performance with a linear equalizer, since the optimum without ISI is already the minimum bandwidth solution.

7. RELATIVE IMPULSIVE NOISE PERFORMANCE FOR A RANGE OF LINE CODES AND PULSE SHAPES

In this section the approximate model presented in this paper is compared with the NEXT impulsive noise figure (Ref.1). These are compared on the basis of a constraint on total transmit power ($H(f)=1$), for 144 kbit/s continuous transmission over 4 km of 0.4 mm polyethylene insulated copper pair cable. The following approximations for the cable propagation constant, which are valid in the frequency range from 30 to 150 kHz, enable the integral of equation (16) to be computed.

$$\frac{\alpha(f_o)}{\alpha(f)} = \frac{1}{(fT)^{0.2} + (0.05)^{0.02}} \quad (52)$$

$$2\alpha(f)\ell = 8.75 (fT)^{0.2} \quad (53)$$

The values P_o of the power limit and I_o which defines the impulsive noise energy spectrum are removed to produce the quantity (in dB) $10 \log_{10} (\bar{N}_o P_o T / I_p)$ which indicates the relative merit of the various codes and pulse shapes.

The NEXT impulsive noise figure R_{IN} is referred to a frequency of 100 kHz and is for an expected number of errors per event $\epsilon = 10^{-3}$. It does not matter which frequency R_{IN} is referred to as only the relative merit of the various codes and pulse shapes is being considered here. Table 2 compares the two measures of performance for the three codes and several pulse shapes.

The consistent difference of about 30 dB between the last two columns of Table 2 shows that, for a given symbol rate, the total energy in the impulsive noise response at the decision point is a useful measure of relative impulsive noise performance. Comparison of practical pulse shapes with the optimum cases indicates that ordinary rectangular transmit pulses and 100% raised cosine receive pulses give performance within 3 dB of the respective optima for AMI and binary codes. It is also apparent that a penalty of about 6 dB is associated with

TABLE 2 - Summary of Computed Results for $H(f)=1$

CODE	TRANSMIT PULSE SHAPE $S(f)$	RECEIVE PULSE SHAPE $D(f)$	$10 \log_{10}$ of $\frac{\bar{N}_o P_o T}{I_o}$ (dB)	R_{IN} (100kHz) ($\epsilon=10^{-3}$) (dB)
BINARY	Optimum	Optimum	27.4	-
$W(f)T = 1$	Optimum	100% raised cosine (full width)	28.3	-
	Full width pulse	100% raised cosine (full width)	30.2	60.1
	WAL1	100% raised cosine (full width)	36.0	64.2
	WAL1	WAL1 2x1/2 width 100% raised cosine	37.7	68.9
AMI $W(f)T_2 = \sin^2(\pi f T)$	Optimum	Optimum	31.0	-
	Optimum	100% raised cosine (full width)	31.9	-
	0.75 width pulse	100% raised cosine (full width)	32.4	62.4
	full width pulse	100% raised cosine (full width)	33.2	63.5
WAL1	100% raised cosine (full width)	39.0	69.0	
DUOBINARY $W(f)T = \cos^2(\pi f T)$	Optimum	Optimum	27.8	-
	full width pulse	100% raised cosine (full width)	33.2	63.5
BINARY →AMI	WAL1 (BINARY)	100% raised cosine (full width, AMI)	37.2	66.8

NOTE: This case includes a delay by $T/2$ and add operation in the equalizer

the use of WAL1 transmit shaping, compared with full width transmitted pulses. Finally, it appears that the best performance, for practical pulse shapes, can be achieved with binary coding, and provided that dc restoration problems can be overcome in the receiver, binary transmission is preferred. Nonlinear (decision feedback) equalizers may be employed to provide further improvements in performance beyond the optima computed here.

8. CONCLUSIONS

The proposed total energy model for impulsive noise impairment provides a useful measure of relative merit for practical line codes and pulse shapes in local digital transmission systems. The simpler description, compared with the NEXT impulsive noise figure, provides the engineer with greater understanding of the relative merit of the different codes and pulse shapes. Comparison of practical pulse shapes with computed optimum pulse shapes

(with a constraint on total transmitted power) shows that there is little to be gained in optimizing the pulse shapes beyond those which are already used.

The analysis provides a link between compatibility and impulsive noise limitations to system performance, and provides the understanding necessary to optimize impulsive noise performance while satisfying constraints on crosstalk interference from the digital system into other types of system in the same cable. Given this understanding, it is important to identify the other systems

(and hence their $\frac{H(f)}{P_o}$ factors) which may be affected by the local digital reticulation systems. Similarly, detailed statistics of the crosstalk paths are required to define the statistics of the impulsive noise energy I_p and also the scale of $H(f)$; because the gain of the crosstalk path is effectively squared (in I_p and $H(f)$ terms) in the equation (16) for the normalized energy \bar{N}_o ,

the absolute impulsive noise impairment is very sensitive to this factor.

However, the main use of the total energy model is as a conceptual model and detailed analyses of impulsive noise performance should still be based on the NEXT impulsive noise figure (Ref.1).

9. REFERENCES

1. Potter, P.G., and Smith B.M., "Statistics of Impulsive Noise Crosstalk in Digital Line Systems on Multipair Cable", IEEE Trans. Comm., to be published.

2. Campbell, J.C., "The Crosstalk Interference from Primary Level PCM

Signals into other Services", Telecom Australia Research Laboratories Report 7290.

3. Campbell, J.C., "The Crosstalk Interference from Baseband Data Signals into other Systems and Services", Telecom Australia Research Laboratories Report 7364.

4. Duc N.Q., and Smith, B.M., "Line Coding for Digital Data Transmission", Australian Telecommunication Research, Vol 11, 1977, pp.14-27.

5. Gibbs A.J., and Addie R., "The Covariance of Near-End Crosstalk and its Application to PCM System Engineering in Multipair Cable", IEEE Trans. Comm. Vol. COM-27, 1979, pp. 469-477.



BIOGRAPHY

PHILIP G. POTTER received the B.E. and Ph.D. degrees in electrical engineering from Monash University, Australia, in 1974 and 1979 respectively.

Since joining the Research Laboratories of Telecom Australia in 1979, he has worked on various aspects of digital transmission in multipair cable, with particular emphasis on crosstalk and impulsive noise impairments in digital line systems. He is currently with Line and Data Systems Section, Telecom Australia Research Laboratories, Melbourne, Australia and is concerned with the application of systems for local digital reticulation in the Australian telephone network.

Echo Canceller Structures for Digital Loop Access Systems

F.G. BULLOCK

Telecom Australia Research Laboratories

This paper examines various echo canceller structures and adaptation algorithms intended to provide full duplex digital transmission for ISDN access over existing local loops. Basic echo cancellers and algorithms are reviewed, then the convergence speed and cancellation error distribution of various TDL, RAM and multiple-RAM cancellation filters, controlled by stochastic, sign and coarse-quantised algorithms are calculated for binary and ternary line codes. Combining a decision feedback equaliser and adaptive reference estimator with the echo canceller is discussed, the benefits including freer choice of line code and filtering (permitting reduced echo canceller size), equalisation of lines with bridged taps, and faster convergence.

KEYWORDS: Digital Echo Canceller, ISDN Basic Digital Loop Access, Decision Feedback Equaliser, Digital Adaption Filter, Sign Algorithm, Table Look Up Filter.

1. INTRODUCTION

During ISDN development, basic network access at 80 kbit/s or 160 kbit/s full duplex data rate is proposed for each ISDN customer over existing local loops. The most promising transmission techniques are echo cancellation and burst-mode (Refs.1,2). Echo cancellers at each end of the loop separate continuous two-way data signals by adapting precisely to the loop's echo response, whereas burst-mode equipment interleaves compressed bursts of data in each direction.

Full duplex base band echo cancellation offers lower line transmit signal frequencies than any other digital loop access technique. Thus it offers significantly greater service area penetration than other techniques, because of its lower sensitivity to impulsive and crosstalk noise. Burst-mode systems can achieve better penetration only if burst synchronisation between different loops is maintained throughout the service area (to avoid near end crosstalk), if impulsive noise levels are unusually low, and if other systems (e.g. primary rate digital line systems) are excluded from the cable being considered.

An echo canceller for data transmission is much less complicated than a voice echo canceller, because the data echo canceller's filters are driven by the transmitted data stream which has shorter wordlength (e.g. 1 or 2 bits/sample) than a linearly digitised voice signal. Digital loop access echo cancelling filters may also have fewer coefficients than those in long haul echo cancelling data modems.

Furthermore a local loop's characteristics scarcely change from call to call and therefore slow converging algorithms based on simple hardware can be used in conjunction with non-volatile memory which retains the coefficients between calls.

This paper describes the more promising digital loop access echo canceller structures, commencing with the basic structures of the echo cancelling filters and their convergence algorithms and proceeding to decision feedback equalisers and adaptive reference circuits.

Section 2 comments on the unusual problems caused by bridged taps (tees) in the Australian local network, and the potential benefits of combining a decision feedback equaliser with the echo canceller in this situation.

Sections 3,4 and 5 review a basic echo canceller with TDL (tapped delay line) filter and stochastic iteration algorithm (Refs.3,5,6,7). The analysis is then extended to RAM (random access memory table look up) and multiple RAM filters whose advantages include convergence under less stringent conditions than required by TDL filters, nonlinear echo cancellation and reduced power consumption.

Noting the requirement for digital realisation of the filters, the operation of various quantised amplitude algorithms is analysed in section 6. The RAM filter with sign algorithm and dither noise (Refs.4,8) is reviewed, followed by analysis of the zero forced sign algorithm (which operates with ternary line signals or with adaptive reference estimation, without dither noise). The convergence speeds and cancellation error noise distributions of both sign algorithms are calculated. The effect of coarse quantising on the stochastic

Paper received 6 December 1984.
Final revision 18 February 1985.

iteration algorithm is analysed for a RAM filter, readily explaining the error distributions obtained in Ref.3. This section is completed with a brief analysis of multiple-RAM and TDL filters with quantised amplitude algorithms.

Section 7 resumes the discussion of the benefits and methods of combining the echo canceller (EC) with the data receiver and with a decision feedback equaliser (DFE). This simultaneously simplifies the receiver, allows the echo tail to be shortened by high pass line filtering, and provides an equaliser for the forward echoes from bridged line taps. Extension of the DFE provides adaptive reference (AR) estimation, which improves the convergence speed of the canceller. Analysis of the DFE and AR, combined as discussed here, is a straightforward extension of the basic echo canceller analysis (Refs.5,6,7,8) except for the still outstanding problem of blind start-up convergence.

The preceding analyses are used to compare the convergence speeds of various EC-DFE-AR structures and algorithms in section 8.

2. NETWORK CONSTRAINTS

Some local loops, on which ISDN access is desired, have over 40 dB loss at 80 kHz. Thus to obtain a 20 dB margin over the residue, echo suppression of approximately 60 dB is required for satisfactory receiver noise margins.

Local pair cables have frequency and gauge dependent characteristic impedances, with a particularly large capacitive range below 40 kHz. A fixed line balance network will not match all cables, and may have only 14 dB return loss with some gauges at 40 kHz. The capacitive mismatch at low frequencies may cause echo impulse response tails with time constants as long as 0.1ms.

Local loops are constructed with mixed gauges, and the Australian network is one of few which have unused bridged taps and tails, which are difficult and expensive to remove. A bridged tap or tail produces a return echo at the point of tapping with 9.5 dB echo loss, subsequent forward and return echoes with 7 dB loss (plus twice the tap line loss) and 3.5 dB forward signal loss.

The return echoes may therefore be larger than those encountered in other networks, requiring greater output from the echo cancelling filter. The forward echoes may seriously degrade the receiver noise margin, and the start-up of the decision feedback equaliser required to cancel them is a matter requiring special consideration in the context of the Australian local network, in studies of both echo cancelling and burst-mode equipment.

The long echo impulse response tail, caused by capacitive mismatch, can be reduced by attenuating the low frequencies in the line signal spectrum and removing the resulting transmission distortion in a

decision feedback equaliser (see section 7). Alternatively a well balanced line code such as AMI or class 4 partial response could be used. However diphase code, while excellently balanced and producing very short echo impulse response tails, has its peak power spectral density at higher frequencies which reduces the crosstalk and noise sensitivity advantages of echo cancelling equipment in which it is used.

3. BASIC ECHO CANCELLER LAYOUT

A basic echo canceller consists of a conventional data transmitter and receiver, with the echo cancelling circuits functioning simply as a 4 wire to 2 wire converter. An important advantage of this configuration is the near absence of coupling between the cancelling circuits and the data transmitter and receiver.

The echo canceller (Figure 1) is a discrete time filter which samples the received digital signal and cancels the echo components at a multiple of the line transmission rate. Such oversampling is necessary to construct a continuous cancellation signal with the same bandwidth as the echo of the line signal, often twice the Nyquist frequency of the line signal (Ref.3). The canceller is phase locked to the transmitter so that its input sampler can be replaced with direct access to the binary or ternary coded transmitted symbols which can be processed by very simple multipliers in transversal delay line (TDL) filters (Refs. 3, 5-8) or which make acceptably short address words for random access memory (RAM) table lookup filters (Refs. 4,8).

4. BASIC ECHO CANCELLER EQUATIONS

These equations (Refs.3-7) describe the convergence of any one of the M sets of coefficients in a basic echo canceller oversampling at M times the line rate. Each set (or phase) converges similarly but independently to an estimate of the sampled echo impulse response, which differs from phase to phase because the uncancellable signal, consisting mainly of the received signal which is usually phase locked via the customer's transmission loop, has different power in each phase.

At sample times $t_m + kT$, where t_m is the constant offset of the mth sampling phase ($0 < m < M-1$) and where T is the transmit symbol period, the signal at the echo cancellation point and input to the receiver is (Refs.3,4)

$$r(k) = s(k) + e(k) - \hat{e}(k) + n(k) \quad (4.1)$$

where

$t_m + kT$ has been abbreviated to k
(m being arbitrary but fixed),

s(k) is the signal from the distant transmitter

e(k) is the echo from the local transmitter

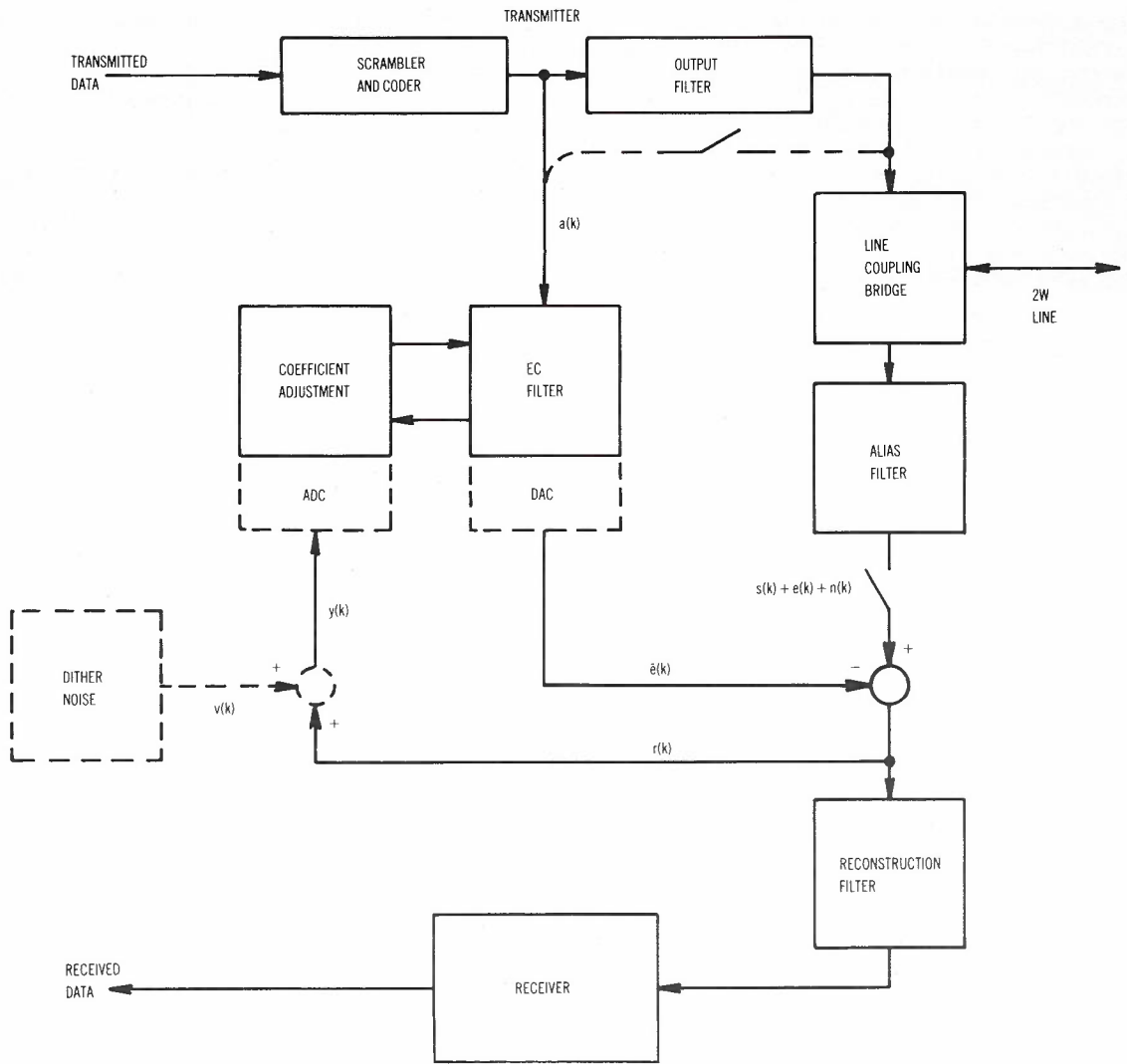


Fig. 1 - Basic Modem Layout

$\hat{e}(k)$ is the echo canceller's estimate of $e(k)$

$n(k)$ is line noise

The filter can cancel the initial and major part of the echo, $e_c(k)$, defined in equations 5.4 and 5.27 for TDL and RAM filters respectively. The uncancellable residue $e_u(k)$ consists of the tail of the echo beyond the time range of the filter's response and, in the case of a TDL filter, non linear components of the initial part of the echo. Hence

$$e(k) = e_c(k) + e_u(k), \quad (4.2)$$

The cancellation error is defined as:

$$z(k) = \hat{e}(k) - e_c(k) \quad (4.3)$$

and the mean excess noise power of the canceller is defined as:

$$\epsilon(k) = E \{z^2(k)\}, \quad (4.4)$$

which as a function of k describes the echo canceller's convergence.

The uncancellable signal is defined as:

$$u(k) = s(k) + e_u(k) + n(k) \quad (4.5)$$

whence:

$$r(k) = u(k) - z(k) \quad (4.6)$$

and the uncancellable signal power is defined as:

$$U = E \{u^2(k)\}, \quad (4.7)$$

The uncancellable signal power may differ before and after system phase lock is achieved but is usually considered to be constant.

The adaptation algorithms reduce but cannot eliminate the cancellation error because the only available control signal is the receiver input signal which also contains the interfering uncancellable signal. However if the data streams are adequately scrambled prior to transmission and if adaptation is relatively slow, the uncancellable signal and the cancellation error are uncorrelated and have zero mean. Then the mean receiver input power

$$R(k) = E \{r^2(k)\} \quad (4.8)$$

can be expressed as

$$R(k) = \epsilon(k) + U \quad (4.9)$$

and minimisation of the receiver input power by adjustment of the echo cancelling filter also minimises the excess noise power. Approximations of steepest descent (gradient) algorithms readily reduce the excess noise power to as small a value as required, with a corresponding characteristic convergence speed.

5. STOCHASTIC ITERATION ALGORITHM

5.1 Transversal Delay Line (TDL) Filter

This algorithm is discussed in many papers (Refs.3,5,7). A TDL filter (Fig.2) has a linear response

$$\hat{e}(k) = \underline{a}^T(k) \hat{\underline{g}}_k = \sum_{n=0}^{N-1} a(k-n) \hat{g}_k(n) \quad (5.1)$$

to the current and the last N-1 transmitted digits

$$\underline{a}(k) = (a(k), a(k-1), \dots, a(k-N+1))^T \quad (5.2)$$

where

$$\hat{\underline{g}}_k = (\hat{g}_k(0), \hat{g}_k(1), \dots, \hat{g}_k(N-1))^T \quad (5.3)$$

is the coefficient array of the TDL filter.

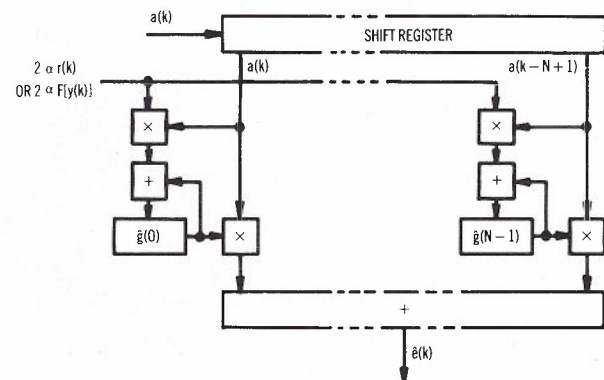


Fig. 2 - TDL Filter and Adaptation Control

It can be used to cancel the echo

$$e_c(k) = \underline{a}^T(k) \underline{g} = \sum_{n=0}^{N-1} a(k-n)g(n) \quad (5.4)$$

of a linear channel whose echo impulse response samples are the components of

$$\underline{g} = (g(0), g(1), \dots, g(N-1))^T \quad (5.5)$$

The transmitter output filter (in Fig.1) can include linear multilevel pulse shaping (e.g. AMI), while the echo canceller operates with binary input, but any nonlinear precoder must be outside the echo cancelling loop. Coders for nonlinear line codes must also be outside the echo cancelling loop.

The cancellation error (4.3) is now

$$z(k) = \underline{a}^T(k) (\hat{\underline{g}}_k - \underline{g}) = (\hat{\underline{g}}_k - \underline{g})^T \underline{a}(k) \quad (5.6)$$

If convergence is slow (i.e. if $\hat{g}_k \approx E\{\hat{g}_k\}$) and if a_k has zero mean and is uncorrelated with $u(k)$, then substituting 4.6 and 5.6 in 4.8 yields the mean receiver input power in the form

$$R(k) = E\{ (u(k) - z(k))^2 \} = (\hat{\underline{g}}_k - \underline{g})^T A (\hat{\underline{g}}_k - \underline{g}) + U \quad (5.7)$$

where

$$A = E\{ \underline{a}(k) \underline{a}^T(k) \} \quad (5.8)$$

Then if the transmitted digits are uncorrelated, matrix A reduces to $(1-P_0)I$ where

$$P_0 = P\{a_k = 0\} \quad (5.9)$$

is the probability of transmitting a zero digit when ternary transmission is used (for binary, $P_0=0$ and $A=I$). Then $R(k)$ is a simple quadratic function of the filter coefficients and differentiating yields

$$\underline{\text{grad}} R(k) = \left(\frac{\partial R(k)}{\partial \hat{g}_k(0)}, \dots, \frac{\partial R(k)}{\partial \hat{g}_k(N-1)} \right)^T \quad (5.10)$$

$$= 2(1-P_0) (\hat{\underline{g}}_k - \underline{g}) \quad (5.11)$$

showing that the gradient algorithm

$$\hat{\underline{g}}_{k+1} = \hat{\underline{g}}_k - 2 \alpha \underline{\text{grad}} R(k) \quad (5.12)$$

directly reduces the coefficient errors in this case.

Differentiating 5.7 before taking the mean yields

$$\text{grad } R(k) = -2E\{\underline{a}(k)r(k)\} \quad (5.13)$$

in terms of the available control signals, and substitution produces the correlation algorithm

$$\hat{\underline{g}}_{k+1} = \hat{\underline{g}}_k + 2\alpha E\{\underline{a}(k)r(k)\} \quad (5.14)$$

This is approximated by the stochastic iteration algorithm

$$\hat{\underline{g}}_{k+1} = \hat{\underline{g}}_k + 2\alpha a(k)r(k) \quad (5.15)$$

which requires no separate correlator memories and which can adjust the filter coefficients at every line symbol period. Substitution of $r(k)$ (from 4.6 and 5.6) and of $\alpha_0 = (1-P_0)\alpha$ yields a recurrence relation for the mean error of each coefficient (assuming $\hat{\underline{g}}_k$ and $\underline{a}(k)$ are independent and $\underline{a}(k)$ has zero mean and is uncorrelated with $u(k)$):

$$E\{\hat{\underline{g}}_{k+1} - \underline{g}\} = (1-2\alpha_0)E\{\hat{\underline{g}}_k - \underline{g}\} \quad (5.16)$$

which converges to zero mean error of each coefficient if $0 < \alpha < 1/(1-P_0)$.

However, stronger conditions are required for convergence of the mean excess noise power. If $\hat{\underline{g}}_{k+1}$ and \underline{a}_{k+1} are independent, substituting 5.6 and 5.8 in 4.4 yields

$$\epsilon(k+1) = E\{(\hat{\underline{g}}_{k+1} - \underline{g})^T A(\hat{\underline{g}}_{k+1} - \underline{g})\} \quad (5.17)$$

Now assuming that the transmitted digits are independent and have zero mean, note that

$$E\{\underline{a}^T(k)\underline{a}(k)\} = N(1-P_0) \quad (5.18)$$

and

$$E\{\underline{a}(k)\underline{a}^T(k)\underline{a}(k)\underline{a}^T(k)\} = ((1-P_0) + (N-1)(1-P_0)^2)I \quad (5.19)$$

and substituting first 5.15 then 4.6 and 5.6 in 5.17, rearranging assuming $\underline{a}_k, \hat{\underline{g}}_k$ and $u(k)$ are independent, and finally substituting 5.18 and

5.19 yields the recurrence relation for the mean excess noise power:

$$\epsilon(k+1) = (1-4\alpha_0 + 4\alpha_0^2 (N + \frac{P_0}{1-P_0}))\epsilon(k) + 4\alpha_0^2 NU \quad (5.20)$$

This converges if $0 < \alpha < 1/(N(1-P_0) + P_0)$ and can then be solved as

$$\epsilon(k) - \epsilon(\infty) = (1-4\alpha_0 + 4\alpha_0^2 (N + \frac{P_0}{1-P_0}))^k \times (\epsilon(0) - \frac{\alpha_0 NU}{1-\alpha_0 (N + \frac{P_0}{1-P_0})}) \quad (5.21)$$

where

$$\epsilon(\infty) = \frac{\alpha NU(1-P_0)}{1-\alpha(N-(N-1)P_0)} \quad (5.22)$$

$$\approx \alpha NU(1-P_0) \quad \text{if } \alpha \text{ is small.} \quad (5.23)$$

Convergence of $\epsilon(k) - \epsilon(\infty)$ is exponential, proceeding at approximately

$$17\alpha(1-P_0) = 17\epsilon(\infty)/NU \text{ dB/line symbol period.} \quad (5.24)$$

If there is any correlation between the transmitted digits, there are non zero off-diagonal terms in the matrix A and $R(k)$ (5.7) is no longer a simple quadratic function of the filter coefficients. Consequently $-\text{grad } R(k)$ is not necessarily in the direction of steepest descent and the filter's convergence may be severely impeded. However, note that adaptation problems caused by correlation introduced solely by linear pseudo-ternary coding (e.g. AMI, class 4 partial response) can be avoided by tapping the data stream $\underline{a}(k)$ from the transmitter before the linear conversion of binary to ternary digits. Although the number of filter taps must be increased according to the duration of the code's intersymbol interference, filter convergence is improved and the complications of ternary digit manipulations are avoided also.

5.2 RAM Table Look Up Filter

The N transmitted digits which are input to a TDL filter can alternatively be used to address a random access memory which stores the echo estimates in a function table (Fig.3) (Refs.4,8). The echo estimates:

$$\hat{\epsilon}(k) = \hat{G}_k(\underline{a}(k)) \quad (5.25)$$

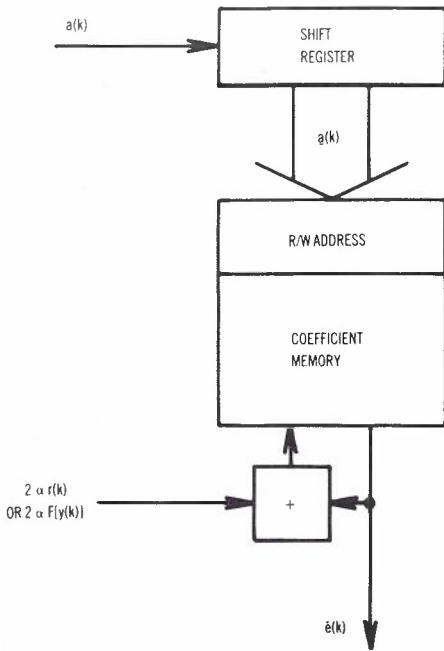


Fig. 3 - Table Lookup Filter (1-RAM)

can cancel the echo

$$e_c(k) = \underline{a}^T(k) \underline{g} \quad (5.26)$$

of a linear channel and can compensate for nonlinearities with short memory in the transmitter, the echo path or in the filter's own output circuit, in which case the cancellable echo is written

$$e_c(k) = G(\underline{a}(k)) \quad (5.27)$$

Nonlinearities which can be compensated by this filter, but usually not by a TDL filter, are transmitted pulse asymmetries, nonlinearities in the filters and AD converters (if any) in the echo path, and monotonic nonlinearities in the cancellation loop (e.g. in a DA converter).

Nonlinearities with long memory, for example nonlinear pseudoternary encoders or binary precoders, must remain outside the echo cancelling loop.

Another advantage of this type of filter over TDL filters is the reduced arithmetic load, power consumption and complexity when the address length N is small. However, the size and convergence time of a table lookup filter grow exponentially with the address word length, effectively restricting the choice of line code to one which has a very short echo impulse response tail, that is a code which has good DC balance and little low frequency spectral power. Diphase code has been used (Ref.4), at the expense of reduced crosstalk and impulse noise immunity, and binary code has been used with a 2-tap TDL transmit filter designed to reduce the echo impulse response duration

(implying that the line code resembles a balanced partial response code) (Ref.8).

Each coefficient in a table lookup filter adapts similarly but independently and it is sufficient to discuss the adaptation of an arbitrary coefficient $\hat{G}_K(a'(k))$ at successive random occurrences of its address a' , simply indexed by $K = 1, 2 \dots$ in the discussion.

The cancellation error for the fixed address a' is now

$$z(K) = \hat{G}_K - G \quad (5.28)$$

and the expression

$$R(K) = E\{(u(K)-z(K))^2\} = (\hat{G}_K - G)^2 + U \quad (5.29)$$

for the mean receiver input power is obtained assuming only that the cancellation error and the uncancellable signal are uncorrelated and have zero mean and that G_K is changing slowly (i.e. $\hat{G}_K = E\{\hat{G}_K\}$). Differentiation yields

$$\frac{\partial R(K)}{\partial \hat{G}_K} = 2(\hat{G}_K - G) = -2E\{r(K)\} \quad (5.30)$$

and, as before, the gradient algorithm for minimisation of the cancellation error power directly reduces the cancellation error and can be approximated by the stochastic iteration algorithm

$$\hat{G}_{K+1} = \hat{G}_K + 2\alpha r(K) \quad (5.31)$$

This algorithm is performed by the structure shown in Figure 3, with only one addition per symbol period, whereas a TDL filter of the same size normally adds N times per symbol period to adjust its coefficients and N times to form each output sample.

The recurrence relations

$$E\{z(K+1)\} = (1-2\alpha) E\{z(K)\} \quad (5.32)$$

and

$$E\{\epsilon(K+1)\} = (1-4\alpha+4\alpha^2) E\{\epsilon(K)\} + 4\alpha^2 U \quad (5.33)$$

are easily obtained, again assuming only that the uncancellable signal and the cancellation error are uncorrelated and have zero mean. Convergence occurs if $0 < \alpha < 1$ when

$$E\{\epsilon(K)\} = (1-4\alpha+4\alpha^2)^K \left(E\{\epsilon(0)\} - \frac{\alpha U}{1-\alpha} \right) + \frac{\alpha U}{1-\alpha} \quad (5.34)$$

As a result of the less stringent convergence conditions, RAM filters can be used with non linear pseudo ternary line codes (originating in the precoder in Fig.1).

In a filter with address word length N, each utilised address occurs with equal probability x^{-N} (where x is the number of transmitted levels) if the transmitted digits are independent and identically distributed (note that memories addressed by decoded ternary words are usually not fully utilised). The mean excess noise power from the entire filter at each line symbol period is then

$$\epsilon(k) = (1 - 4\alpha + 4\alpha^2)^{kx^{-N}} \left(\epsilon(0) - \frac{\alpha U}{1-\alpha} \right) + \frac{\alpha U}{1-\alpha} \quad (5.35)$$

which converges to:

$$\epsilon(\infty) = \frac{\alpha U}{1-\alpha} \quad (5.36)$$

at approximately

$$17\alpha x^{-N} = 17\epsilon(\infty) x^{-N} / U \text{ dB/line symbol period.} \quad (5.37)$$

After convergence, all coefficients (of the same phase in an over-sampling echo canceller) have the same mean excess noise power. Therefore unequal probabilities of occurrence of the address words, or transmitted digit dependence, merely slow the convergence of part of the memory and cause no other performance degradation, whereas a TDL filter may not converge correctly under these conditions.

5.3 Multiple RAM Table Look Up Filter

The exponential dependence of filter size and convergence time on the address word length N can be overcome by dividing the address into P parts which address P separate RAMs (Fig.4). The outputs are added (still with a lower arithmetic load than in a TDL filter) to form the echo estimates

$$\hat{e}(k) = \sum_{p=0}^{P-1} \hat{G}_{p,k} (a_{\sim p}(k)) \quad (5.38)$$

where the a_p are the parts of the filter input address a . These estimates can cancel the echoes from a linear channel, and if the first partial address word is long enough to include all relatively large components of the echo, this filter can compensate for mild nonlinearities in the transmitter, echo path or filter output as before.

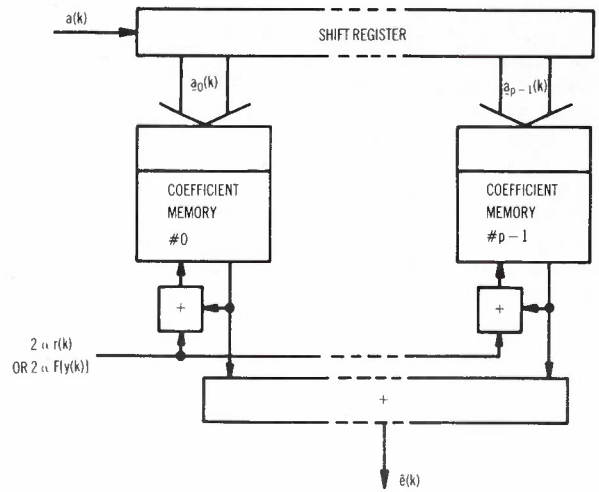


Fig. 4 - Multiple RAM Table Lookup Filter and Adaptation Control

The adaptation of one coefficient $\hat{G}_{p',k}$ in the p'th RAM, at successive occurrences of its partial address $a_{p'}$ is indexed by $K = 1, 2, \dots$ in the following discussion. The stochastic iteration algorithm is now

$$\hat{G}_{p',K+1} = \hat{G}_{p',K} + 2\alpha r(K) \quad (5.39)$$

or

$$z_{p',(K+1)} = z_{p',(K)} + 2\alpha(u(K) - z(K)) \quad (5.40)$$

$$= z_{p',(K)}(1 - 2\alpha) + 2\alpha u_{p',(K)} \quad (5.41)$$

where

$$z_{p',(K)} = \hat{G}_{p',K} - G_{p'} \quad (5.42)$$

is the cancellation error of the p'th RAM, and

$$u_{p',(K)} = u(K) - \sum_{p \neq p'} z_p(K) \quad (5.43)$$

is uncancellable by the p'th RAM.

The recurrence relationship for the mean of this coefficient's error is:

$$E\{z_{p',(K+1)}\} = E\{(1 - 2\alpha)z_{p',(K)} - 2\alpha \sum_{p \neq p'} z_p(K)\} \quad (5.44)$$

which shows considerable interference from the coefficients in the other RAMs. This interference ceases for the stationary solution

$$E\{z(\infty)\} = \sum_{\text{all } p} E\{z_p(\infty)\} = 0 \quad (5.45)$$

which can be reached while each RAM holds a non-zero mean error provided that the sum of these mean errors is zero. Typically this occurs in echo cancellers which do not reset their memories before adaptation. The dynamic range of each RAM in such cancellers need not exceed that required to store echo estimates with zero mean, provided that saturating arithmetic is used in the adaptation adders. However the output adders must have $\log_2 P$ bits over-range capacity to handle partial sums without error.

Because of the non-zero mean, it is appropriate to discuss the recurrence of the variance of the error which is:

$$\text{var}\{z_p, (K+1)\} = E\{z_p^2, (K+1)\} - (E\{z_p, (K+1)\})^2 \tag{5.46}$$

$$= (1-4\alpha)\text{var}\{z_p, (K)\} + 4\alpha^2 \text{var}\{z(K)\} + 4\alpha^2 U \tag{5.47}$$

assuming that the partial addresses are independent and therefore the corresponding echoes are uncorrelated, that the cancellable and uncancellable signals are uncorrelated and that the uncancellable signal has zero mean. This equation also shows interference from the other RAMs, but assuming that all coefficients are converging similarly, then

$$\text{var}\{z(K)\} \approx P \text{var}\{z_p, (K)\} \tag{5.48}$$

and

$$\text{var}\{z(K+1)\} \approx (1-4\alpha+4P\alpha^2)\text{var}\{z(K)\} + 4\alpha^2 PU. \tag{5.49}$$

The filter converges if $0 < \alpha < 1/P$, to mean excess noise

$$E\{z^2(\infty)\} = \epsilon(\infty) = \text{var}\{z(\infty)\} = \frac{\alpha PU}{1-\alpha P} \tag{5.50}$$

at approximately $17\alpha x^{-N/P} \approx 17\epsilon(\infty)x^{-N/P}/PU$ db per line symbol period. $\tag{5.51}$

6. ALGORITHMS WITH AMPLITUDE QUANTISATION

Digital coefficient storage is required to avoid the drifting and adaptation errors which would occur with analogue storage. Other parts of the canceller may be digitalised for economy. Digital wordlengths and DAC and ADC locations must be chosen with regard to their effect on echo canceller cost and performance.

The required resolution of the DACs and ADCs is determined by their quantising noise. The coefficient memory must have finer resolution, matching the convergence increments.

The feedback constant is usually chosen so that multiplication is simply a bit shift operation.

ADCs have higher cost functions than DACs, therefore analogue echo cancellation is preferred, with a fine resolution DAC at the output of the echo cancelling filter as shown in Figure 1. If a digital receiver is used, AGC at the input to the ADC can reduce the ADC's dynamic range requirement, and the digitised signal can be used for echo canceller adaptation provided the feedback constant is adjusted to cancel the AGC in the adaptation loop.

If the adaptation circuit's ADC is separate from the receiver (as in Fig.1) coarse error amplitude quantisation can be used to reduce the ADC or coefficient wordlength. In the extreme, a sign detector is used, resulting in the sign algorithm. However these techniques produce convergence control signals which are coarse step or stair functions of the echo cancellation error, which consequently executes unacceptable random walks. Continuous variation of the control signals is obtained by adding a uniformly distributed dithering noise signal (random reference noise) to the error signal input to the ADC (Refs.3,4,8), resulting in a normal distribution of cancellation errors with acceptable power.

Such a dither noise generator is shown in Fig.1. When algorithms using it are discussed, the receiver input signal $r(k)$, its uncancellable component $u(k)$ and the cancellation error $z(k)$ are defined as before (4.1, 4.3, 4.5), $v(k)$ is the dithering noise signal,

$$w(k) = u(k) + v(k) \tag{6.1}$$

is the uncancellable signal input to the adaptation circuit, and

$$y(k) = r(k) + v(k) \tag{6.2}$$

$$= w(k) - z(k) \tag{6.3}$$

is the input signal to the adaptation circuit.

The dither noise signal is uniformly distributed over the range $\pm a$, and in practice can be a sampled low frequency triangular waveform.

Dither noise is not required with the sign algorithm when ternary line signals are used, or when adaptive reference cancellation is used (see Section 7). In these cases the stepped convergence control signal changes sign at zero cancellation error, forcing the error to a narrow geometric distribution.

6.1 RAM Table Look up Filter

The stochastic iteration algorithm (5.31) for a single RAM filter is now replaced by:

$$\hat{G}_{K+1} = \hat{G}_K + 2\alpha F(y(K)) \quad (6.4)$$

or

$$z(K+1) = z(K) + \Delta z(K) \quad (6.5)$$

where

$$\Delta z(K) = 2\alpha F(w(K) - z(K)) \quad (6.6)$$

and where $F(y)$ is the appropriate finite precision amplitude quantisation function.

The recurrence relationship for the mean cancellation error is:

$$\overline{z(K+1)} = \overline{z(K)} + \overline{\Delta z(K)} \quad (6.7)$$

and the recurrence relationship for the mean squared cancellation error is:

$$\overline{z^2(K+1)} = \overline{z^2(K)} + 2\overline{z(K)\Delta z(K)} + \overline{\Delta z^2(K)} \quad (6.8)$$

both of which can be solved when the statistics of w and the form of $F(y)$ are known.

After convergence, the cancellation error distribution is typically binomial (asymptotically normal) or modified geometric (flatter than normal), depending on F and w . Noting that z is quantised and assuming $z(K) = jq$ where j is integral, the distribution is obtained by describing $z(K)$ as a Markov process with transition probabilities

$$p_{ij} = P\{z(K+1) = iq | z(K) = jq\} = P\{\Delta z = iq - jq\} \quad (6.9)$$

which in matrix form is

$$p_z(K+1) = \{p_{ij}\} p_z(K) \quad (6.10)$$

The stationary solution, i.e. the solution of

$$\{p_{ij} - \delta_{ij}\} p_z(\infty) = 0 \quad (6.11)$$

is described for the simpler cases.

6.1.1 Sign Algorithm. In this algorithm the finite precision law is the slicing function

$$2\alpha F(y) = q \text{ sign}(y) \quad (6.12)$$

and the transition probabilities are

$$P\{\Delta z = \pm q\} = P\{w > z\} \quad (6.13)$$

6.1.1.1 Binary Signalling. The two echo cancellers on a loop are normally synchronised, hence the samples $s(K)$ of the far end signal have amplitude $\pm r$ with equal probabilities $P\{s = \pm r\} = 0.5$, where the sampled received eye opening is $2r$.

If there is no uncancellable echo, intersymbol interference and line noise, and no dither noise, the distribution of the uncancellable signal is the same, i.e. $P\{w = \pm r\} = 0.5$. Then the transition probabilities (6.13) are constant and equal i.e. $P\{\Delta z = \pm q\} = 0.5$ if $|z(K)| < r$ and the cancellation error follows a random walk bounded by the received eye opening. If there is any bias in the received data stream, the transition probabilities are constant but unequal and the cancellation error is confined to a region near one side of the eye opening. Both these results are unsatisfactory.

Adding uniformly distributed dither noise $v(k)$ of peak to peak amplitude $2a$ (greater than the eye opening $2r$) distributes the uncancellable signal, i.e. $p(w) = 1/2a$ if $|w| < (a-r)$ (Fig.5). Now the transition probabilities vary continuously:

$$P\{\Delta z(K) = \pm q\} = .5 \mp z(K)/2a; (|z| < a-r) \quad (6.14)$$

and the mean excess noise power can be reduced (Ref.4).

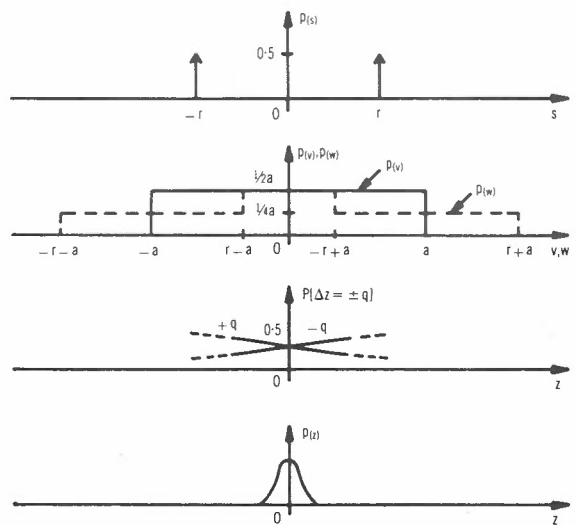


Fig. 5 - Sign Algorithm with Dither Noise

To solve the recurrence relations of the cancellation error, assume that the ensemble of echo estimates (for a given memory address) all start at a given value $z(0)$ and converge slowly so that

$$z(K) \approx \overline{z(K)} \quad (6.15)$$

TABLE 1 - Tail Areas of Modified Geometric Distribution

n	P{z > nσ _z }		Q(n) (Normal)
	P ₀ = .5 (AMI)	P ₀ = .25 (3B-2T)	
1	.11	.14	.16
3	.0037	.0067	.001
5	1.5 × 10 ⁻⁴	3.1 × 10 ⁻⁴	3 × 10 ⁻⁷
8	1.9 × 10 ⁻⁶	5.3 × 10 ⁻⁶	-
11	2.3 × 10 ⁻⁸	5.3 × 10 ⁻⁸	-

Initial convergence is approximated by the stochastic iteration algorithm. Finally, if there is no random reference noise, the uncancellable signal w takes the values ±r, the coefficient transition probabilities

$$P\{\Delta z = NQ\} = P\{(N-1/2)Q < w-z < (N+1/2)Q\} \tag{6.38}$$

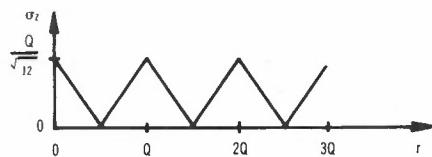
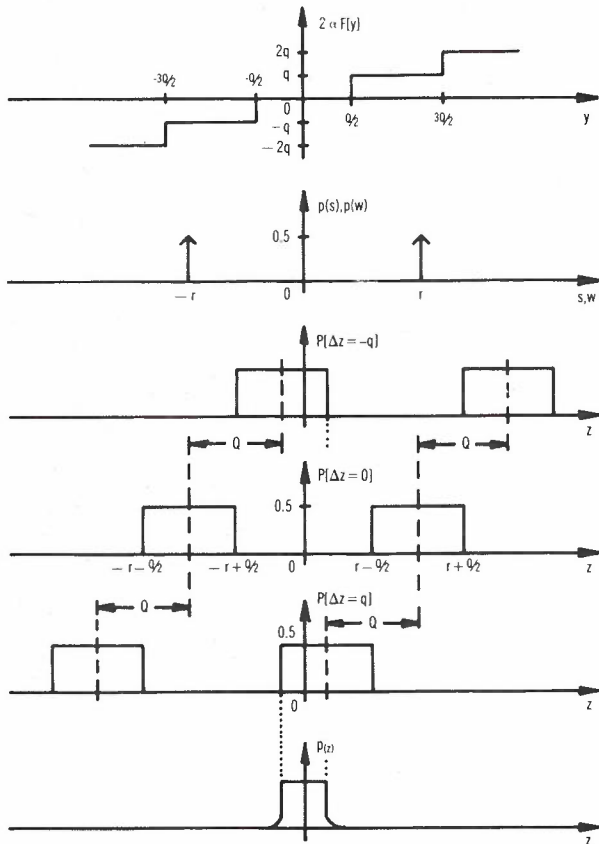


Fig. 7 - Coarse Quantised Algorithm Without Dither Noise

are step functions of the cancellation error and a random walk occurs (Fig.7). The walk is limited by the minimum distance between the discrete values of the sampled received signal and the steps in the quantising function. The limits and the RMS amplitude of the walk are therefore cyclic functions of the received binary signal amplitude r and the quantising increment Q, as illustrated in Fig.7 (and in Ref. 3 on log scales). The random walk is undesirable because its amplitude depends cyclically on the received signal amplitude, i.e. on the line length, and is usually excessive. Similar random walks occur even with ternary signals, because the coarse quantising function has a zero (or dead zone) for $-Q/2 < y < Q/2$.

Stable operation is obtained by adding uniform dither noise v with peak to peak amplitude 2a which is greater than the quantising increment Q, distributing the uncancellable signal w as shown in Fig.8. Now two or more of the transition probabilities (6.38) vary continuously with the cancellation error, preventing random walks. Fig. 8 shows the transition probabilities for typical signal, quantising and dither amplitudes (note the use of symmetry to reduce the number of graphs). An approximate analysis of the algorithm is presented below.

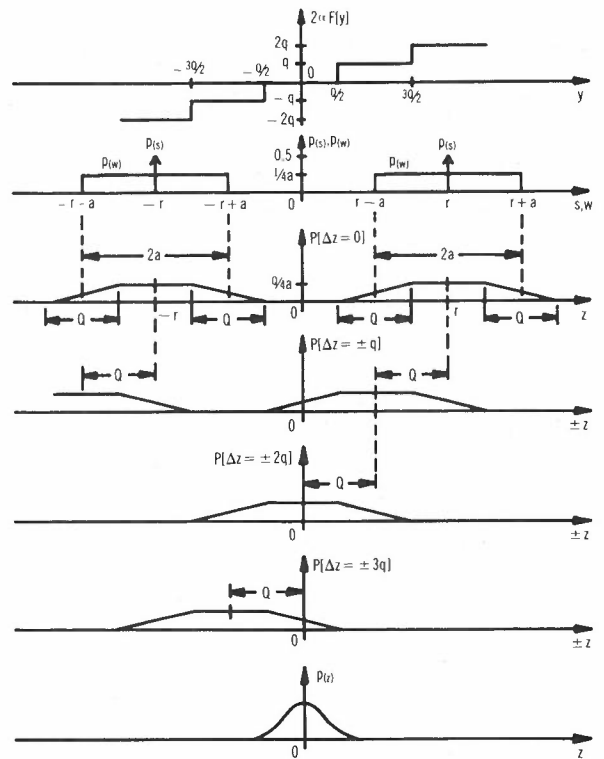


Fig. 8 - Coarse Quantised Algorithm with Dither Noise

The transition probability matrix is difficult to write and solve because the number of non-zero diagonals depends on the amplitudes of the received signal and the dithering signal, even for small cancellation errors. However the non-zero elements furthest from the leading diagonal of the matrix (i.e. the probabilities of $\max|\Delta z|$) are linearly dependent on small cancellation errors (e.g.

$P\{\Delta z = \pm 3q\}$ on Fig.8). This is similar to equation 6.25 (for the sign algorithm with dither noise) whose solution is a binomial distribution. Thus the excess noise of the coarse-quantised algorithm, whose RMS error usually exceeds $\max |\Delta z|$, can be usefully approximated by a binomial or normal distribution.

The excess noise power itself can be found more easily from the recurrence relation for the mean squared error (6.8), although there are still many forms of the expression, depending on the amplitudes of the received and dithering signals. The general form is

$$\overline{z^2(K+1)} = \overline{z^2(K)} (1-R) + C \quad (6.39)$$

where

$$R = -2\overline{z(K)\Delta z(K)} / \overline{z^2(K)}$$

and

$$C = \overline{\Delta z^2(K)}$$

whence

$$\sigma_z^2 = \overline{z^2(\infty)} = \frac{C}{R} = -\frac{\overline{\Delta z^2(K)} \overline{z^2(K)}}{2\overline{z(K)\Delta z(K)}} \quad (6.40)$$

and the rate of convergence of a filter with N-digit address lengths (radix x) is approximately

$$4.3Rx^{-N} = -4.3 \frac{\overline{2z(K)\Delta z(K)}}{\overline{z^2(K)}} x^{-N} \text{ dB/line symbol period.} \quad (6.41)$$

Approximate values of the parameters are obtained by further inspection of Fig.8. Assuming $z(K) = z(K)$,

$$\overline{2z(K)\Delta z(K)} \approx 2z(K) \sum_{n=-\infty}^{\infty} nqP\{\Delta z(K) = nq\}. \quad (6.42)$$

Only 4 terms contribute if $|z(K)|$ is small, so this reduces to

$$\overline{2z(K)\Delta z(K)} = \frac{2z^2(K)\alpha}{a} (F(r-a) - F(r+a)) \quad (6.43)$$

and linearising $F(y)$, i.e. putting $F(r-a) - F(r+a) \approx -2a$, yields

$$\overline{2z(K)\Delta z(K)} \approx -4z^2(K)\alpha. \quad (6.44)$$

Again linearising $F(y)$, and noting that the uncancellable noise power $u^2 \approx r^2$, and using 6.6, 6.3,

$$\overline{\Delta z^2(K)} \approx 4\alpha^2 \overline{y^2} \approx 4\alpha^2 (\overline{u^2} + \overline{v^2}). \quad (6.45)$$

These approximations yield

$$\sigma_z^2 = \overline{z^2(\infty)} = \alpha (\overline{u^2} + \overline{v^2}) \quad (6.46)$$

and rate of convergence $\approx 17 \alpha x^{-N}$ dB/line symbol period.

This is similar to the stochastic iteration algorithm, but performance is reduced because the dithering noise is added to the uncancellable noise and a smaller feedback coefficient α must be used.

6.2 Multiple RAM Table Look Up Filter

As before, the potentially long convergence time of a single RAM filter can be reduced by dividing the filter into P parts. The stochastic iteration algorithm for any particular coefficient in a multiple RAM filter (5.39, 5.40) is now replaced by

$$\hat{G}_{p1, K+1} = \hat{G}_{p1, K} + 2\alpha F(y(K)) \quad (6.47)$$

or

$$\Delta z_{p1, K} = 2\alpha F(w(K) - z(K)) \quad (6.48)$$

Adjustments are made at each random occurrence of this coefficient's address word, and there is interference from all the coefficient errors in the other RAMs, also being adjusted at mutually uncorrelated times. Initial convergence of filters using the sign algorithm may be retarded by the interference, which increases the dithering noise power. After convergence, non zero mean errors can remain in each RAM but cause zero mean error at the filter output. Assuming all coefficients converge similarly, the filter's excess noise is P times the excess noise of each RAM.

The sign algorithm with binary signalling and a dither noise generator finally converges with excess noise power less than, and controlled by, the dither noise generator, i.e.

$$\overline{z^2(\infty)} = Paq/2. \quad (6.49)$$

Similarly, the coarse quantised algorithm's final convergence is controlled by the dither generator, hence

$$\overline{z^2(\infty)} = P\alpha (\overline{u^2} + \overline{v^2}). \quad (6.50)$$

The zero driven sign algorithm's final convergence is altered by the multiple RAM

noise, which spreads the central (zero) component of the received signal distribution. This may increase the excess noise power by more than the number of RAMs, i.e. (from 6.36)

$$\overline{z^2(\infty)} > Pq^2/2P_0^2 \quad (6.51)$$

but may also cause small errors to be more normally distributed, moderating the increased width of the modified geometric distribution obtained with one RAM.

6.3 TDL Filter

The algorithm for this filter is

$$\hat{g}_{k+1} = \hat{g}_k + a(k)2\alpha F(y(k)) \quad (6.52)$$

Considering only the n' th coefficient, and substituting 6.3, 5.6,

$$\Delta \hat{g}_k(n') = a(k-n')2\alpha F(w(k) - \sum_{n=0}^N a(k-n)(\hat{g}_k(n) - g(n))) \quad (6.53)$$

Now noting that $a(k-n') = -1, 0, +1$ only,

$$\Delta \hat{g}_k(n') = \begin{cases} 0 & \text{if } a(k-n') = 0 \\ 2\alpha F(w_n'(k) - (\hat{g}_k(n') - g(n'))) & \text{if } a(k-n') = \pm 1 \end{cases} \quad (6.54)$$

where

$$w_n'(k) = a(k-n')(w(k) - \sum_{n \neq n'} a(k-n)(\hat{g}_k(n) - g(n)))$$

is uncorrelated with the n' th coefficient error if the transmitted digits are independent and uncorrelated with the received digits or with the dithering noise.

This is similar to the algorithm for a multiple RAM table look up filter, except that the interference between the taps now has random sign and non zero mean errors will not occur, and adjustments are made more frequently but only for every non-zero transmitted digit. The discussion of excess noise from the TDL filter follows from the discussion of the multiple RAM filter by substitution of N for P to account for the number of noise components, and multiplication of the noise power by $(1-P_0)$ because a transmitted ternary zero produces no cancellation error.

7. COMBINED RECEIVER AND ECHO CANCELLER

Digital network synchronisation entails phase locking the outstation's transmitter to

its receiver timing recovery circuit, thereby synchronising the network's receiver via the local loop. Then the receiver and echo canceller shown separately in Fig.1 can be combined as shown in Fig.9, principally by using the same sampler for the receiver and for the echo canceller (Refs.4,5,6,8).

This simplifies the equipment because the receiver's input equaliser is now combined with the echo canceller's input band limiting filter and a reconstruction filter is required only in the timing recovery circuit. Also, adaptive reference cancellation can now be used to reduce the uncancellable noise amplitude and to change its distribution, leading to reduced echo canceller convergence time with most algorithms and allowing the zero driven sign algorithm (without a dither generator) to be used with any line code. The adaptive reference amplitude also sets a ternary receiver's decision levels, and AGC is not required.

However, the receiver's equaliser is now in the echo path. In this situation, a linear equaliser and the echo canceller interact strongly and their joint adaptation is unsatisfactory (or even unstable) (Ref.6) because both must use the same convergence error signal $r(k)$. Thus the receiver equalisation and gain must be fixed, and intersymbol interference (ISI) may be excessive.

Similarly, the network receiver's timing recovery circuit must not control its echo canceller timing, because of strong interaction with its echo canceller coefficients. The network receiver is therefore constrained to operate at one of its echo canceller's oversampling phases, locked to its transmitter and to the network clock, thus introducing more ISI. (Note that the outstation receiver's timing recovery circuit controls both its echo canceller and its transmitter timing, resulting in no permanent interaction, and continuous optimum timing adjustments can be used).

7.1 Decision Feedback Equalisation

A decision feedback equaliser (DFE) is easily included in the combined echo canceller and receiver, as shown in Fig.9, where it can be used to cancel the trailing components of the ISI introduced by the restrictions on the combination, without degrading the echo canceller convergence. Extension to adaptive reference (AR) cancellation can enhance the echo canceller convergence.

A DFE is useful, even in a separate receiver, for cancelling trailing ISI resulting from low frequency filtering used to shorten the echo impulse response (because it removes the ISI without restoring the echo impulse response tail) and for adaptively cancelling the trailing ISI produced by line mismatching, gauge changes and bridged taps.

Note that a DFE cannot cancel leading components of ISI. Therefore the fixed

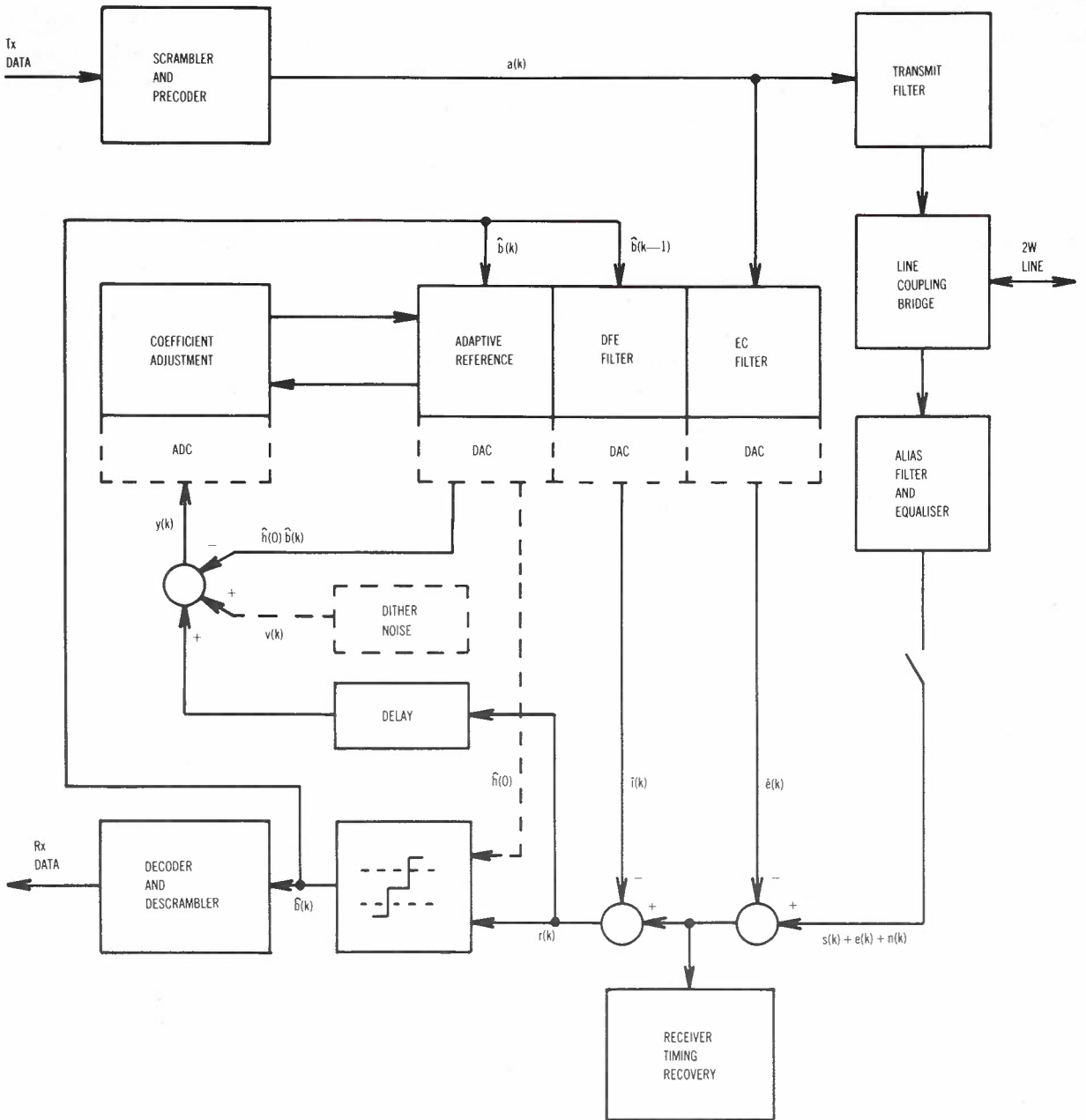


Fig. 9 - Combined Receiver and Echo Canceller with Decision Feedback Equaliser and Adaptive Reference Level

equaliser must be designed to avoid leading ISI, and the network's receiver timing must always be set to the nearest oversampling phase in advance of the optimum.

If the receiver timing is fixed, the joint convergence of echo canceller and DFE is described by simple extension of the basic echo canceller equations (Ref.5). The DFE estimates the received trailing ISI with

$$\hat{i}(k) = \hat{\underline{b}}^T(k) \hat{\underline{h}}_k \quad (7.1)$$

if a TDL structure is used, and can cancel part of the received trailing ISI

$$i_c(k) = \underline{b}^T(k) \underline{h} \quad (7.2)$$

where

$$\underline{b}(k) = (b(k-1), \dots, b(k-J+1))^T \quad (7.3)$$

is the data sequence transmitted from the far end,

$$\underline{h} = (h(1), \dots, h(J-1))^T \quad (7.4)$$

is the impulse response samples of the transmission channel for arbitrary but fixed receiver timing,

$\hat{\underline{b}}(k)$ is an estimate of $\underline{b}(k)$,
and $\hat{\underline{h}}_k$ is the k th estimate of \underline{h} .

If the DFE and the echo canceller use the same algorithm and feedback constant, then

$$N' = N + J \quad (7.5)$$

$$\underline{a}'(k) = (\underline{a}^T(k), \underline{b}^T(k))^T \quad (7.6)$$

$$\underline{g}'_k = (\underline{g}_k^T, \underline{h}_k^T)^T \quad (7.7)$$

and

$$\underline{g}' = (\underline{g}^T, \underline{h}^T)^T \quad (7.8)$$

can be substituted in the basic echo canceller equations, showing that joint convergence is similar to convergence of the echo canceller alone. The uncancellable signal is now

$$u'(k) = b(k)h(0) + i_u(k) + e_u(k) + n(k) \quad (7.9)$$

where

$$i_u(k) = \sum_{j=-\infty}^{-1} b(k-j)h(j) + \sum_{j=J}^{\infty} b(k-j)h(j) \quad (7.10)$$

is the uncancellable ISI.

This uncancellable signal power is not much less than that handled by an echo canceller without a DFE, so similar convergence rates and excess noise levels occur.

DFE convergence depends on correct receiver decisions. Before convergence, the far end signal is masked by the echo of the locally transmitted signal, and the receiver decisions resemble the transmitted data. The combined filters initially behave as an echo canceller with an increased feedback coefficient. When the received signal emerges, the receiver decisions no longer resemble the transmitted data and the echo canceller continues to converge alone. The receiver must now change its timing phase and make sufficient correct decisions for successful DFE convergence. Failure may result in continuous receiver errors and varying DFE coefficients, or the receiver and DFE may lock onto strong ISI and suffer severe interference from the wanted signal itself. These problems may be aggravated by the presence of bridged taps in the local network and further study is required to find operating conditions and equipment parameters which guarantee correct DFE operation.

The impulse response samples h of the transmission channel depend on the receiver timing relative to the remote transmitter timing. The receiver timing must be derived independently of the DFE coefficients h_k if interaction of the DFE and timing feedback loops is to be avoided. Fig.9 shows

a suitable timing recovery point. Note that the DFE and the echo canceller use separate DAC's and that the recovered timing must be in advance of the optimum to avoid leading uncancellable ISI.

The recovered timing may change as the echo canceller completes its convergence. This has little effect in the outstation because all outstation timing is locked to its receiver. However the network receiver timing is restricted to the oversampling phases of the network echo canceller and abrupt phase changes may occur at any time (even after convergence) and may lead to receiver errors while the DFE reconverges. These errors can be avoided by always operating the DFE at the oversampling phases on, ahead of and behind the current receiver decision phase, and changing the DFE coefficient memory addressing appropriately when a receiver phase jump occurs.

7.2 Adaptive Reference (AR)

The DFE can be extended to estimate the current received pulse $b(k)h(0)$ with $b(k)h_k(0)$ where $h_k(0)$ is the adaptive reference level (Ref.7). The adaptation is controlled by cancelling the pulse in the path to the adaptation circuit only, as shown in Fig.9. Joint convergence can be studied by including the 0th term in the DFE vectors, and the calculated excess noise reduced by the 0th term's contribution to obtain the excess noise input to the receiver.

Now the uncancellable signal is only

$$u''(k) = i_u(k) + e_u(k) + n(k) \quad (7.11)$$

which has considerably less power and a narrower amplitude distribution than before. The stochastic iteration algorithm can be used with increased feedback, for faster convergence, and the zero driven sign algorithm now operates also with binary signals, without any dithering noise. Improvement of the coarse quantised algorithm's performance is limited, because the dither noise must be retained to smooth the quantising steps.

The adaptive reference signal can also be used to control the decision levels of a ternary receiver, although this function could also be provided by AGC or decision level circuits driven by the receiver input signal.

The adaptive reference output is delayed because the receiver decision is not instantaneous and the control signal $r(k)$ must be delayed by the same small amount before input to the convergence control circuit. AR convergence at multiple oversampling phases, to allow for network receiver phase jumps, requires an extra delay of one oversampling period. The total delay is less than one line period and does not effect the convergence speed or stability of the

filters although it complicates the memory address sequence. (Larger delays are considered in Ref.7).

A 1-digit table lookup (RAM) filter cannot be used in the AR circuit, if another RAM filter is used either in the echo canceller or in the DFE, because the AR RAM may converge with non zero mean, producing a DC offset at the receiver input and in the received eye. A 1-tap TDL filter can be used because it always has zero mean error and the combined structure converges with zero offset at both the receiver and the adaptation control input.

8. COMPARISON OF ALGORITHMS

To compare algorithms with exponential and linear convergence, and with normally and geometrically distributed excess noise, with and without adaptive reference circuits, consider a typical long loop situation:

- 40 dB line transmission loss
- 10 dB coupling bridge return loss
- 20 dB signal to excess noise ratio required (normal distribution)
- (26 dB if the excess noise is geometrically distributed)
- 15 dB received to uncancellable signal ratio with adaptive reference cancellation.

Algorithms with linear and exponential convergence can be compared by calculating k_c , the number of line periods required to converge from 10 dB echo loss to a loss 3 dB less than the required long term echo loss, i.e. $\epsilon(k_c) = 2\epsilon(\infty)$. The convergence time is $T_c = k_c T$. The comparison is simplified by calculating the convergence time per coefficient:

i.e.

$$k_{cc} = \begin{cases} k_c/N & \text{N-tap TDL filter} \\ k_c/x^N & \text{equivalent 1-RAM filter} \\ k_c/P \cdot x^{N/P} & \text{equivalent P-RAM filter} \end{cases}$$

noting that N and P are the total number of taps and RAMs respectively if structures with DFE or AR estimation are considered.

8.1 Stochastic Iteration Algorithm

From equations 5.24, 5.37 and 5.51, and from Sections 7.1 and 7.2,

$$k_{cc} = (10 \log \frac{\epsilon(0)}{\epsilon(\infty)}) \frac{U}{17\epsilon(\infty)} \tag{8.2}$$

for TDL, RAM and multiple RAM echo canceller (EC) filters, for TDL and multiple RAM EC-DFE filters (partitioned as in Fig.9), and for TDL EC-DFE-AR filters.

Substituting:

$$\epsilon(0) = 10^{-1}$$

$$\epsilon(\infty) = 10^{-6}$$

$$U = \begin{cases} 10^{-4} & \text{without adaptive reference} \\ 3 \times 10^{-6} & \text{with adaptive reference} \end{cases}$$

yields

$$k_{cc} = \begin{cases} 300 & \text{without adaptive reference} \\ 9 & \text{with adaptive reference} \end{cases}$$

(Note that $k_{cc} = 9$ must be regarded as an approximation because such speed may be inconsistent with the assumptions used in deriving the recurrence relations of the stochastic iteration algorithm).

8.2 Coarse Quantised Algorithm

This algorithm approximates the stochastic iteration algorithm, with dither noise added.

If the algorithm is used with an 8 bit ADC, which must handle unit received signal amplitude on short lines, the ADC resolution is $Q = 2^{-7} = .008$ and dither amplitude $a = .004$ is sufficient. Hence the dither noise power is $\sqrt{2} = 5 \times 10^{-6}$ and the performance for the structures noted in 8.1 (from 8.2 and 6.46) is:

$$k_{cc} = (10 \log \frac{\epsilon(0)}{\epsilon(\infty)}) \frac{U + \sqrt{2}}{17\epsilon(\infty)} \tag{8.3}$$

$$= \begin{cases} 310 & \text{without adaptive reference} \\ 24 & \text{with adaptive reference} \end{cases}$$

8.3 Sign Algorithm

The sign algorithm with fixed dither noise must handle unit received signal amplitude, so the dither amplitude must be $a = 1$. Consequently the coefficient resolution is (from 6.22)

$$q = 2\epsilon(\infty)/a = 2 \times 10^{-6}$$

and the convergence performance for a single RAM echo canceller is (from 6.23)

$$k_{cc} = (10 \log \frac{\epsilon(0)}{\epsilon(\infty)}) \frac{a}{8.7q} = 3 \times 10^6 \tag{8.4}$$

If adaptive dither noise tracks the received signal amplitude precisely, i.e. a_{min} = half eye opening = $r = .01$, the coefficient quantising interval (from 6.22) can be increased to $q = 2 \times 10^{-4}$. Initial convergence is linear, from error amplitude $|z(0)| = \sqrt{.1}$, requiring (from 6.24 and 6.23)

$$k_{cc} = \frac{|z(0)|-r}{q} + (10 \log \frac{a^2 \min/3}{\epsilon(\infty)}) \frac{a_{\min}}{8.7q} = 1600 \quad (8.5)$$

8.4 Zero-Driven Sign Algorithm

The zero driven sign algorithm, used with ternary signalling and a 1-RAM echo canceller filter, has geometrically distributed excess noise. Increasing the signal to excess noise ratio to 26 dB and assuming $P_O = .5$ (e.g. for AMI code) the coefficient step size is (from 6.36) $q = .35 \times 10^{-3}$. Convergence has two linear segments (6.32), from $|z(0)|$ to r and from r to zero, and requiring

$$k_{cc} \approx \frac{|z(0)|-r}{q} + \frac{r}{qP_O} = 932. \quad (8.6)$$

8.5 Comment

In this example the stochastic iteration and coarse quantised algorithms are similar in terms of convergence speed (with and without adaptive reference) and both are superior to the sign algorithms. Without adaptive reference, the stochastic iteration algorithm is about 3 times faster than the zero forced sign algorithm with AMI line code and with adaptive reference it is about 100 times faster.

Adaptive reference cancellation significantly improves the convergence speed of the stochastic iteration and the coarse quantised algorithms by factors of approximately 33 and 13 respectively.

The speed of the sign algorithm with adaptive dither noise depends on the dither amplitude tracking accuracy, and even with perfect tracking it is only about half as fast as the zero forced sign algorithm with AMI line code. The simple sign algorithm with fixed dither noise amplitude is extremely slow.

Actual convergence times depend on the number of coefficients in the adaptive filters. For example a RAM filter with 10 address bits has 1024 coefficients and if operated with the zero forced sign algorithm and with AMI line code at 160 kilobaud has a convergence time of 6 seconds. This is fast enough for initial convergence at the time of installation of a fixed line terminating unit, but the coefficients must then be stored between ISDN calls.

The convergence speed of several combinations of algorithm and EC-DFE-AR structures have not been analysed. These include EC-DFE multiple RAM structures with unequal RAM sizes and EC-DFE-AR structures with multiple RAMs and a 1 tap TDL filter for the AR estimate. Approximate comparisons can sometimes be made by multiplying the convergence time per coefficient by the total of the number of RAMs and TDL taps and by the number of coefficients in the largest (and slowest) RAM section, because the excess noise

from this section is uncancellable by the faster sections and retards their convergence.

9. CONCLUSION

Reliable adaptively converging echo cancelling filters for ISDN basic access can be made with a variety of structures and algorithms, several of which have been discussed in this paper.

One attractive structure combines the data receiver with the echo canceller. It uses a decision feedback equaliser to cancel the forward echoes produced by bridged taps on the customer's loop and to cancel the transmission distortion produced by low frequency cutoff which can be used to shorten the return echo duration.

Multiple RAM table look up filters combine adequate convergence speed with reduced digital processing load, by comparison with TDL filters. Their less stringent convergence conditions allow the use of non linear pseudo ternary line codes for bandwidth reduction, and they are capable of compensating for minor channel, transmitter and DAC nonlinearities.

Fine resolution ADCs are not required if analogue echo cancellation is used together with sign algorithm adaptation, which offers further digital processing economy in comparison with the stochastic iteration algorithm. The zero forced sign algorithm can be used with ternary line codes and has speed and simplicity advantages over the sign algorithm with a dither noise generator.

Adaptive reference estimation is obtained from an extension of the decision feedback equaliser, providing a considerable speed advantage to most of the algorithms. It allows the zero forced sign algorithm to be used with any line code, and it provides a replacement for conventional line signal level detectors.

The required echo canceller size is strongly dependent on the low frequency content of the line signals, and although the decision feedback equaliser is capable of cancelling the distortion caused by low frequency filtering, its initial convergence is a subject requiring further study especially in the context of bridged taps in the Australian local distribution network.

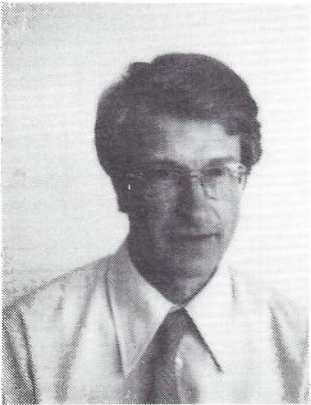
10. ACKNOWLEDGEMENT

Valuable criticisms and suggestions have been contributed by N. Demytko and A.J. Jennings during the preparation of this paper.

11. REFERENCES

1. B. Aschrafi, P. Meschkat and K. Szechenyi, "Field Trial Results of a Comparison of Time Separation, Echo Compensation and

- Four-wire Transmission on Digital Subscriber Loops", Proceedings of IEEE International Symposium on Subscriber Loops and Services, Toronto, September 1982, (ISSLS 82) pp. 181-185.
2. J.O. Andersson, B. Carlqvist and G. Nilsson, "A Field Trial with Three Methods for Digital Two-wire Transmission", *ibid* pp. 186-190.
 3. N.A.M. Verhoeckx, H.C. van den Elzen, F.A.M. Snijders, and P.J. van Gerwen, "Digital Echo Cancellation for Baseband Data Transmission", *IEEE Trans. on Acoustics, Speech, and Signal Processing*, vol ASSP-27, No. 6, December 1979, pp 768-781.
 4. N. Holte and S. Stueflotten, "A New Digital Echo Canceller for Two-wire Subscriber Lines", *IEEE Trans. Communications*, vol. COM-29, No. 11, November 1981, pp. 1573-1581.
 5. K.H. Mueller, "Combining Echo Cancellation and Decision Feedback Equalisation", *Bell Syst. Tech. Journal*, February 1979, pp. 491-500.
 6. D.D. Falconer and K.H. Mueller, "Adaptive Echo Cancellation/AGC Structures for Two-wire, Full-Duplex Data Transmission", *B.S.T.J.* September 1979, pp. 1593-1616.
 7. D.D. Falconer, "Adaptive Reference Echo Cancellation", *IEEE Trans. COM-30*, No. 9, September 1982, pp. 2083-2094.
 8. P.J. van Gerwen and N.A.M. Verhoeckx, "A Digital Transmission Unit for the Local Network", *IEE Conference Proceedings, "Communications 82"*, pp. 65-69.



BIOGRAPHY

FRED G. BULLOCK gained his B.E. (Hons) degree at the University of Adelaide in 1968. He then joined the Philips group where he was involved in the design of telecommunications line equipment and air traffic control equipment, in Australia and the Netherlands. He joined the Transmission Systems Branch of the Telecom Australia Research Laboratories in 1974. There he has investigated CATV distribution, filter design, transmission problems in switched network digitalisation, coaxial cable problems, and ISDN terminal access and local reticulation. He is now studying wideband customer access and fixed point to multipoint digital radio systems.

Protocols for Message Handling

R. EXNER

Telecom Australia Research Laboratories

The CCITT has recently defined a new global telecommunications service known as Message Handling, which combines electronic mail with established telematic services such as telex and facsimile. The global feasibility of this new service owes much to the protocols that have been defined for message transfer and manipulation. This paper describes these protocols, and analyses their structure and foundation as application layer protocols in the Reference Model for Open Systems Interconnection. The paper identifies their dependence on the services of the session layer, and the potential problems in accommodating a presentation layer. The reasons for the overall simplicity of the protocols are elucidated, and applications outside Message Handling are identified.

KEYWORDS: Protocols, Message Handling, Telecommunications service, OSI Reference Model

1. INTRODUCTION

The problems of interconnecting computer-based message systems (CBMSs), together with a desire to integrate these with the established telematic services (telex, teletex and facsimile), have led the International Telegraph and Telephone Consultative Committee (CCITT) to develop a new generic telecommunications service known as Message Handling (Refs. 1-10). The service comprises a flexible model of Message Handling (MH) system, a defined set of basic and optional facilities, and a set of protocols to support these facilities between telecommunicating entities.

Of particular interest are the protocols that have been defined for Message Handling (Refs. 6-8, 11, 12). If the messaging system is to be a global one, i.e. if local and national systems are to be successfully interconnected, then common, internationally accepted protocols are required. The protocols defined by CCITT are application layer protocols within the Open Systems Interconnection (OSI) Reference Model (Ref. 13), and make extensive use of the lower layers of the model. This paper describes these protocols, and analyses their structure, their complexity, and their relationship to the presentation and session layers of the Reference Model. The directions in which the protocols may need to be extended or modified in the future, and the possible use of the protocols or the techniques underlying them in other application areas, are also identified.

2. OVERVIEW OF MESSAGE HANDLING

A Message Handling system is modelled as in Figure 1, and comprises two types of

entities: User Agents (UAs) which assist the (human) user in the preparation, submission, delivery and filing of his messages, and Message Transfer Agents (MTAs) which exchange messages between User Agents. MTAs form a network called the message transfer service, which provides the UAs in the system with a means of exchanging messages. The UAs provide their users with a service known as the inter-personal messaging service.

To send a message, a user first prepares it with the assistance of his UA. The UA then submits it, together with an "envelope" to the MTA to which it is connected. If the recipient's UA is served by the same MTA, the MTA delivers it directly, otherwise it forwards it through the message transfer service to the appropriate MTA. Delivery of messages may not occur immediately - the MH system offers several delivery priorities as well as delivery after a specified time or date - but once it occurs, the recipient UA holds it: it may advise its user of the incoming message, and will assist him in reading it, filing it and so on.

The model of Figure 1 is a conceptual one, and does not constrain actual implementations. In particular, a UA may be co-resident with its MTA, and an MTA may in fact be a distributed collection of processors. A stand-alone UA might well be a special application program running on the user's personal computer.

2.1 Service Elements

Message Handling has been designed to provide an extensive range of user services and facilities. The current and projected services include:

- A directory to allow addressing by name and organisation (among other things).

Paper received 19 June 1984.
Final revision 31 January 1985.

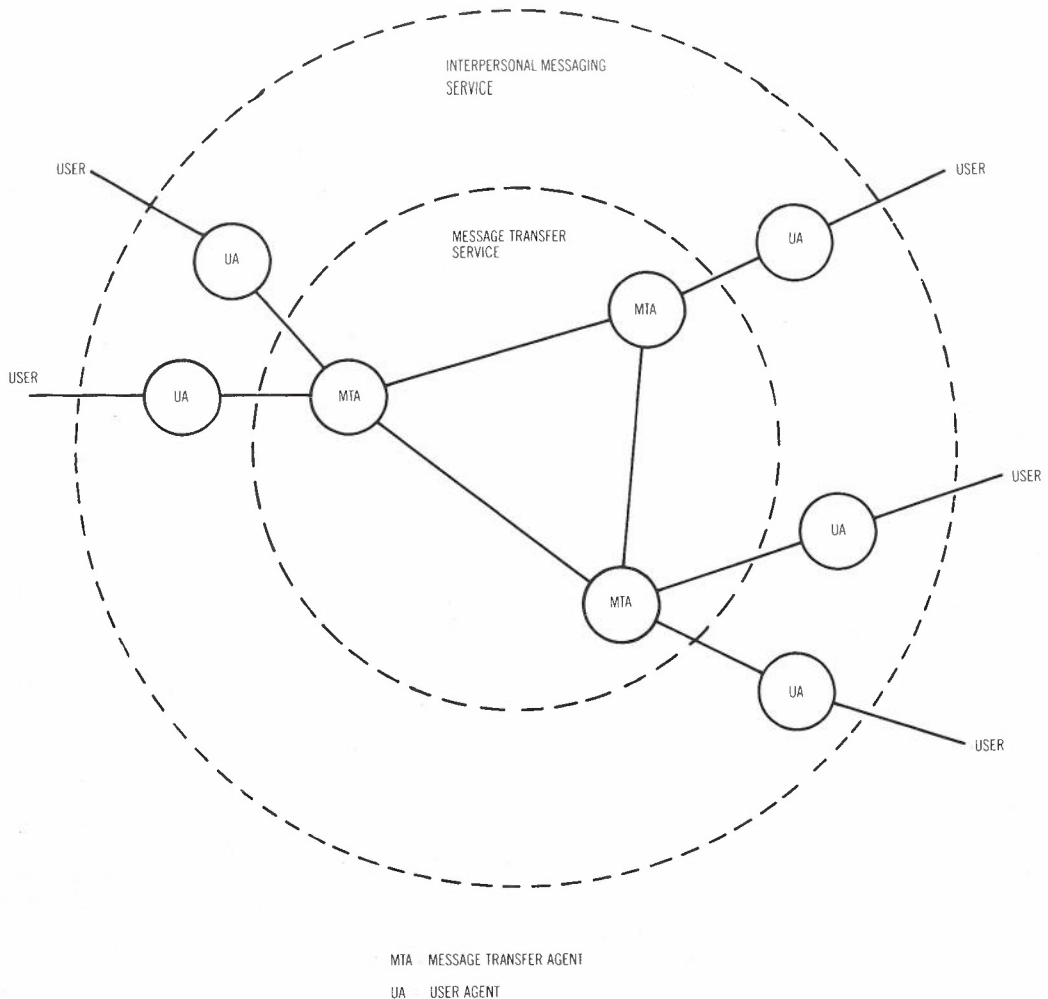


Fig. 1 - Model of a Message Handling System

- . Automatic conversion of message content type from one form (e.g. text) to another (e.g. facsimile), to suit the capabilities of the recipient's UA.
- . Time stamping of message submission and delivery.
- . Delivery verification and non-delivery notification.
- . Autoforwarding of messages
- . Multirecipient addressing, and so on.

This list is by no means exhaustive, but it does indicate the range and power of the facilities that an MH system may offer. Not all facilities will always be available, but there must be support for all of them in the MH protocols.

2.2 Protocols

Message Handling has been defined as an application layer service conforming to the OSI Reference Model, so the MH protocols are application layer protocols which make use of standard protocols in the lower layers. In the application layer there are three protocols of importance:

1. The Message Transfer Protocol (P1) for relaying messages between MTAs.
2. The Interpersonal Messaging Protocol (P2) used between UAs to convey the syntax (content type) of the message and to specify actions to be performed by the recipient UA.
3. The Submission and Delivery Protocol (P3) used between UAs and MTAs in the submission and delivery of messages.

These are shown in Figure 2, which reveals that the application layer is in fact sub-layered for Message Handling, with the P1 and P3 protocols conveying the protocol data units (PDUs) of P2. Section 3 examines these protocols in detail, in the order in which they are encountered when sending a message.

In the OSI Reference Model, application protocol data units are communicated between end systems by the operation of protocols in the lower layers, from Presentation through Session, Transport, Network, Data Link, and Physical. For Message Handling, the protocols are X.225 (Ref.14) at the session layer and X.224 (Ref.15) at the transport layer; no protocol operates at the presentation layer. At lower layers the protocols depend on the network over which the MH system is

implemented. The function of these protocols is essentially the reliable transfer of bulk data between end systems. The specific requirements that Message Handling places on these lower layer protocols are examined in Section 4.

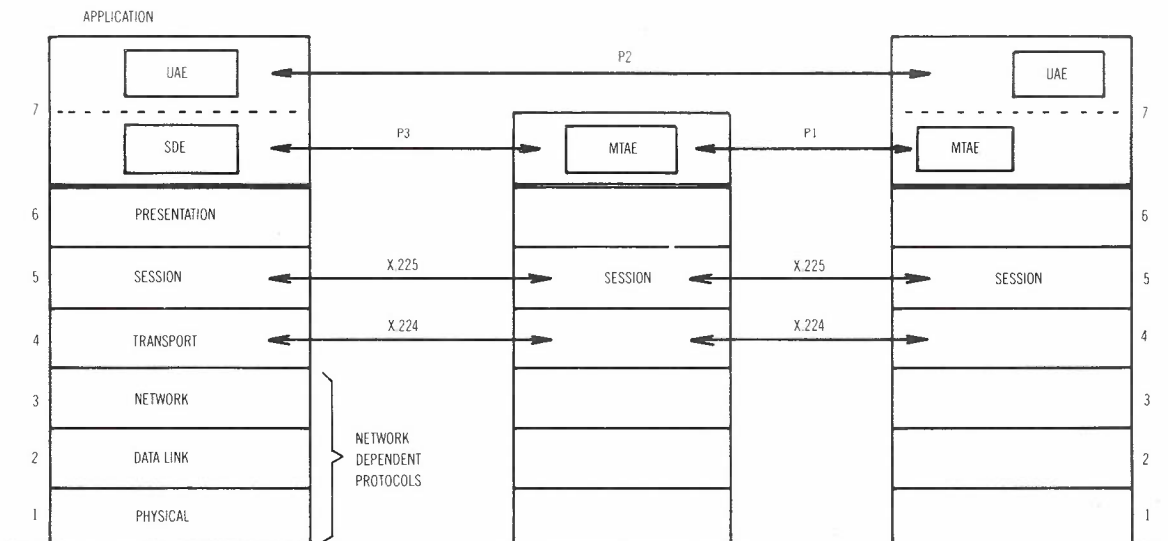
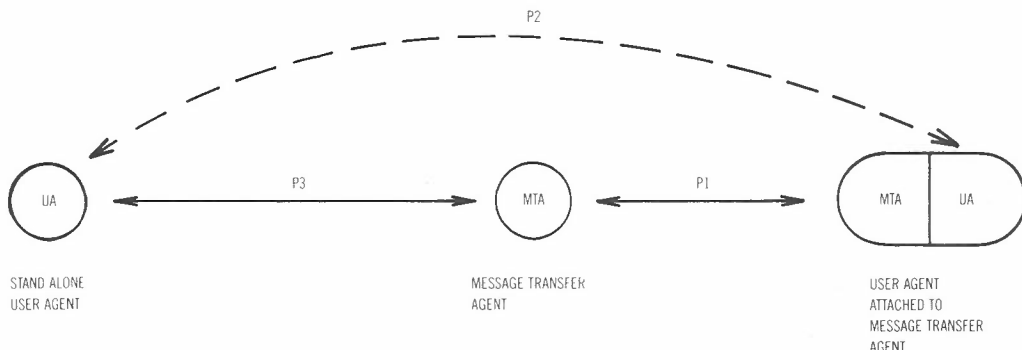
3. APPLICATION LAYER PROTOCOLS

The three application layer protocols of Message Handling are rather unlike other current protocols of the OSI Reference Model in that they are essentially connectionless, and in the case of P1 and P2, non-interactive. A connectionless protocol is one in which all parameters relating to an exchange of information are passed with that exchange, rather than in a previous (connection establishment) exchange. A non-interactive protocol is one in which responses from the receiving party are not required to complete the exchange.

These differences make the MH protocols very simple in terms of their logical operation, and consequently they are primarily concerned with the description of

the complex data types and optional parameters of the protocol data units.

The P1 protocol is used for relaying messages between MTAs. It is required whenever the originating UA and recipient UA are associated with different MTAs. If one models an administration's mail network with a single MTA then P1 is the inter-network protocol, connecting one electronic mail system with another. This accounts for the considerable interest accorded P1 by messaging system operators, and reflected in the priorities of CCITT. P1 is needed to permit interconnection of messaging systems (including existing CBMS systems) across administrative and international boundaries, and is arguably the most important of the MH protocols. In practice, P1 is also likely to be used internally, within an administration's network, to support message transfer between geographically separated message processors. The P3 protocol is needed if a system provides for stand-alone User Agents, and P2 is needed to support multiple message



UAE = USER AGENT ENTITY (PART OF USER AGENT)
 SDE = SUBMISSION AND DELIVERY ENTITY (PART OF USER AGENT)
 MTAE = MESSAGE TRANSFER AGENT ENTITY

Fig. 2 - Layered Protocols for Message Handling

recipient's UA, two peer protocols are encountered. They are the Submission and Delivery or P3 protocol, and the Message Transfer or P1 protocol. The existence of two protocols reflects the fact that interactions between MTAs may also be required in the delivery of a message, and that these interactions are rather different from those between UAs and MTAs.

The P3 protocol is used between a stand-alone UA and the MTA to which it is connected. (If the UA is directly attached to its MTA, interactions between the two are internal to the message processor, and no standardized protocol is required). P3 is primarily for the submission and delivery of user messages (to the MTA and to the UA respectively). It is also the means by which control or management actions, and enquiries or reports about messages, are communicated between UAs and their MTAs.

As previously mentioned, the P3 protocol is an example of a more general application layer protocol called the Remote Operations protocol. This protocol, itself derived from the Xerox Remote Procedure Call protocol (Ref.16), provides a means of specifying operations to be performed on a remote system, and specifying the results, including errors, which the remote system may return in response to a request for an operation.

There are 4 types of Operation Protocol Data Unit (OPDU):

- Invoke OPDU: Invokes a remote operation.
- Result OPDU: Reports the successful completion of an operation.

- Error OPDU: Reports the unsuccessful completion of an operation.
- Reject OPDU: Reports that an OPDU is malformed and therefore rejected.

Not all operations report results or errors. In Message Handling the OPDU's are carried by the session protocol which is fully responsible for their correct delivery. Hence there is no requirement for confirmation at the application layer of their delivery; it is only the outcome of an operation that might need to be reported.

The OPDUs carry parameters, as illustrated in Figure 3. The Invoke OPDU carries an identifier to uniquely reference it, and the others carry that same parameter as a cross-reference. The Invoke OPDU carries a code identifying the operation type, and an "argument" containing the data associated with the operation. The Result OPDU carries a "result" parameter containing data returned by the operation. The Error OPDU carries a code identifying the error, and a "parameter" component further describing the error.

The P3 protocol is specified in terms of eight remote operations, which are summarised in Table 1. The eight operations correspond to eight identifiable services provided by the message transfer layer to UA entities: register, to allow the UA to make (long term) changes to its registration parameters; control, to advise temporary restrictions (and implement, for example, a "hold for delivery" service); change password; submit, to submit a message to the

TABLE 1 - P3 Operations and Parameters

Operation	Code	Argument	Result	Errors	Invoked By
register	1	parameters	confirmation only	"invalid parameters"	UA
control	2	parameters	several items	"invalid parameters"	UA or MTA
chge pw	8	old, new passwords	confirmation only	"invalid passwords"	UA or MTA
submit	3	envelope, content	event ID, time	several e.g. "invalid originator"	UA
probe	4	envelope	event ID, time	several	UA
cancel	7	event ID	confirmation only	several, e.g. "message already sent"	UA
deliver	5	envelope, content, event ID, time	-	"control violation"	MTA
notify	6	event ID, delivery or non-delivery notification	-	"control violation"	MTA

MTA for delivery; probe, to determine whether a particular message would be deliverable (in terms of whether the address is valid, whether the recipient UA can accept a message of a particular content type, etc.); cancel, to delete a message submitted for deferred delivery; deliver, used by the MTA to deliver a message to the recipient UA; and notify, used by the MTA to advise the successful or unsuccessful delivery of an earlier message.

A message for the P3 protocol - as for P1 - comprises an envelope part and a contents part. The envelope contains information used by the MTA in the delivery of the message, and may in fact be modified as the message passes from originator to recipient - much as a real envelope gains postmarks and routing marks in the postal system. The contents contains a User Agent PDU (i.e. a P2 User Message or Status Report), and is ordinarily unmodified as the message passes from originator to recipient. If the MTA performs content conversion, a defined service element in Message Handling, the contents are in fact modified by translation from one syntax or form to another, where possible, in accordance with X.408 (Ref.3).

A message is transferred using the P3 protocol by passing it as the argument of a Submit or Deliver operation.

3.3 The Message Transfer Protocol P1

The P1 protocol requires only three types of protocol data unit, known as Message Protocol Data Units (MPDU's). They are:

User MDPU

Delivery Report MPDU

Probe MPDU.

They are shown in Figure 3. A User MPDU is used to transfer a message, and associated responsibility for the message, to another MTA. A Delivery Report MPDU is used to report that a previous User or Probe MPDU could not be delivered, or alternatively that it has been delivered. A Probe MPDU is used, much like the P3 Probe operation, to determine whether a message with certain attributes would in fact be deliverable.

All three MPDUs have a similar structure, consisting of an envelope part and a contents part, though in the case of a Probe MPDU the contents are absent. The envelope contains similar information to that present in a P3 Submit or Deliver message envelope. Table 2 summarizes the envelope and contents components for each MPDU.

Being non-interactive and connectionless, the P1 protocol is very simple in its operation. An MPDU is transferred to another MTA using lower layer services. If the MPDU is deliverable to the recipient UA, it is delivered (or held for delivery); if it needs to be passed to another MTA, it is queued for transfer; otherwise it is

TABLE 2 - Components of the P1 Protocol Data Units

MPDU	Envelope	Contents
User MDPU	MPDU identifier, originating user, Trace information, Content type, Priority, etc.	User Agent PDU (i.e. User Message or Status Report)
Delivery Report MPDU	MPDU identifier, originating user, Trace information	Original MPDU identifier, intermediate trace information, etc.
Probe MPDU	(almost) same as for User MPDU; + Content length	-

discarded and a Delivery Report MPDU is generated and returned to the originating MTA.

One might ask why there should be any difference between the P1 and P3 protocols - why a subset of P3 cannot be used for the transfer of messages between MTAs. Some of the operations of P3 would not be required (e.g. register, control, change password), and others would contain some redundancy (e.g. submit and deliver), but in principle P3 is as appropriate for inter-MTA message transfer as it is for UA-to-MTA transfers. Yet two separate and quite different protocols have been defined.

The reason for this lies largely in the greater need for reliability (i.e. confirmation) in the transfer of responsibility for messages between UAs and MTAs than between two MTAs. In the latter case, having to confirm a message transfer results in unacceptable inefficiencies, so a separate protocol is justified. But another factor which cannot be disregarded is the history of the development of P1 and P3. P1 was relatively complete before the requirements of UA-to-MTA message transfer were properly analysed, and P1 could not be readily adapted to interactive operation. The extent of the difference between P1 and P3 is regrettable from an implementor's point of view, but it should not prove particularly difficult to tolerate.

4. PROTOCOLS BELOW THE APPLICATION LAYER

The P1 and P3 protocol data units are communicated between end systems by the operation of protocols in the lower 6 layers of the OSI Reference Model. Of particular interest is the relationship of the MH protocols to the presentation and session layers.

4.1 Presentation Layer

The presentation layer serves to determine a common transfer syntax for the exchange of application layer PDUs between application entities. Where the syntax preferred or used by each application entity differs, the presentation layer would provide a mapping or translation (conversion) of one syntax to another, or each into a common transfer syntax.

This function of syntax conversion is particularly important in Message Handling, as one of the features of MH systems is the automatic conversion by the system of user data of one kind (e.g. text), to data of another kind (e.g. facsimile). A presentation protocol could be used to determine conversion requirements, and relieve the application protocol from these considerations. But the development of suitable protocols and conversion algorithms for a general presentation layer have lagged the work - and requirements - of Message Handling by some years. In order to achieve functioning MH protocols in time for the 1984 CCITT Plenary, Message Handling was designed to bypass entirely the presentation layer. The presentation layer is being defined to permit this type of approach, in which application entities can access session services directly, so Message Handling remains consistent with the OSI Reference Model.

But in the future, as the presentation layer is developed, and systems that implement presentation layer functions are connected to MH systems or use MH protocols, this bypass approach may prove a hindrance. It is likely that the P1 and P3 protocols will need to be revised to align Message Handling with the concept of a functioning presentation layer. As long as the MH standards are viewed as evolving, this should be possible. One factor that will aid this process is the development for Message Handling of a very general presentation transfer syntax in X.409 (Ref.4) (see also Section 4). There is currently strong interest outside Message Handling in using all or part of this syntax in the presentation layer area, and this should narrow the current gap between Message Handling and intended OSI use of the presentation layer.

4.2 Session Layer

In the absence of a presentation layer protocol in MH systems, the session layer is directly responsible for the delivery of P1 and P3 protocol data units between UAs and MTAs. The session layer serves to synchronize, and in the event of errors, resynchronize, a dialogue between two communicating entities. For Message Handling, the session layer is responsible for the secure delivery of entire application PDUs.

The session protocol, defined in CCITT recommendation X.225 (Ref.14), is a large and complex protocol with many options. The option set selected for Message Handling is the half duplex Basic Activity Subset

(BAS) with certain restrictions. It is the same set as used by the telematic services, particularly teletex and Group 4 digital facsimile.

The BAS subset is highly appropriate to MH applications. It has two strengths: reliability of data transmission, which it achieves through use of the activity concept, and minimization of retransmission required after errors, which it achieves through use of checkpoints or synchronization points inserted into the data stream.

Both these properties are very important to Message Handling. Because the local session entity confirms delivery of an application PDU, many of the protocol elements of P1 and P3, including those used to transfer user messages from an MTA to another MTA or a UA, are not confirmed. This leads to simpler, more efficient application protocols.

Application PDUs can be very long, for an entire (even multi-page) user message is carried in a single application PDU. The use of checkpoints to minimize retransmission following errors is therefore very important in keeping down overheads. It should be noted that the type of errors encountered in the session layer are procedural errors or failures of the underlying transport connection; actual transmission errors are dealt with in the lower layers of the OSI Reference Model.

The BAS subset performs its functions - reliability of data transmission, and efficient recovery from errors - very well. But this is at the cost of significant overhead in exchanging the turn in a half-duplex interaction. For P1 and P3 this is of no consequence. For human-interactive dialogues though, this overhead makes the protocol rather slow. So as Message Handling is extended to support, say, an on-line directory service, it is likely that a different subset of the session service will be required. The simplicity of having all Message Handling application protocols use the same session layer protocol will then be lost.

4.3 Transport Layer and Below

The CCITT Message Handling standards (Refs. 1-8) specify that Class 0, or optionally Class 1, of the OSI transport protocol X.224 (Ref.15) be used. Once again, this has been designed for compatibility with the other telematic services: Class 0 is the simple teletex transport protocol. Class 1 is a more complex protocol with basic error recovery (i.e. recovery from network disconnects).

Protocols below the transport layer are network dependent, and are not specified for Message Handling. Message Handling systems can thus be implemented over any telecommunications network providing adequate quality of service with the class of transport protocol used. In practice, Message Handling would often be implemented on a packet switched network with X.25 the appropriate protocol.

5. PROTOCOL ENCODING

The encoding of the protocol data units for the P1, P2 and P3 protocols is specified in CCITT recommendation X.409 (Ref.4). X.409 defines both the "abstract syntax" used to define the structure of the PDUs in Refs. 6 and 7, and the encoding or "concrete syntax" used to represent data elements defined in the abstract syntax. Like the Remote Operations protocol, it owes its origins to Ref. 16.

Every data element, whether part of a PDU or one of its parameters, is typed, and its encoding specifies the type as well as the value. An encoded element has three parts in its representation, as shown in Figure 4. The identifier part declares the type of the element, and also whether the contents part is atomic (e.g. an integer or a character string), or itself a list of data elements in their standard encodings. Elements (and types) are thus recursively defined. The length part specifies the length of the contents, and the contents part conveys the value of the element.



IDENTIFIER: 1 OR MORE BYTES, SPECIFYING:

CLASS: e.g. UNIVERSAL, APPLICATION SPECIFIC, etc.

ID CODE: A CODE UNIQUELY SPECIFYING THE IDENTIFIER WITHIN ITS CLASS

FORM: SPECIFYING WHETHER "CONTENTS" IS ATOMIC OR A SERIES OF DATA ELEMENTS IN THEIR STANDARD ENCODINGS

LENGTH: 2 TO 127 BYTES, SPECIFYING THE LENGTH OF THE CONTENTS

CONTENTS: 0 OR MORE BYTES, SPECIFYING THE VALUE OF THE ELEMENT. IT MAY BE A SINGLE VALUE (e.g. A BYTE STRING), OR A SERIES OF ENCLOSED DATA ELEMENTS EACH HAVING IDENTIFIER, LENGTH, AND CONTENTS PARTS.

Fig. 4 - Data Element Encoding in P1, P2, P3

The encoding used for the session protocol and specified in X.225 is superficially similar to that of X.409 and also follows Figure 4. However, its structure is less general than that of X.409, and the bit-level representation of the identifier and length parts is, regrettably, incompatible with it. There would be significant advantages to be gained from aligning these formats, and the development of a concrete transfer syntax for the presentation layer may be influential in resolving the problem.

Faring rather better is the "abstract syntax" defined in X.409. This powerful language is ideal for specifying the complex, highly optioned data types so often encountered in PDU and parameter descriptions, and it has been generally well received in the standards bodies. It should find wide-spread application outside Message Handling,

particularly in presentation layer syntax descriptions.

6. CONCLUSIONS

This paper has considered the developing protocols for Message Handling, a new, generic telecommunications service for electronic messaging. The relationship between the protocols and the upper layers of the OSI Reference Model has been clarified. The protocols have been revealed as very simple in their logical operation, and the reasons for this have been identified. Though the protocols may need to be extended or modified in the future, particularly as they are applied to new and unforeseen applications, they are clearly an important development in application layer protocols, and should receive much use.

7. REFERENCES

1. CCITT, "Message Handling Systems: System Model - Service Elements", Recommendation X.400, 1984.
2. CCITT, "Message Handling Systems: Basic Service Elements and Optional User Facilities", Recommendation X.401, 1984.
3. CCITT, "Message Handling Systems: Encoded Information Type Conversion Rules", Recommendation X.408, 1984.
4. CCITT, "Message Handling Systems: Presentation Transfer Syntax and Notation", Recommendation X.409, 1984.
5. CCITT, "Message Handling Systems: Remote Operations and Reliable Transfer Server", Recommendation X.410, 1984.
6. CCITT, "Message Handling Systems: Message Transfer Layer", Recommendation X.411, 1984.
7. CCITT, "Message Handling Systems: Interpersonal Messaging User Agent Layer", Recommendation X.420, 1984.
8. CCITT, "Message Handling Systems: Access Protocol for Teletex Terminals", Recommendation X.430, 1984.
9. Bartoli, P., "CCITT Message Handling Facilities", A.T.R. Vol. 16 No. 3 pp. 53-62, 1982.
10. Redell, D.D. and White, J.E., "Interconnecting Electronic Mail Systems", Computer Vol. 16 No. 9 pp 55-63, Sept. 1983.
11. Cunningham et al., "Emerging Protocols for Global Message Exchange", Proc. Compcom 82 Fall pp. 153-161, Sept. 1983.

12. Deutsch, D.P., "International Standardization of Message Transfer Protocols: An Overview", Proc. Compcom 82 Fall pp. 162-167, Sept. 1982.
13. CCITT, "Reference Model of Open Systems Interconnection for CCITT Applications", Recommendation X.200, 1984.
14. CCITT, "Session Protocol for CCITT Applications", Recommendation X.225, 1984.
15. CCITT, "Transport Protocol for CCITT Applications", Recommendation X.224, 1984.
16. Xerox Corporation, "Courier: the Remote Procedure Call Protocol", Xerox System Integration Standard XSIS-038112, Dec. 1981.



BIOGRAPHY

ROLF EXNER received the B.Sc and B.E.(Honours) degree from the University of Tasmania in 1975 and 1977 respectively. In 1979 he completed an M.A.Sc. degree at the University of British Columbia, Canada, in the field of computer speech analysis.

He joined the Telecom Australia Research Laboratories in 1980, where he has been involved in investigations into facsimile communications, Message Handling, and most recently, electronic directory services. He is currently a senior engineer in the Telematic and Message Services Section.

A Model for Carrier Recovery, Timing Recovery and Adaptive Equalisation in High-Capacity Digital Radio Systems

P.V. KABAILA and J.L. ADAMS

Telecom Australia Research Laboratories

In this paper a model is presented for carrier recovery, timing recovery and transversal equalisation for the types of high-capacity digital radio systems, employing QAM, which are currently available. Our basic aim is to derive a model which is accurate but not so complicated that we are forced to analyse it using a simulation of the whole system. Our model is notable in that it incorporates a realistic timing recovery scheme and that noise is not neglected. We include noise in our model because, with the introduction of adaptive equalisation schemes, the contribution of noise to the degradation in system performance may become significant in comparison with the degradation due to inter-symbol interference.

We use this model to generate signatures for a two-path channel model. The calculated signatures are compared to measured system signatures using as the criterion the relative probability that the bit-error-rate exceeds 10^{-3} . Using the same criterion we investigate the variation in performance of the system when the number of taps in the transversal equaliser is varied. Currently, five-tap transversal equalisers are implemented. For a nine-tap transversal equaliser the calculated probability that the bit-error-rate exceeds 10^{-3} is approximately one half that calculated for a five-tap transversal equaliser. We also consider the efficacy of the simple timing recovery scheme we have modelled. It would appear that this scheme performs reasonably well.

KEYWORDS: Digital Radio, Signature, Two-Path Model

1. INTRODUCTION

We will present a relatively simple mathematical model for the types of currently available microwave radio systems employing QAM. This model will be an "idealised" model in the sense that it will not possess many of the details (and imperfections) of actual equipment.

Our main contributions in this paper are as follows. In our model we include an analysis of a realistic timing recovery scheme. Although it would have been easier to derive the timing instants by supposing that they were to be selected according to some "optimality" criterion, the timing recovery scheme we have chosen more closely resembles those currently implemented. Some analyses of receivers which do not employ adaptive equalisation neglect noise in their calculation of system performance because the degradation in performance (during frequency selective fading) is dominated by intersymbol interference. We include noise in our model because, with the introduction of adaptive equalisation schemes, the contribution of noise to the degradation in system performance may become significant in comparison with the degradation due to intersymbol interference. Results for PAM systems can be translated to

results for QAM systems, by considering complex-valued signals which are analogous to the real-valued signals of the corresponding PAM systems. Also, we put the results into a form which is convenient for the numerical computation of system performance as measured by bit-error-rate. We have attempted, as far as possible, to use analytical methods in deriving those quantities which are fundamental to the calculation of system performance.

Studies which are related to ours are numerous. Coutts and Campbell (Ref.1) have considered a model in which carrier phase offset, timing and gain are optimised. Their modelling exercise differs from ours in that they do not consider degradations in performance due to noise, they do not include the use of a transversal equaliser and their results are put in a form which is geared to a mean-square-error measure of performance. Foschini and Salz (Ref.2) derive bounds on digital radio system performance. Their modelling exercise differs from ours in that they consider equalisers with an infinite number of taps, they assume complete removal of phase distortion at the receiver and their results are put in a form which is geared to bounding performance. Taylor *et al* and McMillen *et al* (Refs.3,4 and 5) consider a much more detailed model than the one we present. Their modelling exercise differs from ours in that the performance of their modelled system can

Paper received 11 April 1984.
Final revision 16 November 1984.

only be found by the use of extensive simulations. Sari (Ref.6) has considered a model for a high-capacity digital radio system which includes adaptive equalisation. Sari's modelling exercise differs from ours in that Sari does not consider degradation of performance due to noise and in that Sari's measure of performance is the maximum distortion.

In Section 2, the various types of approximations made in modelling the system will be outlined. The mathematical model will be derived in detail in Section 3. In Section 4, we consider in more detail the particular case of no adaptive amplitude equalisation and a two-ray channel model. We assess system performance from the system "signature" which is the locus of channel parameter values (some of which may be fixed *a priori*) for which the bit-error-rate = 10^{-3} .

For the particular case we consider, there is no need to resort to computer simulations in order to predict system performance. However, extensive computations are required. The computational techniques used are described in detail in Section 4.2.

We compare in Section 4.3 system signatures computed from our mathematical model with measured system signatures. We have also investigated the likely improvement in performance obtained by increasing the number of taps in the transversal equaliser. The efficacy of the simple timing recovery scheme modelled is also considered.

2. PRELIMINARIES

2.1 Notation

In this Section, an explanation of some of the notation used is given. The Fourier transform of a function $f(\cdot)$ will be denoted $F(\cdot)$ where:

$$F(\omega) = \int f(t) \exp(-j\omega t) dt$$

Here, as elsewhere in this paper, when the range of integration is not given explicitly it is supposed to extend from $-\infty$ to ∞ . Similarly, if the range of a summation (\sum_n) is not given explicitly it is assumed to extend from $n = -\infty$ to ∞ . We use $\text{Re}(a)$ and $\text{Im}(a)$ to denote the real and imaginary parts respectively, of the complex number a , and $f(\cdot) * g(\cdot)$ denotes the function which is the convolution of $f(\cdot)$ and $g(\cdot)$. We use $E(\cdot)$ to denote the expected value (or "ensemble average"). $\text{Pr}\{A\}$ denotes the probability of the event A . Finally, T denotes the baud period, $\text{Arg}(\cdot)$ denotes the argument of a complex variable ($-\pi \leq \text{Arg}(x) \leq \pi$ for all x).

2.2 Assumptions Made About the Radio System

The channel for a high-capacity digital radio system may be considered to be linear and time-invariant over intervals of, say, 0.01 seconds (during which time a very

large number of symbols will have been transmitted). The impulse response of the channel during an interval of this length will be denoted $f(\cdot)$. Later, we specialise to a particular kind of impulse response which corresponds to a "two-ray" model.

It should be stressed that, in the next Section, we derive an equivalent form for a QAM system which does not represent a simplified block diagram of an actual digital radio system. Thus, for example, automatic gain control (usually carried out at IF) is included as part of the transversal equaliser structure.

The transmitter's in-phase carrier is $\cos(\omega_c t + \theta_0)$ where ω_c is the carrier (angular) frequency of the transmitted signal. The receiver forms an estimate of θ_0 and this estimate is denoted $\hat{\theta}$. As shown in Fig.1 the value taken by $\hat{\theta}$ is determined by the control signal applied to the VCO where ω_i denotes the intermediate (angular) frequency. The control signal for the VCO is derived using the outputs of the decision circuits, i.e. the carrier recovery is decision-directed. We will assume that $\hat{\theta} - \theta_0$ may be approximated by a signal which varies slowly in comparison with the time required by the transversal equaliser to adjust to new channel conditions.

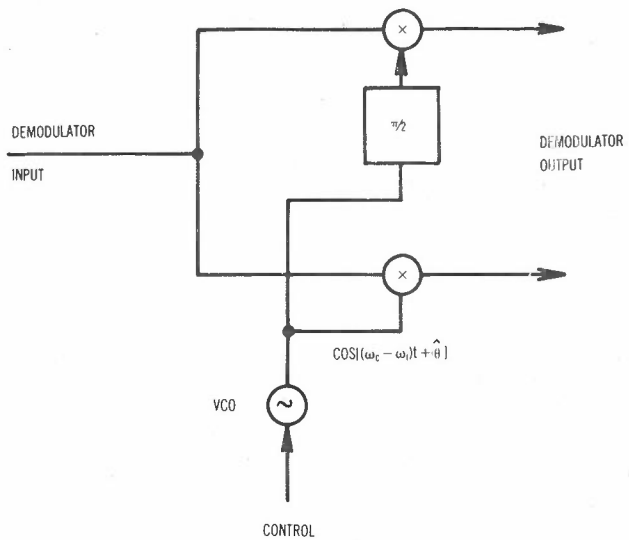


Fig. 1 - Decision directed Carrier Recovery Scheme

Amplitude equalisers use the powers of the outputs of a number of narrowband filters to derive an estimate of $|F(\omega)|^2$ over the bandwidth of the signal. Some receivers use this estimate to adjust what is referred to as an "amplitude equaliser". One possible option is to assume that $f(\cdot)$ is minimum-phase so that $F(\omega)$ is the minimum-phase spectral factor of $|F(\omega)|^2$ (over the bandwidth of the signal). The "amplitude equaliser" is then set to have an amplitude response approximating the inverse of the minimum-phase spectral factor of the estimate of $|F(\omega)|^2$.

We will consider only "zero-forcing" transversal equalisers which are controlled

in such a way that certain intersymbol interference terms are forced to zero. These equalisers are more commonly implemented than minimum mean-square-error equalisers since zero-forcing equalisers tend to have a simpler hardware implementation than minimum mean-square-error equalisers.

We will assume that the timing information is recovered at baseband. The timing recovery schemes considered rely upon the cyclostationarity of the baseband signal. For the case of transversal equalisation, a continuous waveform is available after equalisation from which timing information can be extracted. A simple timing recovery scheme is that of a memoryless nonlinearity followed by a bandpass filter (with centre frequency the inverse of the baud rate). The output of this filter is nearly sinusoidal, and the zero crossings of this waveform determine the timing instants. The nonlinear operation we consider is that of a squarer and we expect that the performance results obtained for other nonlinearities will be similar.

The in-phase and quadrature symbol streams are assumed to be independent. This leads to a rectangular signal constellation, so that, in our model, the in-phase and quadrature streams are decoded independently.

Let ω_{max} be the minimum angular frequency at which the transmitted signal contains no appreciable power. We assume that $\pi/T < \omega_{max} < 2\pi/T$. In fact, in many digital radio systems $\omega_{max} = 3\pi/(2T)$. We assume that the equivalent transfer function of the transmitter filters is real-valued and the same as the equivalent transfer function of the fixed receiver filters. It is noted that the most important contributors to noise at the decision points are the thermal noise at the receive antenna, the waveguide and in the RF preamplifier.

3. DERIVATION OF THE MODEL

As may be seen from the results presented in the Appendix of Kobayashi's paper (Ref.11),

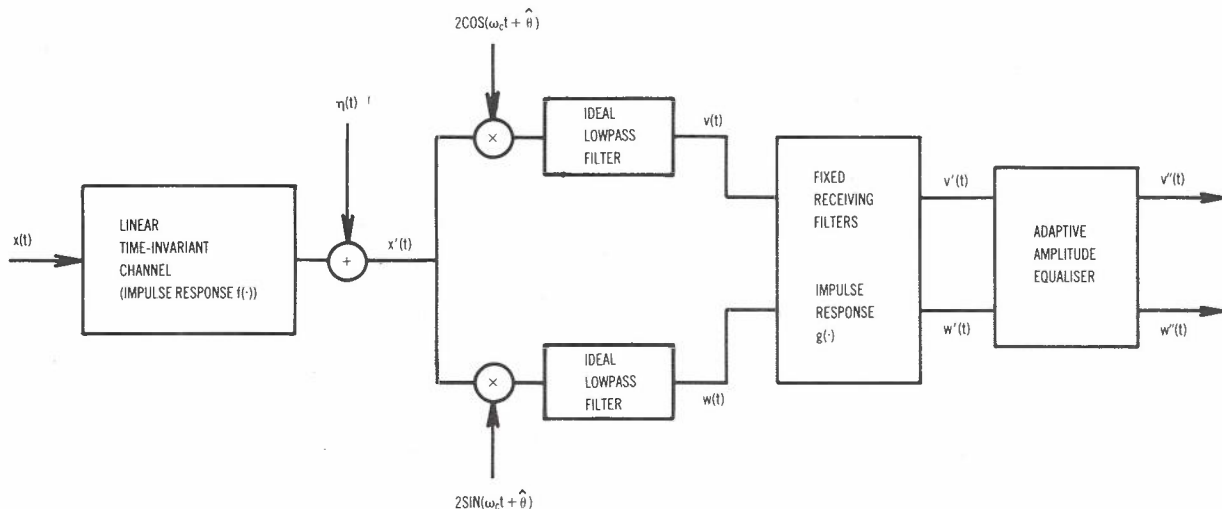


Fig. 2 - Receiver "front end"

QAM systems may be analysed in a manner which is highly analogous to the way in which PAM systems are analysed. In subsection 3.1 we derive a model for the "front-end" which includes the effects of the channel, thermal noise, demodulation, fixed receiving filters and adaptive amplitude equaliser. In subsection 3.2 we derive a model for a transversal equaliser and its associated timing recovery circuit.

3.1 Model for the "Front End"

Let the in-phase symbol stream be denoted $\{a_k\}$ and let the quadrature-phase symbol stream be denoted $\{b_k\}$. Also let $c_k = a_k + jb_k$. An equivalent form for the "front-end" is shown in Fig.2. Here, $x(\cdot)$ represents the transmitted signal and is given by:

$$x(t) = \text{Re} \left\{ \sum_k c_k d(t-kT) \exp(-j(\omega_c t + \theta_0)) \right\}$$

where ω_c is the carrier angular frequency, T is the baud period, and θ_0 is an unknown "true value" of the carrier phase. Let $D(\cdot)$ denote the Fourier transform of $d(\cdot)$. Here, as defined previously, ω_{max} is the smallest ω' for which $D(\omega) = 0$ for all $\omega > \omega'$.

Since $f(\cdot)$ (the impulse response of the channel) is a real-valued function, the signal (after transmission through the channel) can easily be seen to be:

$$x'(t) = \text{Re} \left\{ \sum_k c_k h(t - kT) \exp(-j(\omega_c t + \theta_0)) \right\} + \eta(t)$$

where the power spectral density of $\eta(\cdot)$ is equal to N_0 on the interval $(\omega_c - \omega_{max}, \omega_c + \omega_{max})$ and where $h(\cdot) = (f(\cdot) \exp(j\omega_c \cdot)) * d(\cdot)$.

The well-known "envelope" (or "band-pass") representation of noise (see e.g. p503 of Ref.7) gives:

$$n(t) = n_1(t) \cos(\omega_c t) + n_2(t) \sin(\omega_c t)$$

where $n_1(\cdot)$ and $n_2(\cdot)$ are independent, zero-mean stationary Gaussian processes with spectral densities which take on the value $2N_0$ for $|\omega| < \omega_{max}$. The ideal lowpass filters of Fig.2 are assumed to have identical cutoff (angular) frequencies ω_{max} . It is easily shown that the outputs $v(\cdot)$ and $w(\cdot)$ of the ideal lowpass filters are given by:

$$v(t) = \text{Re} \{ y(t) \}$$

$$w(t) = \text{Im} \{ y(t) \}$$

where

$$y(t) = \sum_k c_k h(t - kT) \exp(j(\theta - \theta_0)) + n(t)$$

$$n(t) = n_1(t) + jn_2(t) \quad (3.1)$$

and $n_1(\cdot)$ and $n_2(\cdot)$ are independent, zero-mean stationary Gaussian processes with spectral densities $N_1(\omega)$ and $N_2(\omega)$ where:

$$N_1(\cdot) = N_2(\cdot) = 2N_0 \text{ for } |\omega| < \omega_{max} \quad (3.2)$$

$$= 0 \text{ otherwise}$$

The block showing the fixed receiving filters includes the effect of all fixed RF, IF and baseband filters. We let $g(\cdot)$ denote the inverse Fourier transform of the equivalent baseband transfer function $F(\cdot)$ of these fixed receiving filters. Using relatively simple manipulations it may be shown that the outputs, $v'(\cdot)$ and $w'(\cdot)$, of the block representing the fixed receiving filters are given by:

$$v'(t) = \text{Re} \{ y'(t) \}$$

$$w'(t) = \text{Im} \{ y'(t) \}$$

where

$$y'(t) = \sum_k c_k h'(t - kT) + n'(t)$$

$$n'(\cdot) = g(\cdot) * n(\cdot)$$

$$h'(\cdot) = g(\cdot) \exp(j(\theta - \theta_0)) * h(\cdot)$$

From the above result it is clear, for no fading and $\theta = \theta_0$, that cross-channel interference at the output of the fixed receiving filters will be zero only when $g(\cdot)$ is a real-valued function. For this reason $g(\cdot)$ will be assumed to be a real-valued function.

Again using relatively simple manipulations it may be shown that the outputs, $v''(\cdot)$ and $w''(\cdot)$, of the block representing the adaptive amplitude equaliser can be written as:

$$v''(t) = \text{Re} \{ y''(t) \}$$

$$w''(t) = \text{Im} \{ y''(t) \}$$

where

$$y''(t) = \sum_k c_k h''(t - kT) + n''(t)$$

$$n''(\cdot) = p(\cdot) * n'(\cdot)$$

$$h''(\cdot) = p(\cdot) * h'(\cdot)$$

and $p(\cdot)$ is the inverse Fourier transform of $P(\omega)$, which represents the baseband equivalent transfer function of the adaptive amplitude equaliser. That is:

$$P(\omega) = \tilde{P}(\omega - \omega_1) \text{ for } |\omega| < \omega_{max}$$

$$= 0 \text{ otherwise}$$

where $\tilde{P}(\omega)$ is the adaptive amplitude equaliser (operating at intermediate frequency ω_1) transfer function. Note that under multipath fading conditions $p(t)$ will, in general, be complex.

Combining the results obtained so far it follows that:

$$h''(\cdot) = p(\cdot) * \{g(\cdot) \exp(j(\theta - \theta_0))\}$$

$$* \{f(\cdot) \exp(j\omega_c \cdot)\} * d(\cdot)$$

$$n''(\cdot) = p(\cdot) * g(\cdot) * n(\cdot) \quad (3.3)$$

We now consider the carrier-recovery where the variable θ is set to $\hat{\theta}$ which is the receiver's estimate of θ_0 . In Section 2 we introduced the assumption that $\hat{\theta} - \theta_0$ varies slowly in comparison with the time required by the transversal equaliser to adjust to new channel conditions. In this case the calculation of receiver performance is not affected by setting $\hat{\theta} = \theta_0$ since, in the analysis of the equaliser, $\exp\{j(\hat{\theta} - \theta_0)\}$ may be considered to be a fixed complex number. Thus, we will proceed with:

$$h''(\cdot) = p(\cdot) * \{f(\cdot) \exp(j\omega_c \cdot)\}$$

$$* \{g(\cdot) * d(\cdot)\} \quad (3.4)$$

and let it be noted that $g(\cdot) * d(\cdot)$ has Fourier transform $G^2(\cdot)$ since $G(\cdot) = D(\cdot)$.

3.2 A Model for the Transversal Equaliser and Associated Timing

In this subsection we are concerned with the derivation of a model for the transversal equaliser and the associated timing recovery. The transversal equaliser and associated timing and decision circuitry are shown in Fig.3. The transversal equaliser has $2K + 1$ complex tap coefficients denoted by $\alpha_{-K}, \alpha_{-K+1}, \dots, \alpha_K$. The continuous-time output of the transversal equaliser is obviously:

$$z(t) = \sum_{k=-K}^K \alpha_k y''(t - kT)$$

$$= \sum_k c_k h'''(t - kT) + n'''(t)$$

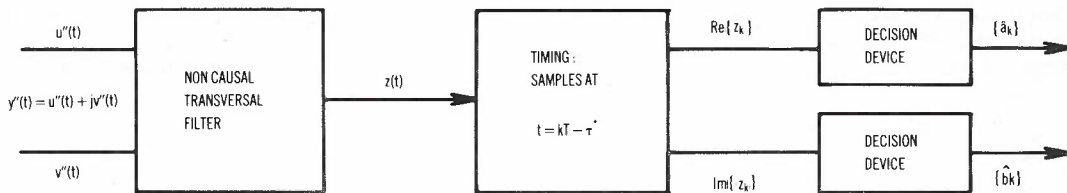


Fig. 3 - Transversal equaliser and associated timing and decision circuitry

where

$$\begin{aligned}
 h''''(t) &= \sum_{k=-K}^K \alpha_k h''(t - kT) \\
 n''''(t) &= \sum_{k=-K}^K \alpha_k n''(t - kT)
 \end{aligned}
 \tag{3.5}$$

Now consider the extraction of timing from the continuous-time output of the transversal equaliser, $z(\cdot)$, as shown in Fig.4. The sampling instants are derived from the zero crossings of the mean timing wave. That is, we do not consider the effect of timing jitter.

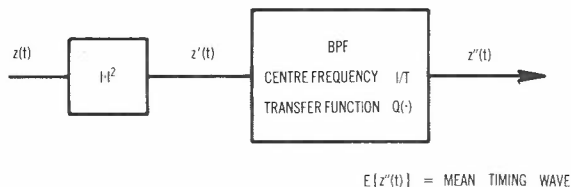


Fig. 4 - Timing recovery circuit

The mean timing wave is derived in the Appendix where it is shown that the k 'th sampling instant is at:

$$t = kT - \tau^*$$

The sampled output of the transversal equaliser is denoted $\{z_k\}$ where:

$$z_k = z(t = kT - \tau^*)$$

That is:

$$z_k = \sum_l c_l \sum_{m=-K}^K \alpha_m h''_{k-l-m}(\tau^*) + n_k''''$$

where:

$$n_k'''' = n''''(t = kT - \tau^*) \tag{3.6}$$

and

$$h_k''(\tau^*) = h''(t = kT - \tau^*) \tag{3.7}$$

$$\tau^* = \frac{T}{2\pi} \text{Arg} \left\{ \tilde{H} \left(\frac{2\pi}{T} \right) \right\} \tag{3.8}$$

Since we have assumed (see Section 2) a zero-forcing equaliser the complex-valued tap coefficients $\alpha_{-K}, \dots, \alpha_K$ are specified by the following $2K + 1$ equations.

$$\sum_{l=-K}^K \alpha_l h''_{m-l}(\tau^*) = 0$$

$$\text{for } m = -K, -K+1, \dots, -1, 1, \dots, K \tag{3.9}$$

$$\sum_{l=-K}^K \alpha_l h''_{-l}(\tau^*) = 1 \tag{3.10}$$

From (A.2) (or A.3) and (3.8) it is clear that τ^* is a function of $\alpha_{-K}, \dots, \alpha_K$. On the other hand, it is clear from (3.7), (3.9) and (3.10) that $\alpha_{-K}, \dots, \alpha_K$ depend on τ^* . In other words, τ^* and $\alpha_{-K}, \dots, \alpha_K$ are determined by the set of nonlinear equations (A.2) (or (A.3) and (3.7) - (3.10).

Now,

$$z_k = \sum_l c_l h_k'''' + n_k''''$$

where:

$$h_k'''' = \sum_{m=-K}^K \alpha_m(\tau^*) h_{k-m}''(\tau^*) \tag{3.11}$$

Note, from equation (3.4), that:

$$H''(\omega) = P(\omega) F(\omega - \omega_c) G^2(\omega) \tag{3.12}$$

Also, from (3.11),

$$\begin{aligned}
 h_k'''' &= \frac{1}{2\pi} \int_{-\pi/T}^{\pi/T} \left[\sum_{m=-1}^1 H''(\omega + \frac{2\pi m}{T}) \sum_{l=-K}^K \alpha_l \exp(-j(\omega + \frac{2\pi m}{T})(lT + \tau^*)) \right] \\
 &\quad \exp(j\omega kT) d\omega \tag{3.13}
 \end{aligned}$$

Now n_k'''' can be written as follows:

$$n_k'''' = \int n(u) a(u) du$$

where $a(\cdot)$ is a complex-valued function. From (3.1) and the above expression it is easy to show that $\text{Re}\{n_k''''\}$ are independent zero-mean, Gaussian random variables with the same variance. It then follows that the variance of $\text{Re}\{n_k''''\}$ is $(1/2) \times E\{|n_k''''|^2\}$. Further, since each symbol stream is decided on separately we need

only consider one stream for the calculation of performance. That is, we need only consider $\text{Re}\{z_k\}$ where, obviously,

$$\text{Re}\{z_k\} = \text{Re}\{\sum_l c_l h_{k-l}''''\} + \text{Re}\{n_k''''\} \quad (3.14)$$

Now:

$$E\{|n_k''''|^2\} = E\{|n''''(t)|^2\}$$

It follows from equations (3.1), (3.2), (3.3) and (3.5) that:

$$E\{\text{Re}(n_k''''')^2\} = \frac{N_0}{\pi} \int_{-\omega_{\max}}^{\omega_{\max}} \left| \sum_{l=-K}^K \alpha_l(\tau^*) \exp(-j l T \omega) \right|^2 |P(\omega)G(\omega)|^2 d\omega \quad (3.15)$$

4. AN APPLICATION OF THE MODEL

In this Section, we deal with the particular case of no adaptive amplitude equalisation and a two-ray channel model. The system signature is used to assess system performance. We do not need to resort to computer simulations in order to predict system performance. However, extensive computations are required. The computational techniques used are described in detail in Section 4.2.

We compare in Section 4.3 system signatures computed from our mathematical model with measured system signatures. We have also investigated the likely improvement in performance obtained by increasing the number of taps in the transversal equaliser. The efficacy of the simple timing recovery scheme modelled is also considered.

4.1 Details of the Model

Some more details concerning the model and the notation adopted are presented in this Section.

4.1.1 Modulation Scheme. We consider a 16 QAM system where the a_k 's and b_k 's are independent, identically distributed random variables and where each a_k or b_k takes on each of the values $-3, -1, 1$ and 3 with probability $= 1/4$. At the receiver the decision devices have decision levels $-2, 0$ and 2 .

4.1.2 Two-Path Channel Model. The transfer function corresponding to the two-path channel model is:

$$F(\omega) = a(1 + b \exp(-j\omega\Delta))$$

where ω is the angular frequency. It is usual to interpret the parameter a as an attenuation common to both a "main" and a "secondary" path. The "secondary" path, involving a delay of Δ seconds relative to the "main",

has an attenuation relative to the "main" specified by b . The baseband equivalent transfer function of the channel is:

$$\begin{aligned} \tilde{F}(\omega) &= F(\omega - \omega_c) \\ &= a(1 + b \exp(-j(\omega - \omega_c)\Delta)) \end{aligned}$$

The disadvantage of the above parametrisation (with 3 independent parameters - a, b and Δ) is that the transfer function, considered over the interval in which the transmitted signal contains appreciable power, is very sensitive to small variations in Δ . For this reason we make the following transformation:

$$\tilde{F}(\omega) = a(1 - b \exp(-j(\omega - \omega_0)\Delta))$$

where $\omega_0 = \omega_c - \omega_n$ and ω_n is defined as that angular frequency, which is of the form $\pi(2n + 1)/\Delta$, closest to ω_c . If Δ were known to a high precision then ω_0 would be determined by the value of Δ . In practice, Δ is not known to a high precision and so we interpret a, b, ω_0 and Δ as four independent parameters where the value of Δ is only approximately specified. It will be convenient to define $B = -20 \log_{10}(1-b)$ because we will often consider b to be close to 1. Finally, in this paper, we set $a = 1$.

4.1.3 The Fixed Receiver Filters. We assume that the equivalent transfer function of the combined transmitting and receiving filters is a raised cosine function, with rolloff α , defined by:

$$G^2(\omega) = G(\omega) D(\omega) = \begin{cases} T & , -\frac{\pi}{T}(1-\alpha) \leq \omega \leq \frac{\pi}{T}(1-\alpha) \\ \frac{T}{2} (1 - \sin(\frac{T}{2\alpha}(\omega - \frac{\pi}{T}))) & , \frac{\pi}{T}(1-\alpha) \leq |\omega| \leq \frac{\pi}{T}(1+\alpha) \\ 0 & , \text{otherwise} \end{cases}$$

The corresponding impulse response is denoted $r_c(t)$.

We present numerical results only for the case of $\alpha = 0.5$, i.e. a 50% raised cosine, as this is a filter commonly used in digital radio systems.

4.1.4 Specification of the Noise. Let us suppose that the channel is not fading, i.e. there is no multipath activity or attenuation beyond the free-space loss.

From (3.14) we see that:

$$\begin{aligned} \text{Re}(z_k) &= a_k h''(0) + \text{Re}(n_k''''') \\ &= a_k + \text{Re}(n_k''''') \end{aligned}$$

since $h''(\cdot) = g(\cdot) * d(\cdot)$. Also, from (3.15) we see that:

$$E\{\text{Re}(n_k''')\}^2 = 2N_o$$

Let us suppose that the flat-fade margin of the system is zero. This means that the b.e.r. (bit-error-rate) of the output stream is 10^{-3} under non-fading conditions. Each symbol at the output of each decision device takes on one of four values. Thus:

$$\text{Pr}\{\text{symbol error}\} = 1.5 \text{Pr}\{\text{Re}(n_k''') > 1\}$$

Since Gray coding is used, 1 symbol error corresponds to 1 bit in error for two bits in the output stream. Thus:

$$\text{b.e.r.} = 0.75 \text{Pr}\{\text{Re}(n_k''') > 1\}$$

and it follows that:

$$N_o = \frac{1}{18}$$

With a flat fade margin of 46.5 dB (which is assumed in this paper)

$$N_o = \frac{10^{-4.65}}{18}$$

4.2 Computational Methods

In this Section we outline the computational methods used in calculating system signatures. We have wherever possible used analytic expressions rather than numerical approximations. This has dictated, to a large extent, whether time domain or frequency domain expressions are used.

4.2.1 Timing Offset, Intersymbol Interference and Noise Variance Calculations. We used the following simple expression for $h''(t)$

$$h''(t) = r_c(t) - b r_c(t-\Delta) \exp(j\omega_0\Delta)$$

Now consider the calculation of the timing offset τ^* , defined in Section 3.2. As was discussed in that section, τ^* and $\alpha_{-K}, \dots, \alpha_K$ are determined by a set of nonlinear equations. We set out our method of solving these equations as follows. Define $\alpha_{-K}(\tau), \dots, \alpha_K(\tau)$ by solving the following set of equations which are linear in the $\alpha_\ell(\tau)$'s.

$$\sum_{\ell=-K}^K \alpha_\ell h''_{m-\ell}(\tau) = 0$$

$$\text{for } m = -K, -K+1, \dots, -1, 1, \dots, K$$

$$\sum_{\ell=-K}^K \alpha_\ell h''_{-\ell}(\tau) = 1$$

where the $h''_k(\tau)$ are defined by equation (3.7).

Define $\Gamma(\tau)$ by

$$\Gamma(\tau) = \frac{T}{2\pi} \text{Arg}\{\tilde{H}(\frac{2\pi}{T})\}$$

where \tilde{H} is defined by equation A.3.

We then define

$$\Lambda(\tau) = \Gamma(\tau) - \tau$$

In other words, τ^* is the solution of $\Lambda(\tau) = 0$. The discontinuities, if any, of $\Gamma(\tau)$ are necessarily jumps of size T . It follows then that only when $\Lambda(\tau)$ has discontinuities which are jumps of size T will there be any possibility of the equation $\Lambda(\tau) = 0$ having no solution. We have found, for all the examples we have examined in detail, that $\Lambda(\tau)$ is an approximately linear function of τ . In fact, for the case of a transversal equaliser with a single central tap it can be shown that $\Lambda(\tau)$ is a linear function of τ .

We find the solution of $\Lambda(\tau) = 0$ using the well-known Regula Falsi technique. The calculation of $\tilde{H}(\frac{2\pi}{T})$ involves a numerical integration which is most conveniently performed on the frequency domain expression given by equation (A.2).

To perform numerical integrations we use Simpson's rule with repeated halving of the step length until the estimated relative error in $\text{Re}\{\tilde{H}(\frac{2\pi}{T})\}$ and $\text{Im}\{\tilde{H}(\frac{2\pi}{T})\}$ is less than some pre-specified value ϵ . The relative error is estimated using the approximate formula given on p. 178 of Ref.8. Let $\Lambda(\tau)$ denote the approximate value of $\Lambda(\tau)$ obtained from the numerically determined value of $\tilde{H}(\frac{2\pi}{T})$. It is not difficult to show that for any given value of τ

$$|\Lambda_a(\tau) - \Lambda(\tau)| \leq \frac{\epsilon \cdot T}{(1-\epsilon)\pi}$$

We are then able to bound the error in the numerical approximation to τ^* . Once τ^* has been calculated the $\{h''_{k-l}\}$ are determined using equation (3.11). $E\{\text{Re}(n_k''')\}^2$ is calculated using equation (3.18).

4.2.2 Probability of Error Calculation. As indicated in Section 3.2, we need consider only one symbol stream for the calculation of probability of error. From equation (3.14) it follows (using the fact that the equaliser is zero-forcing) that we need only consider:

$$\begin{aligned} \text{Re}(z_k) = & a_k + \sum_{\ell \neq k} a_\ell \text{Re}(h''_{k-\ell}) \\ & - \sum_{\ell} b_\ell \text{Im}(h''_{k-\ell}) + \text{Re}(n_k''') \end{aligned}$$

The second and third terms on the r.h.s. of this equation are the intersymbol interference terms. It is important to note, in the calculation of signatures, that the variance of the intersymbol interference is commonly very much greater than the variance of the noise, $\text{Re}(n_k''')$. That is, the intersymbol interference "dominates" the noise in its "contribution" to the probability of error.

Now, the probability of symbol error is $1.5 p_s$, where:

$$p_s = \text{Pr} \{ |\text{Re}(z_k) - a_k| > 1 \}$$

By an argument similar to that given in subsection 4.1.4

$$\text{b.e.r.} = 0.75 p_s \tag{4.1}$$

It is easy to see that

$$p_s = \text{Pr} \left\{ \sum_{\ell=0}^{\infty} \beta_{\ell} \xi_{\ell} + n > 1 \right\}$$

where the β_{ℓ} 's are obtained by placing in descending order of magnitude the following set of numbers

$$\{ |\text{Re}(h_{\ell}''')| : \ell \neq 0 \} \cup \{ |\text{Im}(h_{\ell}''')| \}$$

and the ξ_{ℓ} 's are independent random variables taking on each of the values -3, -1, 1 and 3 with probability = 1/4. Also, n is a Gaussian random variable (which is independent of the ξ_{ℓ} 's) having zero mean and variance = $E\{\text{Re}(n_k''')\}^2$.

As already noted it commonly happens that

$$E \left(\sum_{\ell=0}^{\infty} \beta_{\ell} \xi_{\ell} \right)^2 \gg E(n^2)$$

Because of this, care must be exercised with the use of any expansion methods of approximating p_s . We used three methods of approximating/bounding p_s , namely:

Method 1: Based on exhaustive evaluation. An approximation to p_s is the following

$$4^{-M} \sum_{\xi_1 \dots \xi_M} \text{Pr} \left\{ \sum_{\ell=1}^M \beta_{\ell} \xi_{\ell} + \tilde{n} > 1 \right\}$$

where \tilde{n} is a Gaussian random variable (independent of the ξ_{ℓ} 's) having zero mean and variance $E \left(\sum_{\ell=M+1}^{\infty} \beta_{\ell} \xi_{\ell} \right)^2 + E(n^2)$.

For the calculation of system signatures, made in this paper, the approximation is likely to be reasonable when

$$E \left(\sum_{\ell=M+1}^{\infty} \beta_{\ell} \xi_{\ell} \right)^2 < E(n^2)$$

For the results presented in this paper a value of $M=9$ has been used.

Method 2: The lower bound given by equation (23) of Ref.9.

Method 3: The following (easily proved) upper bound on p_s

$$p_s \leq \text{Pr} \left\{ \sum_{\ell=1}^J \beta_{\ell} \xi_{\ell} + n > 1 - 3 \sum_{\ell=J+1}^{\infty} |\beta_{\ell}| \right\}$$

For the results presented in this paper a value of $J = 7$ was used.

4.2.3 Determination of System Signatures.

System performance is assessed from the system signature. The signature is the locus of those B and f_o ($f_o = \frac{\omega_o}{2\pi}$) values (for a given Δ) for which $\text{b.e.r.} = 10^{-3}$.

For a fixed Δ , the b.e.r. is a function, $e(B, f_o)$, of B and f_o . To obtain the system signature, we determine the zeros of the function $e(B, f_o)$. We calculate each signature by first fixing Δ . Then for a series of f_o values, we determine that value of B for which $e(B, f_o) - 10^{-3} = 0$, using several iterations of the bisection rule followed by a linear interpolation.

For the system we consider the signatures are symmetric about $f_o = 0$. Furthermore the signatures for $\Delta = \Delta'$ and $\Delta = -\Delta'$ are identical. Thus, it is sufficient to consider $\Delta > 0$ only so that for $|b| < 1$ the channel transfer function is minimum-phase.

4.2.4 Comparison of System Signatures. We will compare measured and predicted system signatures. Clearly, we need to have some measure of "distance" between these signatures. If two signatures with the same value of Δ do not intersect, a useful measure of distance between them is the relative probability that $\text{b.e.r.} > 10^{-3}$. The relative probability that $\text{b.e.r.} > 10^{-3}$ also provides us with a measure of the improvement in performance as the number of equaliser taps is increased.

Let us consider signature pairs similar to those shown in Fig.5, that is, non-intersecting and such that there is approximately a constant difference between them for $|f| < f_{o1}$. In this case, the relative probability that $\text{b.e.r.} > 10^{-3}$ is given by:

$$R_{12} = \frac{\text{Pr} \{ \text{b.e.r.} > 10^{-3} \text{ for signature 1} \}}{\text{Pr} \{ \text{b.e.r.} > 10^{-3} \text{ for signature 2} \}}$$

$$\approx \left(\frac{f_{o1}}{f_{o2}} \right) 10^{((B_2 - B_1)/20)}$$

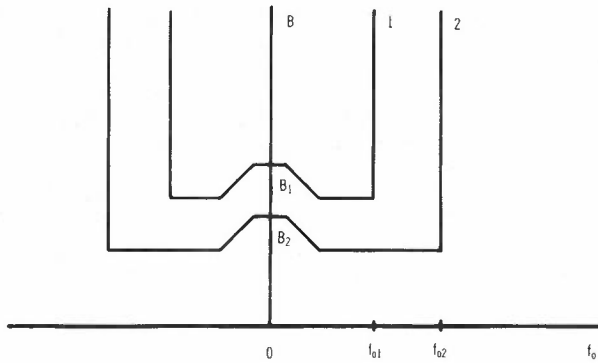


Fig. 5 - Signature pairs used in defining R_{12}

In determining this relation we have assumed that the probability density of b is approximately uniform on the interval $(b_2, 1)$ where b_2 is defined by:

$$b_2 = 1 - 10^{(-B_2/20)}$$

and we have made the very reasonable assumption that f_0 is a uniformly distributed random variable.

4.3 Comparison of Measured and Calculated Signatures: Improvement in Performance with Increase in Number of Equaliser Taps

A series of measurements to obtain system signatures have been performed on a commercially-available 140 Mbit/s, 16 QAM, high capacity digital radio system. The signatures were measured for a basic system employing a decision-directed carrier recovery scheme and a timing recovery scheme similar to the one used in our model (see Fig.4). This basic system corresponds to our model having a 1 tap transversal equaliser. Signatures were also measured for a basic

system to which a 5 tap, zero-forcing transversal equaliser has been added. The measured signatures for $\Delta = 2ns$ are compared with those calculated from our model in Fig.6.

As mentioned in the previous Section, a useful measure of "distance" between non-intersecting signatures is R_{12} , where signature 1 corresponds to the calculated signature and signature 2 corresponds to the appropriate measured signature. This measure of "distance" has been applied to the signatures presented in Fig.6 and the approximate values of R_{12} are given in Table 1. We have chosen to idealise our model to the extent that carrier phase jitter and timing jitter are ignored. Thus, given the very reasonable hypothesis that such jitter only degrades performance, the bit-error-rate we calculate will be a lower bound on the bit-error-rate of the actual system. The difference between the measured and calculated signatures could be accounted for by the following effects:

- (a) The carrier phase jitter and timing jitter.
- (b) Additional equipment imperfections such as incorrect decision levels etc.

TABLE 1 - R_{12} as a Measure of "Distance" Between Calculated and Measured Signatures

NUMBER OF EQUALISER TAPS	R_{12}
1	0.68
5	0.36

Further, we expect these effects to degrade the measured performance in an increasingly significant way as the number of taps is increased. The results presented in Table 1 are consistent with this expectation.

Let us now consider the improvement in performance predicted by our model as the number of transversal equaliser taps is increased. Fig. 7 depicts results for 1, 5, 7 and 9 equaliser tap coefficients, for $\Delta = 2ns$. A measure of improvement in performance as the number of equaliser taps increases is R_{12} where signature 2 corresponds to 1 equaliser tap and signature 1 corresponds to one of 5, 7, or 9 equaliser taps. This measure has been applied to the signatures presented in Fig.7 and the approximate values of R_{12} are given in Table 2. For a nine-tap transversal equaliser the calculated probability that the bit-error-rate exceeds 10^{-3} is approximately one half that calculated for a five-tap transversal equaliser. However, we would expect (for the reasons given earlier) that the difference between the measured performance

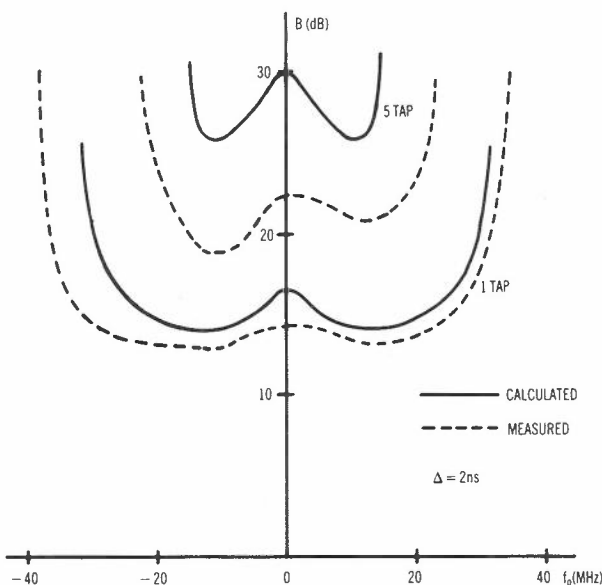


Fig. 6 - System signatures 1 tap and 5 tap

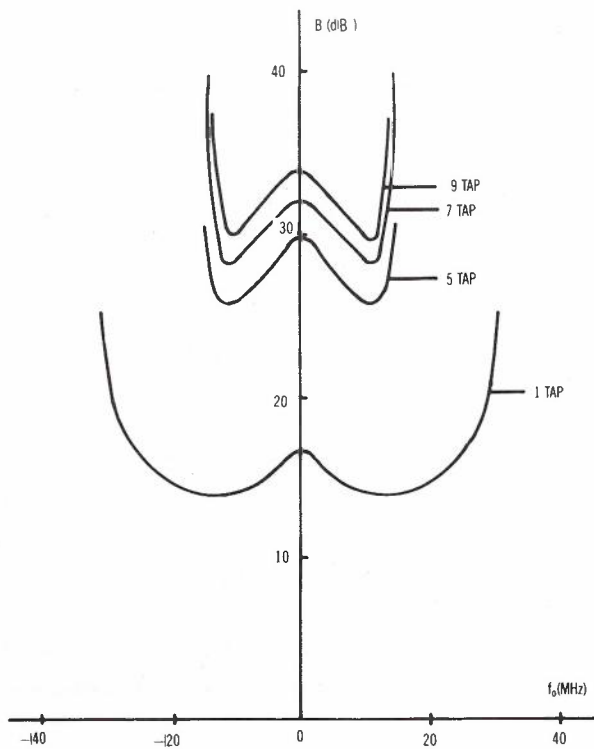


Fig. 7 - Calculated system signatures for 1, 5, 7, 9 taps

of a nine-tap equaliser and a five-tap equaliser would be substantially smaller. Overall, the improvement in performance of actual equipment, when the number of taps is increased from five to nine, is expected to be small in comparison with the improvement in performance of the equipment when the number of taps is increased from one to five.

TABLE 2 - R_{12} as a Measure of Improvement in Performance as the Number of Taps Increases

NUMBER OF EQUALISER TAPS	R_{12}
5	0.1
7	0.07
9	0.05

As described in subsection 4.2.2 we used three methods of approximating/bounding the probability of error. For each system configuration and value of Δ the following curves were calculated:

Curve 1: This is the locus of those B and f_0 values for which the upper bound on b.e.r., determined by Method 3 and equation (4.1), takes on the value 10^{-3} .

Curve 2: This is the locus of those B and f_0 values for which the approximation

to the b.e.r., determined by Method 1 and equation (4.1), takes on the value 10^{-3} .

Curve 3: This is the locus of those B and f_0 values for which the upper bound on b.e.r., determined by Method 2 and equation (4.1), takes on the value 10^{-3} .

Clearly, curve 1 (2) bounds from below (above) the signature evaluated by an exact error probability calculation. For all the signatures calculated by us it was observed that the differences between curves 1, 2 and 3 were negligible. One of the reasons for this is that, in the vicinity of the system signature, there is a rapid variation of b.e.r. with B for a fixed value of f_0 .

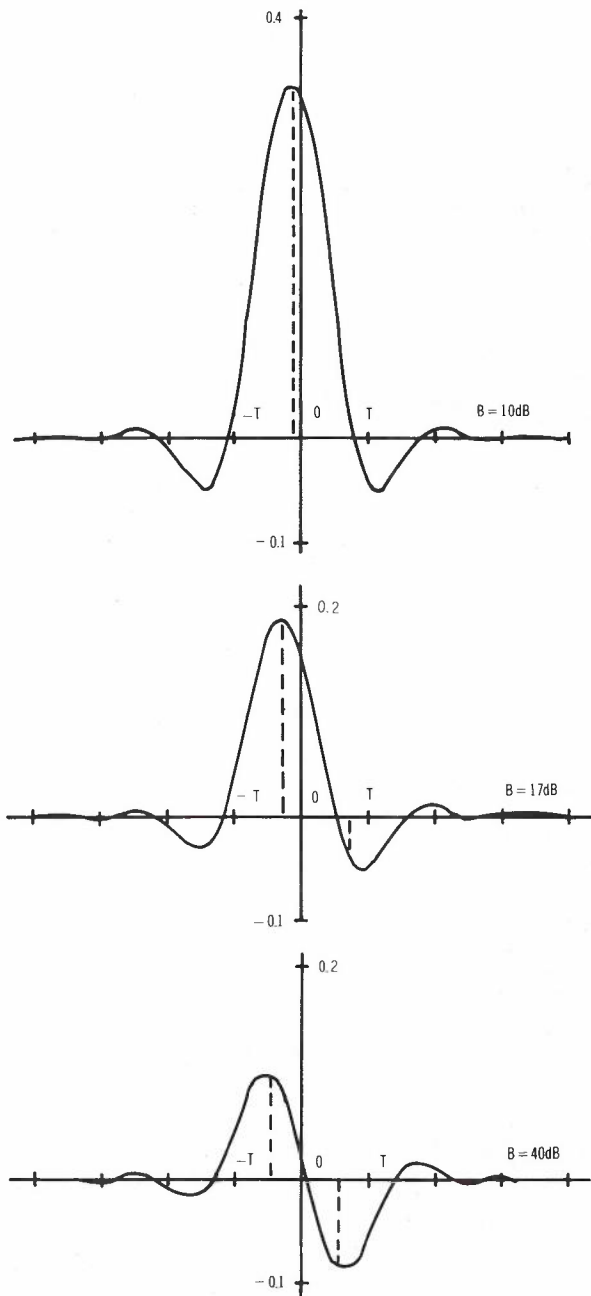


Fig. 8 - $h''(t)$ for $\Delta=2ns$, $f_0 = 0MHz$ for varying values of B. Broken lines indicate timing instants chosen by timing recovery circuit.

4.4 Timing Recovery Performance

The timing recovery scheme we consider is a fairly simple one. It is of interest, therefore, to make some assessment of the performance of this scheme. We can obtain an indication of the performance of the timing recovery scheme from the shape of the $h''(\cdot)$ pulse and the location of the timing instants. Under non-fading conditions $h''(t)$ is the impulse response corresponding to a raised-cosine filter so that it takes on the value unity at $t=0$ and has zero crossings at non-zero multiples of T . Let us now consider Fig.8 which depicts $h''(\cdot)$ for $\Delta = 2ns$, $f_o = 0$ MHz and B taking successively the values 10 dB, 17 dB and 40 dB (i.e. for increasing severity of fading). It is evident that, as the severity of fading increases, there is a shift of the peak of the $h''(\cdot)$ pulse away from $t=0$, a diminution of the height of the peak and an increase in asymmetry of the pulse. Also, the timing instants, depicted by the broken vertical lines follow the shift in the position of the peak. In summary, it would appear that the simple timing recovery scheme performs reasonably well. Note that the potential intersymbol interference, which must be minimised by the transversal equaliser, increases with the severity of fading.

5. CONCLUSION

We have presented, in detail, a mathematical model for microwave radio systems employing QAM. The model has been chosen so as to be able to approximate currently available systems. For this reason, we have considered a simple timing recovery circuit and zero-forcing equalisers. We have not considered, for example, equalisers with fractional tap spacing, minimum mean-square-error equalisation or more complex timing schemes.

Numerical methods are required to calculate system performance. However, we have, as far as possible, used analytical methods to derive those quantities which are fundamental to the calculation of system performance. In particular, we do not need to resort to computer simulation.

We have used the mathematical model to calculate system signatures for the particular case of a transversal equaliser, no adaptive amplitude equaliser and a two-path fading channel. Using as a criterion the relative probability that the bit-error-rate exceeds 10^{-3} , we have compared measured system signatures with calculated system signatures and we have considered the effect on performance of increasing the number of taps of the transversal equaliser.

It was noted that the model provides a lower bound on the bit-error-rate of the actual system, since we have not included carrier phase and timing jitter in the model and since other degradations may be present in an actual system.

For a nine tap transversal equaliser the calculated probability that the bit-error-rate exceeds 10^{-3} is approximately one half that calculated for a five-tap transversal equaliser. However, our calculations neglect jitter and other additional equipment imperfections. Overall, the improvement in performance of actual equipment, when the number of taps is increased from five to nine, is expected to be small in comparison with the improvement in performance of the equipment when the number of taps is increased from one to five.

We have obtained some indication of the effectiveness of the simple timing recovery scheme used in our model and we have shown that it performs reasonably well. How well this simple timing recovery scheme performs in comparison with an optimised timing recovery scheme is a topic which seems worthy of further investigation.

6. ACKNOWLEDGEMENTS

The authors acknowledge helpful discussions held with J. Campbell, R. Coutts, A. Martin, J. Millott, J. Murphy and B. Smith. The authors also acknowledge J. Campbell and A. Martin for providing the measured system signatures.

7. REFERENCES

1. Coutts, R.P. & Campbell, J.C., "Mean Square Error Analysis of QAM Digital Radio Systems Subject to Frequency Selective Fading", Aust. Telecom. Res., Vol. 16, pp23-38, 1982.
2. Foschini, G.J. & Salz, J., "Digital Communications Over Fading Radio Channels", Bell Syst. Tech. J., Vol. 62, pp429-456, 1983.
3. Taylor, D.P. & Shafi, M., "Fade Margin and Outage Computation of 49-QPRS Radio Employing Decision Feedback Equalisation", ICC83, IEEE International Conference on Communications, 1983.
4. Taylor, D.P. & Shafi, M., "Decision Feedback Equalisation for Multipath Induced Interference in Digital Microwave LOS Links", submitted for publication in IEEE Trans. Comm.
5. McMillen, G., Shafi, M. & Taylor, D.P., "Simultaneous Adaptive Estimation of Carrier Phase, Symbol Timing and Data for a 49-QPRS DFE Radio Receiver". Technical Report, Communications Research Laboratory, McMaster University, Canada, 1983.
6. Sari, H., "A Comparison of Equalization Techniques on 16 QAM Digital Radio Systems During Selective Fading", GLOBECOM 82, IEEE Global Telecommunications Conference, Vol. 3, pp1240-1245, 1982.

7. Wozencraft, J.M. & Jacobs, I.M., "Principles of Communication Engineering", John Wiley, 1965.
8. Scarborough, J.B., "Numerical Mathematical Analysis", Johns Hopkins Press (1955).
9. Jenq, Y.C., Liu, B. and Thomas, J.B., "Probability of error in PAM systems with intersymbol interference and additive noise" IEEE Trans. Inf. Th., vol. 23, pp575-582, 1977.
10. Franks, L.E. & Bubrouski, J.P., "Statistical Properties of Timing Jitter in a PAM Timing Recovery Scheme", IEEE Trans. Comm., Vol. 22, pp913-920, 1974.
11. Kobayashi, H., "Simultaneous Adaptive Estimation and Decision Algorithm for Carrier Modulated Data Transmission Systems", IEEE Trans. Comm., Vol. 19, pp268-280, 1971.

APPENDIX

Our derivation of the mean timing wave will use the fact that the operations of $E\{\cdot\}$ and linear, time-invariant filtering commute. It is easy to see that:

$$E\{z'(t)\} = \left\{ \sum_k c_k h''(t-kT) \right\}^2 + C$$

where C is a constant. Thus,

$$E\{z'(t)\} = 2E(a_k^2) \sum_k |h''(t-kT)|^2 + C$$

At this juncture we use the Poisson Summation Formula as do Franks and Bubrouski (Ref.10). Additional manipulations lead us to express the mean timing wave, $E\{z''(t)\}$, in the form:

$$E\{z''(t)\} = C' \sum_k R\left(\frac{2\pi k}{T}\right) \exp\left(\frac{j2\pi kt}{T}\right) \quad (A.1)$$

where:

C' is a constant

$$R(\cdot) = Q(\cdot) \tilde{H}(\cdot)$$

$$\tilde{H}(\omega) = \frac{1}{2\pi} \int H''(v+\omega) H''(v)^* \left| \sum_{k=-K}^K \alpha_k \exp(-jv k T) \right|^2 dv \quad (A.2)$$

$$\tilde{H}(\omega) = \int \left| \sum_{k=-K}^K \alpha_k h''(t-kT) \right|^2 \exp(-j\omega t) dt \quad (A.3)$$

where $Q(\cdot)$ denotes the transfer function of the bandpass filter.

Since $Q(\omega) = 0$ for $\omega < 0$ and $\omega > \frac{2\pi}{T}$, the equation (A.1) reduces to:

$$E\{z''(t)\} = C'' \left| R\left(\frac{2\pi}{T}\right) \right| \cos\left(\frac{2\pi}{T}t + \phi\right)$$

where:

$$\phi = \arg\{R(2\pi/T)\} \text{ and } C'' \text{ is a constant.}$$

The downcrossings of the mean timing wave are given by:

$$t = kT + \frac{T}{4} - \frac{\phi T}{2\pi}$$

The timing instants are offset from the downcrossings by:

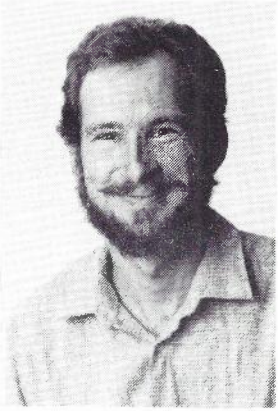
$$\frac{T}{4} - \frac{T}{2\pi} \cdot \text{Arg}\left\{Q\left(\frac{2\pi}{T}\right)\right\}$$

as this gives ideal timing under non-fading conditions. That is, the k' th sampling instant is at:

$$t = kT - \tau^*$$

where τ^* is given by equation (3.8).

BIOGRAPHIES



PAUL V. KABAILA received the B.Sc degree in mathematics and the B.E.(Hons) degree in electrical engineering, both from the University of New South Wales, and the Ph.D degree in electrical engineering from the University of Newcastle in 1979.

From October 1978 to November 1982 he was employed, first as an Experimental Officer and then as a Research Scientist, by CSIRO Division of Mathematics and Statistics. At the Division he had the dual role of conducting research in the field of time series analysis and of acting as a statistical consultant at other divisions of CSIRO. Since December 1982 he has been with Telecom Australia Research Laboratories where he currently holds the position of senior engineer in the Applied Mathematics and Computer Techniques Section. His interests are in statistical consultancy and the application of stochastic process theory in the context of telecommunications research.



JENNIFER L. ADAMS was born in Hobart in 1955. She received the B.Sc, B.Sc(Hons) and PhD degrees in Physics from the University of Tasmania in 1976, 1977 and 1981 respectively.

In 1981, she joined the Telecom Australia, Research Laboratories where she is currently a Science Class 3 in the Transmission Systems Branch. Since joining the Research Laboratories, she has been concerned with various problems associated with optical fibre transmission systems and digital radio systems.

Information for Authors

ATR invites the submission of technical manuscripts on topics relating to research into telecommunications in Australia. Original work and tutorials of lasting reference value are welcome.

Manuscripts should be written clearly in English. They must be typed using double spacing with each page numbered sequentially in the top right hand corner. The title, not exceeding two lines, should be typed in capital letters at the top of page 1. Name(s) of author(s), in capitals, with affiliation(s) in lower case underneath, should be inserted on the left side of the page below the title. An abstract, not exceeding 150 words and indicating the aim, scope and conclusions of the paper, should follow below the affiliation(s).

ATR permits three orders of headings to be used in the manuscript. First-order headings should be typed in capitals and underlined. Each first-order heading should be prefixed by a number which indicates its sequence in the text, followed by a full stop. Second-order headings should be underlined and typed in lower case letters except for the first letter of each word in the heading, which should be typed as a capital. They should be prefixed by numbers separated by a full stop to indicate their hierarchical dependence on the first-order heading. Third-order headings are typed as for second-order headings, underlined and followed by a full stop. The text should continue on the same line as the heading. Numbering of third-order headings is optional, but when used, should indicate its hierarchical dependence on the second-order heading (i.e. two full stops should be used as separators).

Tables may be included in the manuscript and sequentially numbered in the order in which they are called up in the text. The table heading should appear above the table. Figures may be supplied as clear unambiguous freehand sketches. Figures should be sequentially numbered in the order in which they are called in the text using the form: Fig. 1. A separate list of figure captions is to be provided with the manuscript. Equations are to be numbered consecutively with Arabic numerals in parenthesis, placed at the right hand margin.

A list of references should be given at the end of the manuscript, typed in close spacing with a line between each reference cited. References must be sequentially numbered in the order in which they are called in the text. They should appear in the text as (Ref. 1). The format for references is shown in the following examples.

Wilkinson, R.I., "Theories for Toll Traffic Engineering in the U.S.A.", BSTJ, Vol. 35, No. 2, March 1956, pp.541.

Abramowitz, M. and Stegun, I.A., (Eds), Handbook of Mathematical Functions, Dover, New York, 1965.

Four copies of the paper, together with a biography and clear photograph of each of the authors should be submitted for consideration to the secretary (see inside front cover). All submissions are reviewed by referees who will recommend acceptance, modification or rejection of the material for publication. After acceptance and publication of a manuscript authors of each paper will receive 50 free reprints of the paper and a complimentary copy of the journal.

Benefits of Authorship for ATR.

- ATR is a rigorously reviewed journal with international distribution and abstracting.
- Contact with workers in your field in the major telecommunication laboratories in Australia can improve interaction.
- Contributions relevant to the Australian context can contribute to the viability and vitality of future Australian research and industry.
- Publication is facilitated because ATR arranges drafting of figures at no cost to the author, and with no need for the author to spend time on learning journal format standards.

ATR AUSTRALIAN
TELECOMMUNICATION
RESEARCH
ISSN 0001-2777

VOLUME 19, NUMBER 1,
1985

Titles (Abbreviated)

Challenge	2
Satellite Propagation	3
E. BACHMANN	
Local Digital Transmission Pulse Shapes	13
P.G. POTTER	
Echo Canceller Structures	23
F.G. BULLOCK	
Protocols for Message Handling	43
R. EXNER	
High-Capacity Digital Radio System Model	53
P.V. KABAILA, J.L. ADAMS	